REMARKS/ARGUMENTS

I. Status of the claims

With entry of this amendment, claims 34-37 and 40 are amended, claims 47-52 are added, and claims 41-46 are canceled. Claims 34-40 and 47-52 are pending with entry of the amendment.

II. Support for the amendments

Support for the amendments can be found in the specification, drawings and claims as originally filed. For example, support for "at least 30 nucleotides" in claim 34 can be found on, e.g., page 28, lines 8-16 of the specification. Support for the various floral phenotypes recited can be found on, e.g., page 44, lines 12-24 of the specification. Support for increased endosperm size can be found on page 25, lines 20-21 of the specification. Support for new claim 47 can be found on, e.g., page 44, lines 12-24 and page 16, line 9 of the specification. No new matter is added.

III. Interview

Applicants thank the Examiner for the phone interview on July 14, 2004. The relation of decreased expression to organ identity and number and meristem was discussed, as well as overexpression and delayed flowering. Applicant indicated that a terminal disclaimer might be appropriate if the other patentability issues were resolved. Various aspects of claim scope including percent identity and RNAi-type claims were discussed. Applicants believe they have addressed the Examiner's concerns in this Amendment.

IV. Objection to the Abstract and Title

The Examiner objected to the abstract and title as allegedly not clearly indicative of the invention. Applicants have amended the abstract and title as requested. Applicants respectfully request withdrawal of the objections.

V. Objection to claims 40-45

The Examiner objected to claims 40-45 as not further limiting the independent claim. As these claims are canceled or amended, the rejection is moot. Accordingly, withdrawal of the rejection is requested.

VI. Rejection under 35 U.S.C. § 112, first paragraph: enablement

Claims 34-46 were rejected as allegedly not meeting the enablement requirement. Specifically, the Examiner argued that the specification did not enable those of skill in the art to make and use the full scope of the claimed invention. The Examiner questioned whether the homology between endonuclease III, glycosylases and DMT polypeptides was real given the low homology described in the application. The Office Action further questioned whether DMT affected DNA methylation. As DMT does in fact modulate DNA methylation and the specification does enable those of skill in the art to practice the full scope of the claimed invention, Applicants respectfully traverse the rejection.

To establish a *prima facie* case of non-enablement, the Examiner must show that undue experimentation would be required to make and use the claimed invention. Even if the practice of the claimed invention requires a considerable amount of experimentation, it is not necessarily "undue" experimentation:

> The test is not merely quantitative, since a considerable amount of experimentation is permissible, if it is merely routine, or if the specification in question provides a reasonable amount of guidance with respect to the direction in which the experimentation should proceed. *In re Wands*, 8 USPQ2d 1400 (Fed. Cir. 1988) (citing *In re Angstadt*, 190 USPQ 214 (CCPA 1976). MPEP § 2164.06.

As amended, there are two sets of claims under prosecution (claims 34-39 and 47-52). The first set of claims is directed to methods of inhibiting DMT expression, thereby resulting in modulated floral organ identity, modulated floral organ number, or increased meristem size. As described in the specification (e.g., on page 44, lines 12-18), in *dmt/dmt* plants the above-described phenotypes are observed. For example, as illustrated in Choi *et al., Cell* 110:33-42 (2002) (Exhibit A), Figure 2F, both stamen and petal identity is affected. Reduction

of DMT activity due to DMT mutation generates flowers with altered numbers of floral organs. *See* Choi *et al.*, Figures 2B and 2C for petals and sepals, Figure 2H for gynoecia, and Figure 2I for stamens. Moreover, the inventors observe fascinated (i.e., larger, thicker) stems in *dmt/dmt* plants. Fasciation is caused by modulation of meristem size. *See, e.g.*, Leyser *et al.*, *Development* 116:397-403 (1992) (Exhibit B). Please note that the inventors have since abbreviated the *DEMETER* gene name as *DME* rather than *DMT*. In view of the above evidence, it is clear that reducing DMT activity or expression results in the recited phenotypes.

Claim 34 recites that DMT expression may be reduced by expressing an "expression-inhibiting polynucleotide comprises at least 30 contiguous nucleotides of a polynucleotide encoding SEQ ID NO:2." This claim encompasses the inhibition of DMT expression using various RNAi technologies, including antisense- and sense-based suppression as provided in the specification on page 27, line 22 to page 28, line 29 and page 29, line 22 to page 30, line 17. RNAi-based suppression of endogenous gene expression was well-known as of the filing date of the present application. For example, in 2000, Chuang *et al.* (*Proc. Natl. Acad. Sci. USA* 97(9):4985-4990 (2000) (Exhibit C) demonstrated that use of gene fragments (*see, e.g.*, last sentence of "constructs" paragraph on page 4985) were useful for knocking out endogenous gene expression. The paper concludes that RNAi "... is a useful method for determining the loss-of-function phenotypes of genes ...."

The length of expressed sequences effective in RNAi can be as short as 23 nucleotides of complete identity. *See, e.g.*, Thomas *et al.*, *Plant J.* 25(4):417-25 (Feb., 2001) (Exhibit D). Thus, those of skill in the art could have readily used the sequences recited in claim 34 to reduce expression of DMT. Accordingly, the full scope of claim 34 is enabled by the specification.

Claim 47 recites a method of delaying flowering time by introducing into a plant an expression cassette comprising a promoter operably linked to a DMT polynucleotide, or a complement thereof, encoding a polypeptide at least 80% identical to SEQ ID NO:2, wherein the polypeptide comprises a leucine zipper and a nuclear localization signal sequence. In response to the Examiner's questions regarding the function of DMT, Applications submit Choi *et al.* (Exhibt A) and Xiao *et al.*, *Develop. Cell* 5:891-901 (2003) (Exhibit E). As illustrated in Figure

3 of Choi *et al.*, the proposed glycosylase domain of DMT comprises a large number of conserved amino acids with known DNA glycosylases, including two highly conserved glycines and an aspartate (*see*, page 3 of Choi *et al.*). Xiao *et al.* demonstrates that mutations that suppress the effect of DMT mutations can be found in a methyltransferase, thereby providing further evidence that DMT modulates methylation. In view of the sequence conservation with glycosylases and the structure/function knowledge base for glycosylases, those of skill could have readily introduced changes into SEQ ID NO:2 to maintain activity without undue experimentation.

Moreover, Applicants note that claim 47 further recites that the DMT polypeptide comprises a leucine zipper and a nuclear localization signal sequence. Those of skill in the art were well aware of the structures of such domains and therefore it would not have required undue experimentation to make and use sequences within the scope of the claims.

Finally, Applicants note that the exact scope of sequence identity was already issued in the parent application (now U.S. Patent No. 6,476,296) of the present application. The Examiner is reminded that claims issued by the Patent Office are presumed valid.

In view of the above arguments, Applicants respectfully request withdrawal of the enablement rejection.

VII. Rejection under 35 U.S.C. § 112, first paragraph: written description

Claims 34-46 were also rejected under the written description requirement because the application allegedly only teaches one sequence within the scope of the claims and allegedly provides no structural basis to identify other sequences within the scope of the claims. Applicants respectfully traverse the rejection.

"The written description requirement does not require the applicant 'to describe exactly the subject matter claimed, [instead] the description must clearly allow persons of ordinary skill in the art to recognize that [he or she] invented what is claimed.'" *Union Oil Co. v. Atlantic Richfield Co.*, Docket No. 99-1066 (Fed. Cir. 2000) *citing In re Gosteli*, 10 USPQ 2d 1614, 1618 (Fed. Cir. 1989) (brackets in original). Whether claims have met the written description requirement is a factual determination. *See In re Wertheim*, 191 USPQ 90, 96

(CCPA, 1976). When considering whether claims satisfy the written description requirement, it is essential to keep in mind the purpose for the description requirement, i.e., to ensure that, as of the filing date, the inventor conveyed with reasonable clarity to those of skill in the art that he was in possession of the subject matter of the claims. *See Vas-Cath, Inc. v. Mahurkar*, 19 USPQ 2d 1111, 1117 (Fed. Cir. 1991).

With regard to claim 34, and claims depending from claim 34, the specification teaches that polynucleotide fragments comprising as few as 30 nucleotides may be used in the sense orientation (page 30, lines 5-13), antisense orientation (page 28, lines 8-16), or combinations of sense and antisense orientations (page 30, lines 14-17). These descriptions clearly convey to one of skill in the art what size and type of fragments are useful in the invention. Based on the teaching of the specification alone, those of skill in the art could have readily identified all sequences within the scope of the claims. Moreover, as described above in the enablement discussion, as of the filing date, those of skill in the art were able to use gene fragments to inhibit gene expression. Accordingly, amended claim 34 and claims dependent thereon, meet the written description requirement as interpreted by the Federal Circuit.

As described above on the enablement discussion, the structural features recited in the present claims, including clam 47, as well as taught in the specification, confers sufficient information to those of skill in the art such that those of skill in the art would have understood that the inventors were in possession of the full scope of the claimed invention. For example, the specification teaches that DMT affects methylation whose structural basis is related to homology to an endonuclease. The specification further teaches that the protein comprises a leucine zipper and nuclear localization signal sequence. Therefore, sufficient structure/function information is provided to meet the written description requirement for the pending claims.

In view of the above arguments, Applicants respectfully request withdrawal of the written description rejection.

VIII. Rejection under 35 U.S.C. § 112, second paragraph

Claims 34-46 were also rejected under 35 U.S.C. § 112, second paragraph as allegedly unclear. The language objected to by the Examiner has been canceled from the claims. Accordingly, withdrawal of the rejection is respectfully requested.

IX. Obviousness-type double patenting

Claims 34-46 were also rejected under the doctrine of obviousness-type double patenting over claims 10-38 of U.S. Patent No. 6,476,296. Applicants will gladly consider providing a terminal disclaimer to overcome this rejection when the Examiner has indicated that the claims are otherwise allowable.

CONCLUSION

In view of the foregoing, Applicants believe all claims now pending in this Application are in condition for allowance. The issuance of a formal Notice of Allowance at an early date is respectfully requested.

If the Examiner believes a telephone conference would expedite prosecution of this application, please telephone the undersigned at 415-576-0200.

Respectfully submitted,

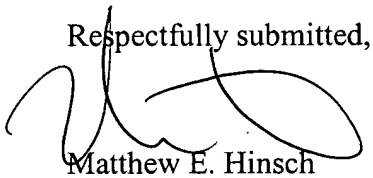

Matthew E. Hinsch
Reg. No. 47,651

TOWNSEND and TOWNSEND and CREW LLP
Two Embarcadero Center, Eighth Floor
San Francisco, California 94111-3834
Tel: 415-576-0200
Fax: 415-576-0300
Attachments
MEH:meh
60340393 v1

Cell, Vol. 110, 1–20, July 12, 2002, Copyright ©2002 by Cell Press

EXHIBIT A

DEMETER, a DNA Glycosylase Domain Protein, Is Required for Endosperm Gene Imprinting and Seed Viability in *Arabidopsis*

Yeonhee Choi,[1] Mary Gehring,[1] Lianna Johnson,[2] Mike Hannon,[1] John J. Harada,[3] Robert B. Goldberg,[2]
Steven E. Jacobsen,[2,4] and Robert L. Fischer[1,5]
[1]Department of Plant and Microbial Biology
University of California, Berkeley
Berkeley, California 94720
[2]Department of Molecular, Cell, and Developmental Biology
University of California, Los Angeles
Los Angeles, California 90095
[3]Section of Plant Biology
Division of Biological Sciences
University of California, Davis
Davis, California 95616
[4]Molecular Biology Institute
University of California, Los Angeles
Los Angeles, California 90095

Summary

We isolated mutations in *Arabidopsis* to understand how the female gametophyte controls embryo and endosperm development. For the *DEMETER* (*DME*) gene, seed viability depends only on the maternal allele. *DME* encodes a large protein with DNA glycosylase and nuclear localization domains. *DME* is expressed primarily in the central cell of the female gametophyte, the progenitor of the endosperm. *DME* is required for maternal allele expression of the imprinted *MEDEA* (*MEA*) Polycomb gene in the central cell and endosperm. Ectopic *DME* expression in endosperm activates expression of the normally silenced paternal *MEA* allele. In leaf, ectopic *DME* expression induces *MEA* and nicks the *MEA* promoter. Thus, a DNA glycosylase activates maternal expression of an imprinted gene in the central cell.

Introduction

In flowering plants, the female gametophyte is the progenitor of the embryo and endosperm. Much is understood about female gametophyte morphology, and genes necessary for female gametophyte development and function have been identified (Drews et al., 1998). However, little is known about the molecular and genetic processes taking place in the female gametophyte that affect subsequent embryo and endosperm development.

The female gametophyte is formed within the ovule. In *Arabidopsis*, a haploid spore undergoes three mitotic divisions to form an 8-nucleus, 7-cell female gametophyte containing the egg, central, synergid, and antipodal cells. Before fertilization, a diploid nucleus is formed in the central cell by the fusion of two haploid nuclei. The endosperm is derived from fertilization of the central cell by a sperm cell; fertilization of the adjacent egg cell by a second sperm cell gives rise to the embryo (Brown et al., 1999). Thus, double fertilization generates a seed with a triploid endosperm and diploid embryo. The embryo generates organs (axis and cotyledon), tissues (protoderm, procambium, and ground meristem), and meristems (shoot and root). The fertilized central cell replicates to form a syncytium, and following cellularization, produces storage proteins, lipids, and starch, and mediates the transfer of nutrients from maternal tissues to be absorbed by the embryo (Brown et al., 1999).

To gain insights into the maternal control of embryo and endosperm development, mutations in a small number of genes have been identified where seed viability depends upon the genotype of the maternal allele. For example, these studies have shown that the female gametophyte provides the embryo with an MCM-related protein, PROLIFERA (PRL), necessary for cytokinesis (Springer and Holding, 2002). Also, wild-type maternal alleles encoding Polycomb group proteins are necessary for proper female gametophyte and seed development. *MEDEA* (*MEA*), *FERTILIZATION INDEPENDENT ENDOSPERM* (*FIE*), and *FERTILIZATION INDEPENDENT SEED2* (*FIS2*) encode SET-domain, WD domain, and zinc finger Polycomb group proteins (Grossniklaus et al., 1998; Kiyosue et al., 1999; Luo et al., 1999; Ohad et al., 1999; Birve et al., 2001). Polycomb group proteins repress gene transcription by forming complexes that remodel chromatin structure at specific regions within the genome (Francis and Kingston, 2001). One function of *MEA*, *FIE*, and *FIS2* is to prevent the onset of central cell proliferation and endosperm development prior to fertilization and to repress endosperm growth and development after fertilization (Kiyosue et al., 1999; Vinkenoog et al., 2000). Thus, to date, no genes have been discovered that function primarily as prefertilization in the female gametophyte to control processes essential for subsequent embryo and endosperm development after fertilization.

Because only the maternal allele is required for seed viability, loss-of-function *mea*, *fie*, *fis2*, and *prl* mutations cause parent-of-origin effects on seed viability. For example, inheritance of a mutant maternal *mea* allele results in seed abortion, even when the paternal *MEA* allele is wild-type. By contrast, inheritance of a mutant paternal *mea* allele has no detectable effect on seed viability. The parent-of-origin effects of *mea* mutations are due, at least in part, to its being an imprinted gene in the endosperm (Kinoshita et al., 1999; Vielle-Calzada et al., 1999; Luo et al., 2000). Only the maternal *MEA* allele is expressed throughout endosperm development while the paternal allele is silenced (Kinoshita et al., 1999). In this regard, *MEA* is distinct, as the *FIE* and *PRL* genes are not imprinted throughout seed development (Yadegari et al., 2000; Springer and Holding, 2002). It is unknown how *MEA* imprinted gene expression is regulated in the endosperm.

We isolated mutations, named *demeter* (*dme*), causing parent-of-origin effects on seed viability to understand how the female gametophyte controls embryo and endosperm development. We found that seed viability depended solely on the maternal *DME* allele. *DME* encodes a 1729 amino acid polypeptide that contains a

[5]Correspondence: rfischer@uclink4.berkeley.edu

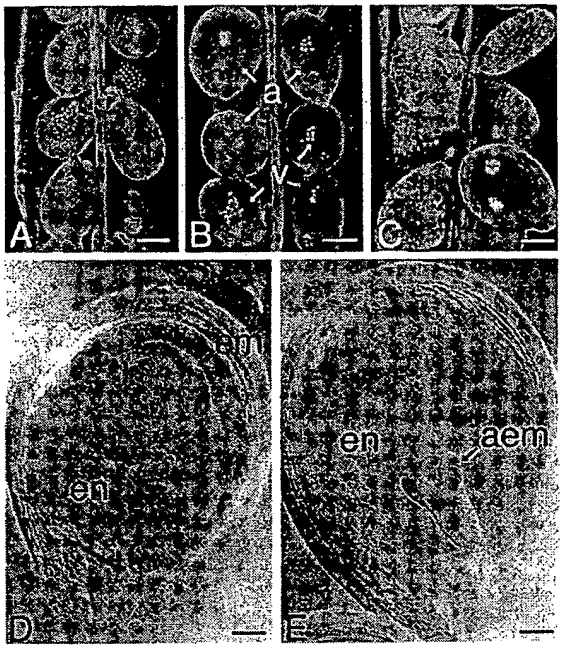

Figure 1. Effect of the *dme-1* Mutation on Embryo and Endosperm Development

(A) Wild-type silique harvested 9 days after pollination.
(B) Heterozygous *DME/dme-1* silique harvested 9 days after pollination.
(C) Homozygous *dme-1* silique harvested 9 days after pollination.
(D) Viable seed obtained from silique in (B).
(E) Aborted seed obtained from silique in (B).
Bars, 0.5 mm (A–C) and 0.1 mm (D and E). a, aborted seed; aem, aborted embryo; em, embryo; en, endosperm; v, viable seed.

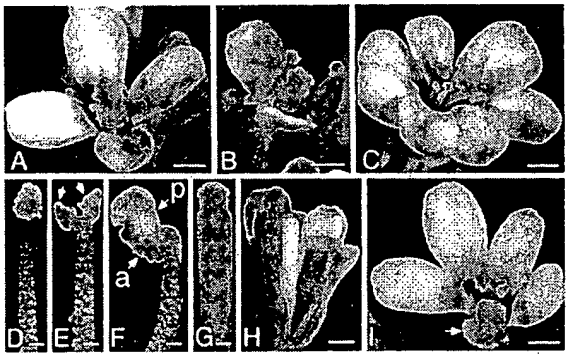

Figure 2. Developmental Abnormalities in Homozygous *dme-1* Mutant Plants

Light micrographs of homozygous *dme-1* and wild-type flowers and floral organs are shown. The percentage of wild-type (n = 105) and *dme-1* (n = 138) flowers with reduced number of petals and sepals was 0% and 3%; increased number of petals and sepals was 2% and 14%; stamens with fused filaments or petal-like anthers was 0% and 9%.
(A) Wild-type flower.
(B) *dme-1* flower with 2 sepals and 2 petals.
(C) *dme-1* flower with 7 sepals and 7 petals.
(D) Wild-type stamen.
(E) Stamens from *dme-1* flower. Arrows point to anthers on a fused filament.
(F) Petal-like stamens from *dme-1* flowers. a, anther-like region; p, petal-like region.
(G) Wild-type gynoecium.
(H) *dme-1* flower with 2 gynoecia.
(I) *dme-1* flower with unfused carpels. Arrow points to large stigma associated with unfused carpels.
Bars in (A–C), (H–I) represent 0.5 mm. Bars in (D–G) represent 0.1 mm.

DNA glycosylase domain and a highly basic region with a nuclear localization signal. *DME*, primarily expressed in the central cell, is required for maternal allele expression of *MEA* in the central cell and the endosperm. When *DME* was ectopically expressed in the endosperm, the expression of the normally silenced paternal *MEA* allele was detected. Ectopic *DME* expression in the leaf activated *MEA* expression and generated nicks in the *MEA* promoter DNA. These results suggest DME is a DNA glycosylase that controls maternal expression of an imprinted maternal gene in the central cell, a process that is essential for subsequent embryo and endosperm viability.

Results

Only the Maternal *DME* Allele Is Necessary for Seed Viability

Whereas seeds from wild-type plants rarely abort (Figure 1A), self-pollinated heterozygous *DME/dme-1* siliques (Figure 1B) have approximately equal numbers of viable and nonviable seeds (552:569, 1:1, $\chi^2 = 0.26$, $P > 0.7$). Likewise, *DME/dme-1* plants pollinated with wild-type pollen-produced siliques with approximately equal numbers (148:147, 1:1, $\chi^2 = 0.003$, $P > 0.95$) of viable seeds with normal embryos (Figure 1D) and nonviable seeds with enlarged endosperm and aborted embryos (Figure 1E). All F_1 viable seeds from this cross were homozygous wild-type *DME*. Thus, inheritance of a *dme-1* mutant allele by the female gametophyte resulted in embryo and endosperm abortion even when a wild-type paternal *DME* allele was inherited. When the reciprocal cross was performed, siliques had no aborted F_1 seed and F_1 plants displayed a 1:1 segregation of the wild-type and *DME/dme-1* genotype (173:142, $\chi^2 = 3:1$ $P > 0.1$). Thus, seed viability depends only upon the presence of a wild-type maternal *DME* allele, and the paternal allele is expendable.

DME Prevents Sporadic Developmental Abnormalities

As described below, *dme-1* is a weak allele, allowing for rare mutant maternal allele transmission and the formation of homozygous *dme-1* plants. Homozygous *dme-1* plants generated normal rosette leaves, an inflorescence, and produced siliques containing nearly all (98%) aborted seeds (Figure 1C). However, we occasionally observed developmental abnormalities in mutant plants. For example, the *Arabidopsis* flower (Figure 2A) is normally composed of four sepals, four petals, six pollen-bearing stamens (Figure 2D), and two ovule-bearing carpels that form the gynoecium (Figure 2G). By contrast, homozygous *dme-1* plants sporadically formed individual flowers with reduced (Figure 2B) or increased (Figure 2C) petal and sepal number. We observed flowers with fused stamen filaments (Figure 2E), petal-like anthers (Figure 2F), two gynoecia (Figure 2H),

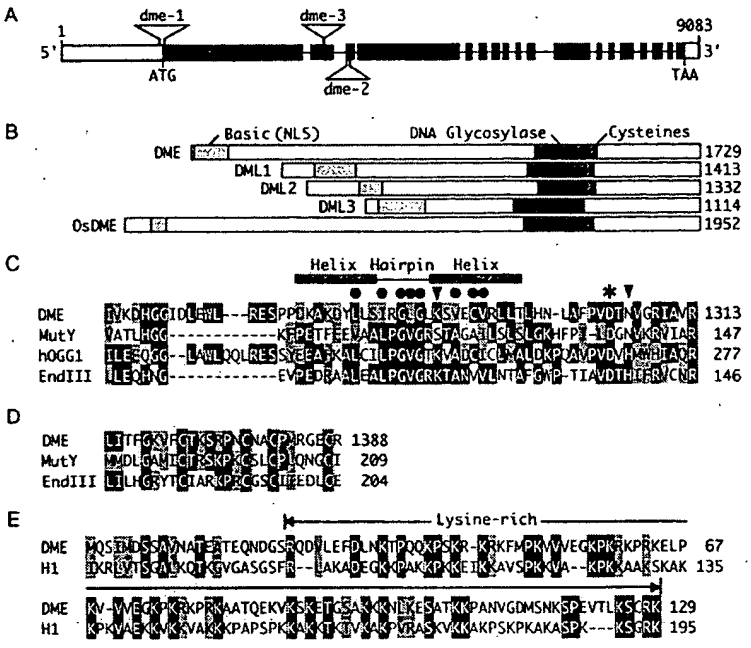

Figure 3. *DME* Gene and Protein Structure

(A) The *DME* gene. Transcription begins at 1 and ends at 9083. *dme-1* T-DNA is associated with a 177 base pair deletion. *dme-2* T-DNA is associated with a 48 base pair deletion. *dme-3* T-DNA is associated with 12 base pairs of unknown origin. Black box, translated exon; white box, untranslated exon; line, intron.

(B) Conservation of DNA glycosylase domain, cysteine cluster, and lysine-rich region in *Arabidopsis DME* gene family and rice (*Oryza sativa*, Os). GenBank Accession numbers for *DME*, *DML1*, *DML2*, *DML3*, and *OsDME* are At5g04560, At2g36490, At3g10010, At4g34060, and BAB16489.1. EST for *OsDME* is AU056357. Compared to DME, percent amino acid sequence identity was 62% over 569 DML1 residues, 55% over 554 DML2 residues, 45% over 519 DML3 residues, and 47% over 1114 OsDME residues. Predicted polypeptide size is shown on the right.

(C) Comparison of the DME helix-hairpin-helix domain to DNA glycosylases. MutY, *E. coli* monofunctional adenine glycosylase; hOGG, human 8-oxoguanine bifunctional DNA glycosylase; and EndIII, *E. coli* bifunctional endonuclease III. Conserved aspartic acid is indicated with an asterisk. Lysine and histidine residues conserved in bifunctional glycosylases are indicated with triangles. Position of helices and hairpin determined with the Jpred (http://jura.ebi.ac.uk:8888/) program.

(D) Comparison of DME to DNA glycosylases with a $(4Fe\text{-}4S)^{2+}$ cluster. Conserved cysteines are in red boxes.

(E) Comparison of DME to *Xenopus laevis* histone H1 (GenBank Accession number P22844).

and improperly fused carpels (Figure 2I). Sporadic abnormalities in leaf and stem morphology were also detected (data not shown). Thus, in *Arabidopsis*, the *DME* gene is required for stable, reproducible patterns of floral and vegetative development. Preliminary efforts to transmit these developmental abnormalities to subsequent generations have not been successful, suggesting that the lesions responsible for the defects are not stable, or that they did not occur in cells that give rise to gametes in *Arabidopsis* (Irish and Sussex, 1992).

Cloning the *DME* Gene

Three mutant T-DNA alleles *dme-1*, *dme-2*, and *dme-3* were obtained (Figure 3A). Each T-DNA cosegregated with the seed abortion phenotype (data not shown). To isolate the *DME* gene, plant DNA flanking the *dme-2* T-DNA was isolated and used to clone the wild-type *DME* gene and cDNA. We rescued the *dme* seed abortion phenotype by introducing a transgene composed of 3.4 kb of 5′-flanking *DME* genomic sequence ligated to a full-length *DME* cDNA (see Experimental Procedures). The *dme-2* and *dme-3* alleles are probably null alleles as their respective T-DNAs inserted into the middle portion of the *DME* gene. The weak *dme-1* allele was created by insertion of the T-DNA at the boundary of the 5′-untranslated region. Low-level transcription from within the *dme-1* T-DNA was detected (data not shown) that would produce a slightly truncated (46 amino acids) DME polypeptide.

DME Encodes a DNA Glycosylase Domain Protein

The *DME* cDNA encodes a 1,729 amino acid protein. A conserved domain search of NCBI databases revealed a 201 amino acid domain (Figure 3B; amino acids 1167–1368) related to the helix-hairpin-helix superfamily of base excision DNA repair proteins (Pfam score of $3e^{-15}$, http://www.sanger.ac.uk/Software/Pfam/). The hallmark of the base excision DNA glycosylase superfamily is a helix-hairpin-helix structural element followed by a glycine/proline-rich loop and a conserved aspartic acid (Krokan et al., 1997; Bruner et al., 2000; Scharer and Jiricny, 2001) all of which are present in DME (Figure 3C). Very highly conserved glycines (G1282 and G1284) are present within the conserved DME hairpin. A conserved aspartic acid (position 1304) present in all DNA glycosylases is distal to the helix-hairpin-helix domain and serves as the electron donor in the base excision reaction. There are two classes of DNA glycosylases. Bifunctional glycosylases couple base excision (DNA glycosylase activity) with 3′-phosphodiester bond breakage (DNA nicking activity). Monofunctional enzymes have DNA glycosylase activity and an AP (apurinic or apyrimidinic) endonuclease is responsible for nicking the DNA (Bruner et al., 2000; Jiricny, 2002). DME is predicted to be a member of the monofunctional class of DNA glycosylases (e.g., MutY and AlkA) where the conserved aspartic acid deprotonates a water molecule, which then displaces the damaged or mismatched base by nucleophilic attack at the anomeric center. Like all monofunctional DNA glycosylases, DME lacks a histidine (position 1306) essential for bifunctional DNA glycosylases (EndoIII and hOGG1) and like monofunctional MutY has asparagine at this position (Figure 3C). DME also has four conserved cysteine residues (Figure 3D) adjacent to the DNA glycosylase domain (Figure 3B) that function to hold a $(4Fe\text{-}4S)^{2+}$ cluster in place. This

cluster, found in many DNA glycosylases, is thought to play a role in DNA binding. Thus, *DME* encodes each of the amino acid residues essential for DNA glycosylase activity.

DME also encodes an amino-terminal 129 amino acids that are highly basic and are related to the carboxy-terminal domain of a *Xenopus laevis* H1 linker histone (31% identity, Figure 3E) that binds linker DNA in chromatin (Kasinsky et al., 2001). It is possible that this basic region of DME facilitates interactions with DNA or chromatin. A bipartite nuclear localization signal is in the basic region (amino acids 43–78).

Three additional *DME-like* (*DML*) genes in the *Arabidopsis* genome, *DML1*, *DML2*, and *DML3*, encode a family of related high molecular weight DNA glycosylase domain proteins (Figure 3B). The structure and organization of the DNA glycosylase domain, the conserved cysteine residues, and the nuclear localization signal are all conserved. Moreover, a highly related gene, *OsDME* (Figure 3B), is expressed in rice suggesting that DME structure and function has been conserved during flowering plant evolution.

Pattern of *DME* RNA Accumulation and Promoter Activity

Measurement of *DME* RNA levels by semiquantitative reverse transcriptase-polymerase chain reaction (RT-PCR) procedures showed that the *DME* RNA is most abundant in immature flower buds (Figure 4A). As flowers mature, *DME* RNA decreases to a low level (Figure 4A). Analysis of dissected flowers revealed that *DME* RNA was abundant in the ovule-bearing carpels and not detectable in pollen-bearing stamens (Figure 4A). *DME* RNA was detected in developing (stage 12) and mature (stage 14) ovules (Figure 4A). However, after fertilization, the level of *DME* RNA dramatically decreased in developing seeds (Figure 4A). These results show that high level *DME* expression is specifically associated with maternal reproductive structures prior to fertilization.

To visualize *DME* gene expression, we transformed *Arabidopsis* plants with two chimeric genes, each with 2.3 kb of 5′-flanking *DME* sequences, 1.9 kb of sequences encoding 148 amino acids of *DME* spanning the putative nuclear localization signal, ligated to the β-*glucuronidase (DME::GUS)* reporter gene (Jefferson et al., 1987) or to the *GREEN FLUORESCENT PROTEIN* (*DME::GFP*) reporter gene (Niwa et al., 1999). Multiple independently isolated lines displayed the same pattern of reporter gene expression. As shown in Figure 4B, GUS staining was detected in the two unfused polar nuclei in the central cell, which will form the diploid nucleus of the central cell, as well as in the synergid cells. The polar nuclei and the synergid cells derive from the third of the haploid mitoses that generate the female gametophyte and are thus closely related in time and space. Later in the development of the mature unfertilized female gametophyte, when the polar nuclei had fused to form the central cell nucleus, GUS staining was primarily detected in the central cell (Figure 4C). No GUS staining was detected in developing (data not shown) or in mature anthers and pollen grains (Figure 4D). Thus, *DME* promoter activity is associated with female gametophyte development, consistent with the expression of the endogenous *DME* gene (Figure 4A). The *DME::GFP* reporter gene showed a similar pattern of expression (Figure 4E). After fertilization, *DME::GFP* promoter activity rapidly decreased. GFP fluorescence was no longer detected prior to the first division of the primary endosperm nucleus (Figure 4F). Nor was GFP fluorescence detected during subsequent endosperm or embryo development (Figures 4G and 4H). These results are consistent with RT-PCR analysis of endogenous *DME* gene expression in prefertilization ovules and developing seed (Figure 4A). These results show *DME* promoter activity is detectable before fertilization in the female gametophyte, primarily in cells leading to the formation of the central cell. Finally, the GFP and GUS used in the construction of reporter transgenes lack any subcellular localization sequences (Niwa et al., 1999). Hence, localization of GUS activity and GFP fluorescence to nuclei (Figures 4B, 4C, and 4E) is due to *DME*-encoded nuclear localization sequences.

DME Regulates *MEA* Expression

Seed viability depends on wild-type maternal *DME*, *MEA*, *FIE*, and *FIS2* alleles that are expressed in the female gametophyte. However, *DME* is distinct in two ways; only *DME* encodes a DNA glycosylase domain protein, and only *DME* is not expressed after fertilization in the embryo and endosperm. One possibility is that the *DME* DNA glycosylase gene controls seed development in a pathway that does not include the *MEA*, *FIE*, and *FIS2* Polycomb group genes. Alternatively, *DME* and the Polycomb group genes may be part of the same pathway. For example, *DME* may be necessary for expression or activity of *MEA*, *FIE*, or *FIS2*. To understand the relationship between the *DME* DNA glycosylase gene and the *MEA*, *FIE*, and *FIS2* Polycomb group genes, we measured their respective RNA levels in wild-type and mutant genetic backgrounds. *MEA*, *FIE*, and *FIS2* RNAs accumulated in developing and mature wild-type flowers. *MEA* RNA was not detected in homozygous *dme-1* flowers, whereas *FIE* and *FIS2* RNA accumulation was not significantly affected by the *dme-1* mutation (Figure 5A), suggesting that *DME* is required for floral *MEA* expression. Moreover, homozygous *mea* plants accumulate normal levels of floral *DME* RNA (Figure 5B), demonstrating that *MEA* is not required for *DME* expression. Thus, *DME* is necessary for *MEA* gene expression prior to fertilization.

To understand the spatial and temporal control of *MEA* gene expression by *DME* during ovule and seed development, we observed the effect of the *dme-1* mutation on transcription of a *MEA::GFP* transgene. A single locus of the *MEA::GFP* transgene consisting of approximately 4.2 kb of *MEA* 5′-flanking sequences ligated to the *GFP* reporter gene was introduced into wild-type *DME/DME* plants. Approximately one-half of prefertilization ovules from transgenic plants hemizygous for the *MEA::GFP* transgene displayed strong fluorescence in the central cell nucleus and cytoplasm prior to fertilization (data not shown), consistent with Mendelian inheritance of the *MEA::GFP* transgene by one-half of the female gametophytes. In a plant hemizygous for the *MEA::GFP* transgene and heterozygous *DME /dme-1*, one-fourth of the prefertilization female gametophytes are predicted to inherit both the wild-type *DME* allele and the *MEA::GFP* transgene, whereas one-fourth will

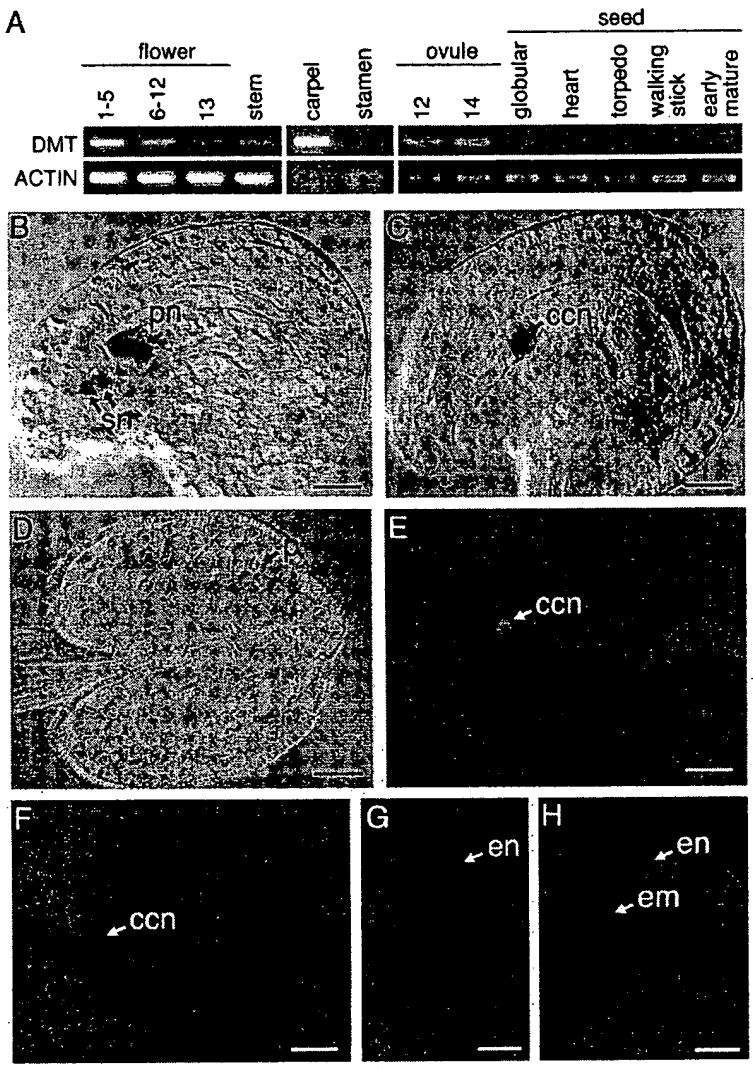

Figure 4. Regulation of *DME* RNA Accumulation and Promoter Activity

(A) Expression of *DME* in wild-type flowers, floral organs, ovules, and seeds. Carpels and stamens were dissected from stage 12 flowers. Ovules were isolated from stage 12 and 14 flowers. Seeds were isolated with embryos at the indicated stages. Upper lane designations refer to tissues used for total RNA isolation. Floral stages are as described (Bowman, 1994). Left-hand side designations refer to the gene specific primers used to amplify RNA by RT-PCR. (B)–(D) are light micrographs of ovules and stamens from transformed plants homozygous for a *DME::GUS* transgene. (E)–(H) are fluorescence micrographs of transformed plants homozygous for a *DME::GFP* transgene. GFP and chlorophyll florescence was converted to green and red, respectively. ccn, central cell nucleus; en, endosperm; em, embryo; p, pollen; pn, polar nucleus; sn, synergid cell nucleus.

(B) Unfertilized ovule prior to fusion of polar nuclei. Bar represents 0.01 mm.

(C) Mature unfertilized ovule after fusion of polar nuclei. Bar represents 0.01 mm.

(D) Mature stamen showing anther and pollen. Bar represents 0.005 mm.

(E) Mature unfertilized ovule after fusion of polar nuclei. Bar represents 0.01 mm.

(F) Seed 8 hr after pollination with wild-type pollen. Bar represents 0.01 mm.

(G) Seed 90 hr after pollination with wild-type pollen. Bar represents 0.3 mm.

(H) Seed at the walking stick stage of embryo development. Bar represents 0.6 mm.

inherit the mutant *dme-1* allele along with the *MEA::GFP* transgene. We found that approximately one-fourth of the prefertilization ovules displayed GFP fluorescence in their central cells (153:396, fluorescent:dark, 1:3, χ^2 = 2.4 P > 0.15), suggesting that female gametophytes inheriting the *dme-1* mutant allele did not express the *MEA::GFP* transgene (Figure 5C). Similar results were obtained in an independently isolated transgenic line where the same *MEA* 5′-flanking sequences were ligated to a *GUS* reporter (81:279, blue central cell:colorless central cell, 1:3, χ^2 = 1.2 P > 0.37). Thus, a wild-type *DME* allele is necessary for transcription of the *MEA::GFP* and *MEA::GUS* transgenes in the central cell of the female gametophyte prior to fertilization.

Normally, the maternal *MEA* allele is expressed after fertilization in the endosperm (Kinoshita et al., 1999) at a time when *DME* is not expressed (Figure 4). We determined the effect of the maternal mutant *dme-1* allele on postfertilization expression of the maternal *MEA::GFP* transgene to see if expression of *DME* in the central cell of the female gametophyte prior to fertilization was necessary for postfertilization maternal *MEA::GFP* allele transcription during endosperm development. Flowers hemizygous for the *MEA::GFP* transgene and heterozygous *DME/dme-1* were pollinated with wild-type nontransgenic pollen. We observed approximately one-fourth seeds with GFP fluorescence (123:332, fluorescent:dark, 1:3, χ^2 = 0.95, P > 0.4) in endosperm cells at 24 hr (Figure 5D) and 90 hr (Figures 5E and 5F) after pollination. This result suggests that female gametophytes that inherited the *dme-1* mutant allele did not express the *MEA::GFP* transgene in the endosperm after fertilization. Thus, the maternal wild-type *DME* allele, expressed prior to fertilization in the female gametophyte, is necessary for transcription of the maternal *MEA::GFP* transgene after fertilization during endosperm development. These results are consistent with the model that *DME* controls maternal *MEA* allele expression in the endosperm, and that the parent-of-origin effects of *dme* mutations on seed viability are due, at least in part, to a failure to express the maternal *MEA* allele during female gametophyte and early seed development.

To determine if *DME* is sufficient for *MEA* gene expression, we generated *CaMV::DME* transgenic plants where transcription of *DME* is under the control of the cauli-

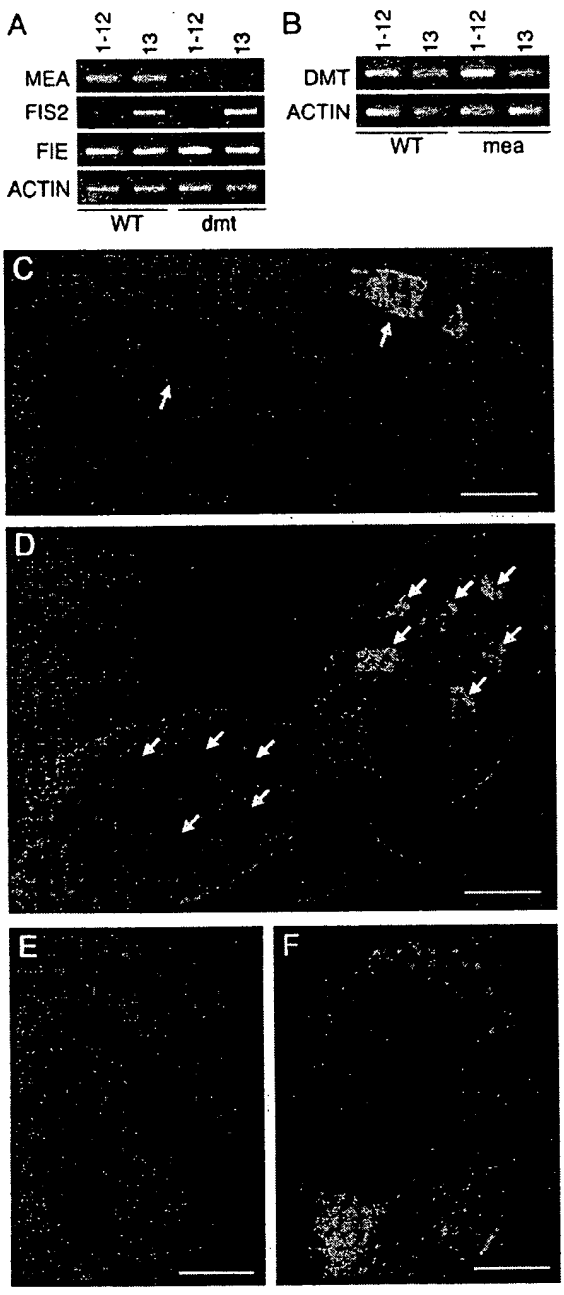

Figure 5. *DME* Controls *MEA* RNA Accumulation and Promoter Activity

For (A) and (B), RNA was isolated from developing floral buds (stage 1-12) and open flowers (stage 13). Floral stages are as described (Bowman, 1994). Left-hand side designations refer to the gene specific primers used to amplify RNA by RT-PCR. Lower lane designations specify the genotype; WT, wild-type; dme, homozygous third generation *dme-1*; mea, homozygous *mea-3*.

(A) *MEA* RNA does not accumulate in *dme-1* flower buds.

(B) *DME* RNA accumulation is the same in wild-type and *mea-3* flower buds. For (C)–(F), fluorescence micrographs were taken from *DME / dme-1* plants hemizygous for a *MEA::GFP* transgene. GFP and chlorophyll fluorescence was converted to green and red, respectively.

(C) Unfertilized ovules from stage 12 flowers. Arrows point to central cell nuclei. Bar represents 0.04 mm.

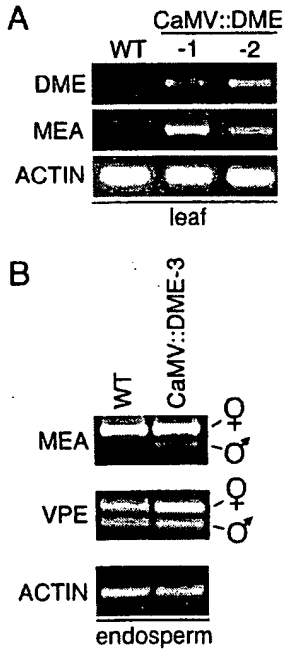

Figure 6. Ectopic *DME* Expression Activates *MEA* Gene Transcription

CaMV::DME-1, CaMV::DME-2, and CaMV::DME-3 represent three independently isolated transgenic lines. WT, wild-type; leaf, cauline leaf.

(A) *DME* is sufficient for *MEA* expression in the leaf.

(B) A *CaMV::DME* transgene activates paternal *MEA* allele gene expression in the endosperm. Endosperm and embryos were dissected from F1 seeds obtained 7 days after wild-type (Columbia *gl* ecotype) plants or *CaMV::DME* (Columbia *gl* ecotype) were pollinated with RLD ecotype pollen. Control biallelic expression of the *VACUOLAR PROCESSING ENZYME* (*VPE*) gene is shown. For the actin control, no attempt was made to distinguish between maternal and paternal alleles.

flower mosaic virus (*CaMV*) promoter (Rogers et al., 1987). Whereas *DME* and *MEA* gene expression were not detectable in wild-type leaf, both *DME* and *MEA* RNAs were present in leaves from independently isolated *CaMV::DME* transgenic lines (Figure 6A). Thus, *DME* is sufficient to activate *MEA* gene expression in the leaf.

The mechanism for paternal *MEA* allele silencing in the endosperm is not known. It is possible that restriction of *DME* expression to the female gametophyte prevents activation of paternal *MEA* allele transcription in the endosperm. To test this hypothesis, we used wild-type pollen (RLD ecotype) to pollinate control wild-type (Columbia *gl* ecotype) plants and *CaMV::DME* transgenic (Columbia *gl* ecotype) plants (Figure 6B). We isolated and dissected F1 seeds, isolated RNA from the endosperm (plus maternal seed coat), and measured the level of maternal and paternal *MEA* RNA using ecotype-spe-

(D) Seeds 24 hr after pollination with wild-type pollen. Arrows point to endosperm nuclear-cytoplasmic domains. Bar represents 0.08 mm.

(E and F) Seeds 90 hr after pollination with wild-type pollen. Bar represents 0.2 mm.

cific restriction polymorphisms (Kinoshita et al., 1999). Whereas only the maternal *MEA* allele was detected in control wild-type endosperm, both maternal and paternal *MEA* expression was detected in the *CaMV::DME* endosperm (Figure 6B). The paternal *MEA* allele in *CaMV::DME* endosperm was expressed at a lower level compared to the paternal allele of a control nonimprinted gene (Figure 6B). The lower expression may reflect inefficient endosperm expression of the *CaMV::DME* transgene. Or, additional mechanisms may control *MEA* expression in the endosperm. However, these results are consistent with the hypothesis that the restricted pattern of *DME* gene expression is responsible, at least in part, for the silencing of the paternal *MEA* allele in wild-type endosperm.

DME Expression Results in Nicks in the *MEA* Promoter

The amino acid sequence of DME (Figure 3C) suggests it is a monofunctional DNA glycosylase that generates an abasic site by carrying out a base excision reaction. The next step in DNA repair is single-stranded DNA cleavage (nicking) 5′ to the abasic site by an AP endonuclease (Bruner et al., 2000; Jiricny, 2002). If DME acts directly on *MEA::GFP* to regulate its expression (Figure 5), the abasic residues should generate sites for AP endonuclease nicking in the 4.2 kb *MEA* promoter region. To test this hypothesis, we devised a sensitive PCR-based procedure to localize nicks produced in vivo. As shown in Figure 7A, to identify nicks on the sense-strand of the *MEA* promoter, a *MEA*-specific primer (MEA sense-R1) was used to initiate first-strand DNA synthesis. Nicks would cause termination of synthesis at specific sites; if there were no nicks, termination would occur randomly. DNA from the first-strand synthesis reaction was then purified and tailed with terminal deoxynucleotidyl transferase and dCTP. A linker with G residues at its 3′ end (linkerGGG) and a second nested *MEA*-specific primer (MEA sense-R2) were used to amplify DNAs by PCR. DNA products from the first PCR amplification were diluted 100-fold into multiple aliquots, and the linker and a third nested MEA-specific primer (MEA sense-R3) were used for a second PCR amplification. PCR products were then analyzed by agarose gel electrophoresis.

It is not possible to isolate DNA and determine the pattern of nicks in the *MEA* promoter in wild-type and *dme* mutant central cells because they are embedded within the female gametophyte and ovule. Because ectopic expression of a *CaMV::DME* transgene induces *MEA* expression in leaves (Figure 6A), we compared the pattern of nicks in the *MEA* promoter isolated from readily accessible wild-type and *CaMV::DME* leaves to test the hypothesis that DME directly regulates *MEA*. Specific DNA bands were detected when template DNAs were isolated from *CaMV::DME* leaves (Figure 7B). Repetition of PCR reactions produced different size DNA bands and DNA sequence analysis verified that these DNA bands were derived from the *MEA* promoter. The fact that different size bands were synthesized in multiple PCR reactions indicates there is a stochastic element to PCR sampling of the *CaMV::DME*-induced nicks, suggesting the molecules with nicks at different

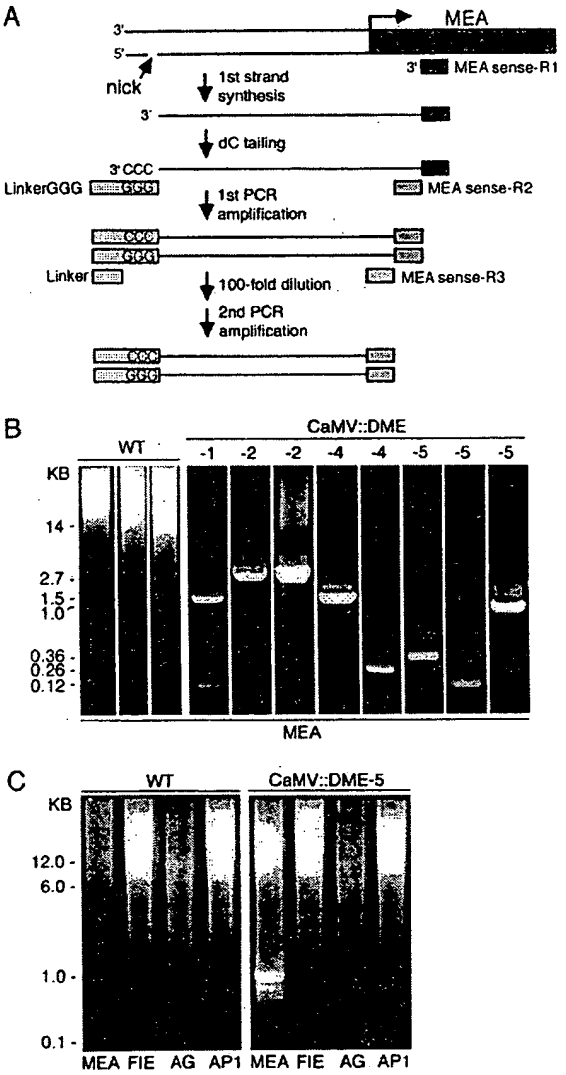

Figure 7. Ectopic *DME* Expression Generates Nicks in the *MEA* Promoter

(A) PCR-based strategy for detecting nicks in the sense-strand of the *MEA* promoter.

(B) PCR products from the sense-strand of the *MEA* promoter. PCR products obtained with DNA templates isolated from leaves from wild-type (WT) and CaMV::DME-1, CaMV::DME-2, CaMV::DME-4, and CaMV::DME-5 independent transgenic lines. Amplifications of multiple aliquots from the first PCR amplification of wild-type and *CaMV::DME* templates are shown as described in the text.

(C) Comparison of PCR products from the sense-strand of the *MEA*, *FIE*, *AG*, and *AP1* 5′-flanking regions using wild-type and *CaMV::DME-5* DNA templates.

sites in the *MEA* promoter were present in very low concentration (Cavrois et al., 1995; Taberlet et al., 1996). By contrast, no discrete DNA bands were detected when wild-type template DNA was isolated from leaves which do not express *MEA* (Figure 7B). The diverse range of high molecular weight PCR products suggested that during the first-strand synthesis reaction the DNA polymerase terminated randomly. The same result was obtained when the entire procedure (i.e., first-strand synthesis, two PCR amplifications) was repeated three

times with wild-type DNA template with multiple aliquots used for the second PCR amplification (data not shown). In control PCR reactions using *MEA* sense-R3 and a primer located in the *MEA* promoter, PCR products were obtained with equal efficiency with wild-type and *CaMV::DME-1* DNA templates (data not shown). Finally, specific PCR products were not detected from the sense-strand of wild-type or *CaMV::DME* template DNA within the 5′-flanking regions of the control *FIE* gene and the floral homeotic (Meyerowitz and Clark, 1994) *AGAMOUS* (*AG*) or *APETALA1* (*AP1*) genes (Figure 7C). Thus, nicking, a property of base excision DNA repair, was detected in the sense-strand of *CaMV::DME* lines and not in the wild-type sense-strand within 14 kb of the start of *MEA* transcription.

Discussion

We isolated mutations in the *Arabidopsis DME* gene to understand how the female gametophyte influences embryo and endosperm development. We demonstrated that seed viability depends solely on the maternal allele and found that DME is a large protein with DNA glycosylase and nuclear localization domains. Transcribed primarily in the central cell, *DME* is necessary for activation of imprinted *MEA* expression in the central cell and the endosperm. Ectopic expression of *DME* results in expression of the normally silenced paternal *MEA* allele. When *DME* was expressed in the leaf, we observed *MEA* expression and in vivo nicking of the *MEA* promoter. We conclude from these results that DME is a DNA glycosylase that mediates imprinting in the central cell and that this process is required for seed viability.

A Model for the Control of *MEA* Gene Imprinting in the Endosperm

Our analysis of DME suggests a mechanism for the regulation of imprinted (maternally expressed, paternally silenced) genes in the endosperm. The reason that the maternal *MEA* allele, and not the paternal *MEA* allele, is expressed in the endosperm is because only the maternal *MEA* allele is accessible to DME in the central cell of the female gametophyte before fertilization. This model is based in part upon the highly restricted pattern of *DME* expression. *DME* is primarily expressed in the central cell of the female gametophyte, and its transcription is turned off soon after fertilization (Figure 4). *DME* RNA and promoter activity was not detected in the male gametophyte producing stamens (Figure 4). Thus, only the maternal *MEA* allele and not the paternal *MEA* allele, is exposed to DME activity. The model is also based on experiments showing *DME* regulates *MEA* gene expression. *MEA* RNA and promoter activity was not detected in *dme* mutants (Figure 5), whereas ectopic *DME* expression in the leaf and endosperm activated *MEA* and paternal *MEA* allele expression, respectively (Figure 6). Finally, we found that ectopic expression of *DME* in leaf caused single-stranded breaks in the *MEA* promoter within 2 kb of the start of *MEA* gene transcription (Figure 7). We propose that DME might mark the maternal *MEA* allele in the female gametophyte, allowing sustained maternal *MEA* allele expression to occur in the endosperm after fertilization. The paternal allele is not marked and therefore not expressed during endosperm development.

A Role for DNA Glycosylases in Controlling Gene Imprinting and Seed Viability

DNA glycosylases represent a diverse array of small (200–300 amino acids), monomeric, structurally related DNA repair proteins that are very highly conserved in evolution (Krokan et al., 1997; Scharer and Jiricny, 2001). These proteins excise mismatched or altered bases (e.g., oxidized, deaminated, alkylated, and methylated) by cleaving the N-glycosidic bond between the base and the sugar-phosphate backbone of the DNA. DNA glycosylases represented by DME, *E. coli* MutY, endonuclease III, human 8-oxoguanine DNA glycosylase, and MBD4 have a conserved helix-hairpin-helix domain. Excision by monofunctional DNA glycosylases results in an abasic site that is mutagenic and must be removed. Single-strand cleavage 5′ to the abasic site by an AP endonuclease generates a 3′-hydroxyl used by a specialized DNA repair polymerase that inserts a single nucleotide and removes the abasic sugar-phosphate (Jiricny, 2002). A DNA ligase seals the nick to complete the repair process. It has been proposed that highly mutagenic oxidized, deaminated, or alkylated bases are associated with pathophysiologic processes such as cancer and aging in mammals. However, mice with mutations in DNA glycosylase genes do not display overt developmental abnormalities (Scharer and Jiricny, 2001). Thus, the role of DNA glycosylases in the control of development or tumor suppression is unknown.

The *Arabidopsis* genome encodes multiple small helix-hairpin-helix DNA glycosylases, some of which have been shown to function in DNA repair (Garcia-Ortiz et al., 2001). However, the DME protein is unique from other DNA glycosylases in several regards. First, the DME-predicted polypeptide is much larger than typical DNA glycosylases that function in DNA repair (Figure 3). Moreover, it has a highly basic region related to histone H1 (Figure 3). This basic region might enhance the ability of DME to interact with DNA or with other chromatin proteins. These unique molecular properties, coupled with the phenotypes of mutant *dme* plants (Figures 1 and 2), and its role in regulating *MEA* gene expression (Figure 5), suggest that any base excision activity of DME is probably not involved solely with DNA repair.

How might DME work to regulate the expression of *MEA*? One possibility is that DME modifies chromatin structure by excising 5-methylcytosine. Genomic imprinting in mammals reflects modifications in DNA methylation (Reik and Walter, 2001) and the sporadic developmental abnormalities observed in *dme* homozygous mutant plants (Figure 2) are reminiscent of genome methylation defective mutants in *Arabidopsis* (Kakutani et al., 1996). Other related DNA glycosylases have been shown to excise 5-methylcytosine from the genome (Jost et al., 2001). However, using bisulfite sequencing methods we have been unable to detect 5-methylcytosine residues in a 2 kb region sufficient for regulation of *MEA* gene expression by DME in seed or leaf from wild-type or mutant *dme* genetic backgrounds (see Experimental Procedures for details).

DME is predicted to be a monofunctional DNA glycosylase (Figure 3). Following base excision, the DNA is nicked 5′ to the abasic site by an AP endonuclease. Consistent with this prediction, we observed nicks on the sense-strand of the *MEA* promoter in multiple independently isolated *CaMV::DME* transgenic lines (Figure 7). The nicked DNA molecules may be very rare because only a fraction of the population of *MEA* genes in *CaMV::DME* leaves may be transcribed at any given time. Also, it is possible that the DME-induced nicks are quickly repaired, thereby lowering their concentration. These results strongly support the hypothesis that DME carries out a base excision reaction with subsequent nicking in the *MEA* promoter by an AP endonuclease, although it is formally possible that the nicking we observed is an indirect effect of the activation of *MEA* gene transcription.

The AP endonuclease-mediated DNA nicking activity that follows DME base excision might catalyze nucleosome sliding, as has been demonstrated for nicks in linker DNA in vitro (Langst and Becker, 2001). The H1 linker histone-related region that is located at the amino terminus of DME might facilitate this process. Nucleosome sliding may allow transcription factors to activate *MEA* gene transcription by RNA polymerase. Once the nucleosome structure has been altered on the maternal *MEA* allele, it may be perpetuated after fertilization, allowing for continued maternal *MEA* allele transcription (Figure 5) in the absence of *DME* expression (Figure 4) in the endosperm.

It is unknown how DME is directed to sites in the *MEA* promoter. One possibility is that DME acts at modified base pairs. Alternatively, it has been shown that a mammalian thymine DNA glycosylase acts in a protein complex to remodel chromatin (Tini et al., 2002). Thus, DME might function in a protein complex that could provide promoter specificity for base excision/DNA nicking of the maternal genome. Finally, it is important to consider that nicks at specific sites in DNA might constitute an essential feature in the control of chromatin structure and gene expression.

Experimental Procedures

Plant Materials and Microscopy

Methods for growing plants, fixing tissues, photography, GUS activity localization, and GFP fluorescence microscopy are as previously described (Yadegari et al., 2000).

Mutagenesis

dme-1 and *dme-2* alleles were obtained by screening 5000 T1 plants (Columbia *gl*) mutagenized with activation T-DNA vector, pSKI015 for siliques with 50% seed abortion. The *dme-3* allele (Wassilewskija) was from the *Arabidopsis* Knockout Facility where mutagenesis was with a nonactivation T-DNA vector, pD991. Mutant lines were crossed to wild-type (Landsberg *er*) six times to remove additional mutations.

Molecular Cloning of *DME*

DNA from *DME/dme-2* plants was used to isolate *DME* sequences flanking the left and right border T-DNA regions. *DME* genomic clones were obtained from a wild-type (Columbia *gl*) genomic library. A cDNA library of floral mRNAs was used to obtain a cDNA clone with a 3′-poly A tail plus 2.7 kb of *DME* sequences (4169–6871). Using reagents and 5′- and 3′-RACE procedures from Clonetech and Gibco Bethesda Research, overlapping cDNA clones (1–2921 and 2279–4973) extending through the *DME* 5′-untranslated region were obtained. Using restriction enzyme sites, clones were ligated into a full-length *DME* cDNA (1–6871). To complement the *dme* mutation, *DME* 5′-flanking sequences (3424 base pairs) were ligated to the full-length *DME* cDNA and inserted into pBI-GFP(S65T). A single locus transgenic T_1 plant was crossed with *DME/dme-1* pollen generating F_1 progeny hemizygous for the transgene and *DME/dme-1*. In self-pollinated F_1 plants, a 3:1 ratio of viable to aborted F_2 seeds (329:121, 3:1, $\chi^2 = 0.86$, $P > 0.43$) was observed.

Analysis of RNA Accumulation

Total RNA was isolated and reverse transcriptase reactions and PCR reactions were carried out (Yadegari et al., 2000). Primers for amplifying *DME* were *cDNA-5* (CAGAAGTGTGGAGGGAAAGCGTCT GGC) and *SKEN-5* (GCAATGCGTTTGCTTTCTTCCAGTCATCT), for *FIE* were *cer1ns8517n* (CTGTAATCAGGCAAACAGCC) and *cer8191n* (TCAAGGTCTCAGGGAGTAGC), and for *FIS2* were *F2-f5/6* (TCAAG GTCTCAGGGAGTAG) and *F2-r7/8* (CTCTCTAGCCTTGTACCGCTT TGCATATAACTG). Primers for *MEA* in Figure 5A and Figure 6A were as described (Kiyosue et al., 1999). For measuring maternal and paternal *MEA* RNA accumulation, RNA was prepared and RT-PCR reactions were carried out as described (Kinoshita et al., 1999). All primer pairs spanned intron sequences so that amplification of RNA could be distinguished from amplification of any contaminating DNA.

Generation of Plants with Reporter Transgenes

Using BamHI and EcoRI, the sGFP(S65T) (Niwa et al., 1999) coding sequence was excised from CaMV35S-sGFP(S65T)-nos3′ and inserted into pBI101.1 (Jefferson et al., 1987), replacing β-glucuronidase-nos3′ to create pBI-GFP(S65T). A portion of the *DME* gene (2282 bp of 5′-flanking sequences plus 1922 bp of the first exon) was inserted into XbaI/BamHI sites of T-DNA pBI-GFP(S65T), introduced into *Agrobacterium*, and five transgenic lines (Columbia *gl*) obtained. For *DME::GUS*, the same sequences were inserted into pBI101.1 upstream of β-glucuronidase-nopaline synthase (Jefferson et al., 1987). For *CaMV::DME*, a full-length *DME* cDNA was inserted downstream of the *CaMV* promoter of vector pMD1. To construct *MEA::GFP* and *MEA::GUS* transgenes, clone 6–22 (Kiyosue et al., 1999) was used as template in a PCR reaction to amplify 4.2 kb of *MEA* 5′ sequences with primers *MEA*4105SaI (5′TATTGTCGACCGT CCTGTCAAACCCGTCCCGT3′) and *MEA*8323Xba (5′ATATTCTAGA CTTTTTTTCTCGTCTTCTCTGATGTTGGT3′). The PCR product was digested with SalI and XbaI and inserted into pBI-GFP(S65T) and pBI101.2 creating the *MEA::GFP* and *MEA::GUS* transgenes with 4193 bp *MEA* 5′-flanking sequences and 26 bp 5′-untranslated sequences ligated to *GFP* and *GUS* reporter genes, respectively.

Bisulfite Sequencing

DNA was isolated from Landsberg *er* leaves, wild-type seeds, and homozygous *dme-1* seeds. Seeds were harvested 2–3 days postpollination. DNAs were treated with bisulfite and PCR products from −2080 to +1 were purified, cloned, and 15–20 clones sequenced (Jacobsen et al., 2000). The 2 kb region represents the overlap of a 7 kb transgene with approximately 2 kb of 5′-flanking sequences that was imprinted like the endogenous *MEA* gene (data not shown), and the *MEA::GFP* transgene (Figure 5).

Detection of DNA Nicks

First-strand DNA synthesis was with 0.5 ug genomic DNA template, *MEA* sense-R1 (5′-CTTCTCCATTAACCACTCGCCTCTT-3′) and 400 uM dNTPs using Ex Taq DNA polymerase from Takara at 95°C 5 min, 52°C 5 min, and 72°C 40 min. Single-stranded DNA was purified (Qiagen PCR Kit) and tailed with 200 uM dCTP and terminal deoxynucleotidyl transferase (TdT; Invitrogen). DNA was treated at 95°C for 3 min, chilled, 1 ul of TdT (10 units) added, and incubated at 37°C for 10 min. TdT was inactivated at 65°C for 10 min. The first PCR amplification was with Invitrogen Abridged Anchor primer (5′-GGCCACGCGTCGACTAGTACGGGIIGGGIIGGGIIG-3′) and *MEA* sense-R2 (5′-CTCGTCTTCTCTGATGTT-3′). After 95°C for 5 min, 35 PCR cycles were carried out (94°C 30 s, 55°C 30 s, 72°C 4 min). PCR products were diluted 100-fold and amplified again with Invitrogen abridged universal amplification primer (5′-GGCCACGCGTCGAC TAGTAC) and *MEA* sense-R3 (5′-GGTGAAAAGGATAATGCAAAG

GGT-3'). *FIE* sense primers, R1 (TGGAGTCAAAGACCCAACTATT GACTCGT), R2 (TCTCTCTCTGTCTGACTCTCGCACAC), R3 (TCG ATTAGACACAGATTCACAGGT); *AG* sense primers, R1 (AGGTA AGGTTGTGCTGGTG), R2 (CATCCATATAGTGTCTTGTC), R3 (CTG GTGTTTCTTTTCAGTAC); and *AP1* sense primers, R1 (CCAAG AATCAGTGGAGTATTCG), R2 (GACCAGCTCTTCTTTTCG), R3 (GAA GAGCTCAGACTTTGGT). For *AG*, the PCR annealing temperatures was 52°C.

Acknowledgments

We thank Nickolai Alexandrov, Tatiana Tatarinova, and Jack Okamuro for insights into DME protein structure. We thank Roger Pennell for critically reading this manuscript and helpful discussions. This research was supported by USDA (2000-01539) and Ceres, Inc. (B970602) grants to R.L.F., a NIH (GM60398) grant to S.E.J., and a NSF Graduate Research Fellowship to M.G.

Received: May 13, 2002
Revised: June 5, 2002

References

Birve, A., Sengupta, A.K., Beuchle, D., Larsson, J., Kennison, J.A., Rasmuson-Lestander, A., and Muller, J. (2001). *Su(z)12*, a novel *Drosophila* Polycomb group gene that is conserved in vertebrates and plants. Development *128*, 3371–3379.

Bowman, J.L. (1994). Flowers: introduction. In Arabidopsis: An Atlas of Morphology and Development, J.L. Bowman, ed. (New York: Springer-Verlag), pp. 135–145.

Brown, R.C., Lemmon, B.E., Nguyen, H., and Olsen, O.-A. (1999). Development of endosperm in *Arabidopsis thaliana*. Sex Plant Reprod *12*, 32–42.

Bruner, S.D., Norman, D.P., and Verdine, G.L. (2000). Structural basis for recognition and repair of the endogenous mutagen 8-oxoguanine in DNA. Nature *403*, 859–866.

Cavrois, M., Wain-Hobson, S., and Wattel, E. (1995). Stochastic events in the amplification of HTLV-I integration sites by linker-mediated PCR. Res. Virol. *146*, 179–184.

Drews, G.N., Lee, D., and Christensen, C.A. (1998). Genetic analysis of female gametophyte development and function. Plant Cell *10*, 5–17.

Francis, N.J., and Kingston, R.E. (2001). Mechanisms of transcriptional memory. Nat. Rev. Mol. Cell. Biol. *2*, 409–421.

Garcia-Ortiz, M.-V., Ariza, R.R., and Roldan-Arjona, T. (2001). An OGG1 orthologue encoding a functional 8-oxoguanine DNA glycosylase/lyase in *Arabidopsis thaliana*. Plant Mol. Biol. *47*, 795–804.

Grossniklaus, U., Vielle-Calzada, J.-P., Hoeppner, M.A., and Gagliano, W.B. (1998). Maternal control of embryogenesis by *MEDEA*, a polycomb-group gene in *Arabidopsis*. Science *280*, 446–450.

Irish, V.F., and Sussex, I.M. (1992). A fate map of the *Arabidopsis* embryonic shoot apical meristem. Devel *115*, 745–753.

Jacobsen, S.E., Sakai, H., Finnegan, E.J., Cao, X., and Meyerowitz, E.M. (2000). Ectopic hypermethylation of flower-specific genes in *Arabidopsis*. Curr. Biol. *10*, 179–186.

Jefferson, R.A., Kavanagh, T.A., and Bevan, M.V. (1987). Gus fusions: β-glucuronidase as a sensitive and versatile gene fusion marker in higher plants. EMBO J. *6*, 3901–3907.

Jiricny, J. (2002). An APE that proofreads. Nature *415*, 593–594.

Jost, J.-P., Oakeley, E.J., Zhu, B., Benjamin, D., Thiry, S., Siegmann, M., and Jost, Y.-C. (2001). 5-methylcytosine DNA glycosylase participates in the genome-wide loss of DNA methylation occurring during mouse myoblast differentiation. Nucleic Acids Res *29*, 4452–4461.

Kakutani, T., Jeddeloh, J.A., Flowers, S.K., Munakata, K., and Richards, E.J. (1996). Developmental abnormalities and epimutations associated with DNA hypomethylation mutations. Proc. Natl. Acad. Sci. USA *93*, 12406–12411.

Kasinsky, H.E., Lewis, J.D., Dacks, J.B., and Ausio, J. (2001). Origin of H1 linker histones. FASEB J. *15*, 34–42.

Kinoshita, T., Yadegari, R., Harada, J.J., Goldberg, R.B., and Fischer, R.L. (1999). Imprinting of the *MEDEA* polycomb gene in the *Arabidopsis* endosperm. Plant Cell *11*, 1945–1952.

Kiyosue, T., Ohad, N., Yadegari, R., Hannon, M., Dinneny, J., Wells, D., Katz, A., Margossian, L., Harada, J., Goldberg, R.B., and Fischer, R.L. (1999). Control of fertilization-independent endosperm development by the *MEDEA* polycomb gene in *Arabidopsis*. Proc. Natl. Acad. Sci. USA *96*, 4186–4191.

Krokan, H.E., Standal, R., and Slupphaug, G. (1997). DNA glycosylases in the base excision repair of DNA. Biochem. J. *325*, 1–16.

Langst, G., and Becker, B. (2001). ISWI induces nucleosome sliding on nicked DNA. Mol. Cell *8*, 1085–1092.

Luo, M., Bilodeau, P., Koltunow, A., Dennis, E.S., Peacock, W.J., and Chaudhury, A.M. (1999). Genes controlling fertilization-independent seed development in *Arabidopsis thaliana*. Proc. Natl. Acad. Sci. USA *96*, 296–301.

Luo, M., Bilodeau, P., Dennis, E.S., Peacock, W.J., and Chaudhury, A. (2000). Expression and parent-of-origin effects for *FIS2*, *MEA*, and *FIE* in the endosperm and embryo of developing *Arabidopsis* seeds. Proc. Natl. Acad. Sci. USA *97*, 10637–10642.

Meyerowitz, E.M., and Clark, S.E. (1994). *Arabidopsis* flower development. In Arabidopsis, E.M. Meyerowitz and C. Somerville, eds. (Cold Spring Harbor, NY: Cold Spring Harbor Laboratory Press), pp. 435–466.

Niwa, Y., Hirano, T., Yoshimoto, K., Shimizu, M., and Kobayashi, H. (1999). Non-invasive quantitative detection and applications of non-toxic S65T-type green fluorescent protein in living plants. Plant J. *18*, 455–463.

Ohad, N., Yadegari, R., Margossian, L., Hannon, M., Michaeli, D., Harada, J.J., Goldberg, R.B., and Fischer, R.L. (1999). Mutations in *FIE*, a WD polycomb group gene, allow endosperm development without fertilization. Plant Cell *11*, 407–415.

Reik, W., and Walter, J. (2001). Genomic imprinting: parental influence on the genome. Nat. Rev. Genet *2*, 21–32.

Rogers, S.G., Klee, H.J., Horsch, R.B., and Fraley, R.T. (1987). Improved vector for plant transformation: expression cassette vectors and new selectable markers. Methods Enzymol *153*, 253–277.

Scharer, O.D., and Jiricny, J. (2001). Recent progress in the biology, chemistry and structural biology of DNA glycosylases. Bioessays *23*, 270–281.

Springer, P., and Holding, D.R. (2002). The Arabidopsis gene PROLIFERA is required for proper cytokinesis during seed development. Planta *214*, 373–382.

Taberlet, P., Griffin, S., Goossens, B., Questiau, S., Manceau, V., Escaravage, N., Waits, L.P., and Bouvet, J. (1996). Reliable genotyping of samples with very low DNA quantities using PCR. Nucleic Acids Res *24*, 3189–3194.

Tini, M., Benecke, A., Um, S.-J., Torchia, J., Evans, R.M., and Chambon, P. (2002). Association of CBP/p300 acetylase and thymine DNA glycosylase links DNA repair and transcription. Mol. Cell *9*, 265–277.

Vielle-Calzada, J.-P., Thomas, J., Spillane, C., Coluccio, A., Hoeppner, M.A., and Grossniklaus, U. (1999). Maintenance of genomic imprinting at the *Arabidopsis medea* locus requires zygotic DDM1 activity. Genes Dev *13*, 2971–2982.

Vinkenoog, R., Spielman, M., Adams, S., Fischer, R.L., Dickinson, H.G., and Scott, R.J. (2000). Hypomethylation promotes autonomous endosperm development and rescues postfertilization lethality in *fie* mutants. Plant Cell *12*, 2271–2282.

Yadegari, R., Kinoshita, T., Lotan, O., Cohen, G., Katz, A., Choi, Y., Katz, A., Nakashima, K., Harada, J.J., Goldberg, R.B., et al. (2000). Mutations in the FIE and MEA genes that encode interacting polycomb proteins cause parent-of-origin effects on seed development by distinct mechanisms. Plant Cell *12*, 2367–2381.

Accession Numbers

The *DME* cDNA sequence has been deposited in GenBank as accession number AF521596.

Development 116, 397-403 (1992)
Printed in Great Britain © The Company of Biologists Limited 1992

Characterisation of three shoot apical meristem mutants of *Arabidopsis thaliana*

H. M. OTTOLINE LEYSER* and IAN J. FURNER

Department of Genetics, University of Cambridge, Downing Street, Cambridge, CB2 3EH, UK

*To whom correspondence should be addressed
Current address: Jordan Hall 142, Department of Biology, Indiana University, Bloomington, Indiana 47405, USA

Summary

The shoot apical meristem of dicotyledonous plants is highly regulated both structurally and functionally, but little is known about the mechanisms involved in this regulation. Here we describe the genetic and phenotypic characterisation of recessive mutations at three loci of *Arabidopsis thaliana* in which meristem structure and function are disrupted. The loci are Clavata1 (Clv1), Fasciata1 (Fas1) and Fasciata2 (Fas2). Plants mutant at these loci are fasciated having broad, flat stems and disrupted phyllotaxy. In all cases, the fasciations are associated with shoot apical meristem enlargement and altered floral development. While all the mutants share some phenotypic features they can be divided into two classes. The pleiotropic *fas1* and *fas2* mutants are unable to initiate wild-type organs, show major alterations in meristem structure and have reduced root growth. In contrast, *clv1* mutant plants show near wild-type organ phenotypes, more subtle changes in shoot apical meristem structure and wild-type root growth.

Key words: fasciation, meristem, *Arabidopsis*, Clavata1, Fasciata1, Fasciata2.

Introduction

The shoot apical meristem of higher plants is laid down during embryogenesis and gives rise to all the aerial parts of the plant. The meristem is usually a dome of cells consisting of a peripheral zone (PZ) of rapidly dividing cells in which leaf initiation occurs, and a central zone (CZ) of more slowly dividing cells which replenish the PZ. Around the base of the peripheral zone, leaves are initiated in a specific pattern (phyllotaxy). In dicotyledonous plants, superimposed on this zonation, there are three generative layers of cells. The layers are maintained by the pattern of cell division in the meristem. The outer layer (L1) divides anticlinally to give rise to the plant epidermis; the middle layer (L2) divides anticlinally in the dome apex, and anticlinally and periclinally in the dome base to give rise to the plant mesoderm; and the inner layer (L3) divides in various planes to give rise to the central tissues of the plant (Satina et al., 1940). Occasional periclinal divisions occur resulting in the insertion of cells derived from one layer into the neighbouring layer, where they adopt a fate appropriate to their new layer. Despite this, the layers are largely ontogenetically separate yet they function in an integrated and coordinated manner to produce the plant body. While it is clear that there is a high degree of structural and functional organisation in the meristem, little is known about how this organisation is achieved or maintained.

We are taking a genetic approach to study the control of meristem structure and function using the model plant *Arabidopsis thaliana*. *Arabidopsis* provides an excellent model system for both genetic and molecular studies because of its rapid life cycle, small genome size and high fecundity, and because of the availability of extensive genetic maps of both visible (Koornneef et al., 1983) and restriction fragment length polymorphism markers (Chang et al., 1988, Nam et al., 1989). *Arabidopsis* has been increasingly used as a model system for the study of the genetics and molecular biology of higher plant development (Finkelstein et al., 1988). For example, a broad spectrum of mutants affecting embryonic (Mayer et al., 1991) and floral (Meyerowitz et al., 1991) development have been isolated and characterised.

In *Arabidopsis*, postembryonic growth starts with the initiation of a variable number of rosette leaves in a spiral phyllotaxy with unextended internodes. The leaf number depends on genotype and growth conditions (Rédei, 1969). At the end of the rosette stage, the bolting stem and a variable number of cauline leaves are initiated. Finally the meristem switches from producing leaf primordia to producing flower primordia. Organ initiation by the apical meristem is in the same spiral phyllotaxy in all three phases of growth, but individual plants show either clockwise or anticlockwise spirals (Smyth et al., 1990).

Previous work has shown that the shoot apical meristem of *Arabidopsis* is typical of dicots. Miksche and Brown (1965) describe the meristem of 6-day-old *Arabidopsis*

plants (ecotype Estland) as a shallow dome, four cells deep and approximately 40 μm in diameter. During vegetative growth, the meristem maintains this shape but increases in size. Vaughn (1952) measured an average diameter of 90 μm for the meristems of 25-day-old *Arabidopsis* plants kept vegetative in short days. On transition to flowering, the dome becomes more convex (Miksche and Brown, 1965, Vaughn and Jones, 1953, Vaughn, 1955). These workers also describe typical zonation patterns within the *Arabidopsis* meristem (Brown et al., 1964).

Here we report the genetic analysis and morphological characterisation of three fasciated mutants of *Arabidopsis*. Fasciation is a term used to describe a variety of developmental abnormalities in the shoot system (Worsdell, 1905). These include distortions in phyllotaxy and broadening, flattening and, in extreme cases, bifurcation of the stem. Fasciations can result from a variety of causes such as wounding (Loiseau, 1959) or pathogen attack (Murai et al., 1980), or they may be genetic (MacArthur, 1926; McKelvie, 1962; Reinholz, 1966; Krickhahn and Napp-Zinn, 1975; Usmanov and Startsev, 1979; Haughn and Somerville, 1988). Fasciation represents a breakdown in the pattern of organogenesis and has been associated with meristematic enlargement (Loiseau, 1959; Krickhahn and Napp-Zinn, 1975). The study of fasciation might reveal how meristem structure and function are established and maintained in normal plants.

Materials and methods

Seed of the Enkheim, Landsberg *erecta* and *fas1* genotype were obtained from the *Arabidopsis* Information Service Seed Bank. Seed of the *clv1-1* genotype was obtained from Vivian Irish and seed of the *flo-5* genotype in the Columbia genetic background was obtained from George Haughn, and then crossed into a Landsberg *erecta* background.

Plants were grown in an autoclaved mix of 80% sand and 20% Fisons Levington multi-purpose compost. The plants were maintained at 25°C in continuous light. Plants were grown axenically on Murashige and Skoog (1962) medium (MS) with 1% sucrose and solidified with 0.6% Difco Bacto Agar. Seedlings were grown in Petri dishes and mature plants were grown in jars or Magenta boxes (Sigma). Seeds were sterilized by soaking for ten minutes in a solution of 10% Clorox and 0.02% Triton X-100 followed by 30 seconds in 70% ethanol. The seeds were then washed in five changes of sterile distilled water and transferred to the MS medium using a sterile toothpick or a Pasteur pipette. The plants were maintained at 25°C in continuous light.

Ethyl methanesuphonate (EMS) mutagenesis

Mutagenesis was carried out in a fume cupboard. Landsberg *erecta* seed was soaked for five hours in a solution of 0.1 M potassium phosphate buffer at pH 5, 5% dimethyl sulphoxide and an appropriate concentration of EMS (between 12 and 500 mM). The seed was then washed twice for 15 minutes in 100 mM sodium thiosulphate and twice for 15 minutes in water. The seed was allowed to dry on Whatman 3MM paper, diluted with dry sand and planted at an approximate density of one seed per cm^2. The mutagenised seed (the M_1 generation) was grown up and their progeny (the M_2 generation) were harvested from each M_1 plant separately to give a collection of M_2 families. Approximately 10 members from each of 1200 families were planted in soil and screened for fasciated individuals.

Shoot apical meristem sections

Shoots from axenically grown seedlings were fixed for at least three days in 2.5% glutaraldehyde, 50 mM PIPES pH 7.2 and 0.1% caffeine. The tissue was then washed in 50 mM PIPES pH 7.2, stained with OsO_4 and dehydrated through an ethanol series of five 3-hour steps ending in absolute ethanol. The ethanol was gradually replaced with epoxy resin to allow infiltration. The resin was polymerised by baking overnight at 67°C. The embedded tissue was sectioned using a pyramitome with glass knives. The sections were stretched in a drop of 100% ethanol and cleared and mounted with Gurr's neutral mounting medium supplied by BDH.

Results

Mutant isolation and genetic analysis of the fasciated mutants

1200 Landsberg *erecta* EMS mutagenised M_2 families were generated and screened for fasciated plants. Ten fasciated lines were isolated but only two were studied further since the remaining eight showed variable penetrance and expressivity. A literature survey revealed a fasciated line isolated by Reinholz (1966) following X-ray mutagenesis of seed of the Enkheim genetic background. This line was named fasciata (Fas1). We obtained seed from this line from the *Arabidopsis* Information Service seed bank.

Genetic analysis of the mutant lines showed that in each case, the fasciations resulted from a single recessive Mendelian mutation (data not shown). Pairwise crosses between the three mutants gave all wild-type plants in the F_1, suggesting that each mutation is in a different gene. The genes were named Fas1 (Reinholz, 1966), Fas2, and Fas3.

The Fas loci were mapped with respect to various of the genetic markers described by Koornneef et al. (1983). Fas1 was found to map between Gl2 and Ch1 on Chromosome1 (Table 1), and Fas2 was found to map between Yi and Ttg on chromosome 5 (Table 2). Fas3 was found to map to chromosome 1 and to be allelic to both *clv1* (Koornneef et al., 1983) and *flo5* (Haughn and Somerville, 1988) (data not shown). Koornneef et al. (1983) mapped Clv1 to chromosome 1, 8.6 map units proximal of Gl2 and Medford had previously shown *flo5* and *clv1* mutants to be allelic (Medford personal communication). In pairwise crosses, *fas3*, *flo5*, and *clv1*, all failed to complement each other in the F_1 and no wild-type plants segregated in the F_2. Therefore the *fas3*, *clv1* and *flo5* mutations are allelic and so *flo5* was renamed *clv1-2* and *fas3* was renamed *clv1-3*.

The *fas1* mutation was isolated in the Enkheim background (Reinholz, 1966) which is wild-type at the erecta locus. When backcrossed into the Landsberg *erecta* genetic background the *fas1* mutant plants show reduced fertility in plants homozygous for the erecta mutation. Because of this, the *fas1* mutation was characterised in the Enkheim (ER^+) background with Enkheim controls.

Phenotypic analysis of the fasciated mutants

Fasciation is characterised by altered phyllotaxy and stem broadening. These aspects of the mutant phenotypes were analysed and the results are presented below. Interestingly, both these aspects of the mutant phenotypes became progressively worse as the plants developed. If plant growth

Table 1. *The F_2 segregation of* fas1 ch1, *and* gl2 *in crosses between* fas1, gl2 *double homozygotes and wild-type plants; and* fas1, ch1 *double homozygotes and wild-type plants*

	F_2 phenotypes						
Markers	+ +	+ −	− +	− −	X^2 linkage	p	Map units
Fas1, Gl2	109	23	22	23	19.8	<0.01	29 ± 7
Fas1, Ch1	96	22	14	16	15.1	<0.01	30 ± 7

Table 2. *The F_2 segregation of* fas2, ttg, *and* yi, *in crosses between* fas2 *plants and* ttg, yi *double homozygotes*

	F_2 phenotypes						
Markers	+ +	+ −	− +	− −	X^2 linkage	p	Map units
Fas2, Yi	252	105	94	11	15.5	<0.01	33 ± 4
Fas2, Ttg	247	106	89	20	5.7	<0.05	41 ± 4
Yi, Ttg	272	89	75	26	0.8	>0.05	No significant linkage

was slowed, for example by low temperatures, then more extreme fasciations developed. Apart from fasciation, the mutants also showed a variety of additional phenotypes including altered floral phyllotaxy, altered floral organ structure and number, unusual leaf shapes and inhibition of root elongation. The analysis of each of these phenotypes is described below.

Disturbed leaf phyllotaxy

For both the wild-type strains used (Landsberg *erecta* and Enkheim), phyllotaxy was found to be spiral with new leaves initiating at an angle averaging 138° from the previous leaf. The direction of the spiral was random and the phyllotaxy did not change on transition to floral growth. All the mutant lines studied show deviations from this phyllotaxy. A precise analysis of leaf divergence angles is not practical for large numbers of plants but major alterations in the relative positions of leaves can be seen in intact plants (Fig. 1). The phyllotaxy of the first six leaves of plants of each genotype were analysed in this way and the percentage of plants showing deviation from the normal phyllotaxy was recorded (Fig. 2). Some individuals in all the mutant lines showed disturbed phyllotaxy within the first six leaves. An allelic series was found within the Clv1 alleles with 60% of *clv1-2* plants, 42% of *clv1-3* plants and 30% of *clv1-1* plants showing phyllotactic distortions within the first six leaves. This figure is 40% for *fas2* plants and 23% for *fas1* plants. These data show that in all five mutant lines examined, some proportion of seedlings initiate leaves in unusual positions with respect to the other early leaves.

Fasciation in the inflorescence

The inflorescence of *Arabidopsis* consists of a bolting stem, cauline leaves and flowers, initiated in the same spiral phyllotaxy as the leaves (Smyth et al., 1990). In all the mutants, the fasciations observed in the rosette persisted into the

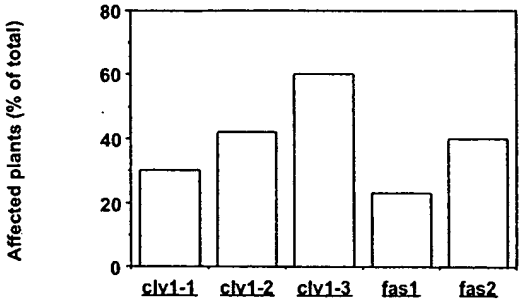

Fig. 2. The graphs show the percentage of *clv1*, *fas1* and *fas2* plants that show deviations from wild-type phyllotaxy within the first six rosette leaves. For each genotype 50 plants were scored except for *fas2* where only 25 plants were scored. No phyllotactic abnormalities were observed in a samples of 50 Landsberg *erecta* plants and 50 Enkheim plants.

inflorescence and tended to worsen with time (Fig. 3 A-F). The severity of inflorescence fasciations varied from plants in which only a single flower was not in the normal phyllotaxy, to plants in which the initiation of flowers failed entirely leaving the meristem exposed. Such exposed meristems occurred frequently in the *fas2* line, more rarely in the *fas1* line and never in the *clv1* mutants.

Other less extreme phenotypes observed include overall stem enlargement, stem flattening (line or ribbon fasciation) (Fig. 3 E-F), and stem flattening accompanied by stem bifurcation. Bifurcation appears to normalise the phyllotaxy somewhat resulting in the establishment of two or more new spiral phyllotaxies. Another feature of the mutant inflorescences is the failure to maintain stem elongation so that the mature structure appears crowded with flowers and siliques.

Changes in the number and structure of floral organs

In addition to fasciations, all the mutant lines show abnormalities in floral phenotype (Fig. 3 A-B). In *clv1* mutants, additional floral organs may arise in all or any of the floral whorls (Fig. 4). The most consistently affected whorl is the carpel whorl. Here the wild-type number of two carpels is seen rarely, and only in *clv1-1* plants. In all three alleles the modal carpel number is four. The organs of *clv1* flowers appear to be structurally wild-type although some double organs arise.

In contrast, both *fas1* and *fas2* mutants have fewer floral organs in their petal and stamen whorls and on average more sepals, while the carpel number is unaffected (Fig. 4). The organs in all whorls are not wild-type. The sepals and petals are narrow and both mutant lines show reduced fertility. In *fas2* mutants, floral initiation can break down entirely or fused partial flowers may arise.

Leaf morphology and root growth

The leaves of *clv1* mutants are slightly rounder than wild-type (Fig. 3 G-H) and occasional double leaves are observed. All three *clv1* mutants have near wild-type root growth (Fig. 5). The *fas1* and *fas2* mutants show variable leaf shapes (Fig. 3 I-J) and reduced root elongation (Fig. 5). The leaves of *fas1* plants are dentate and generally nar-

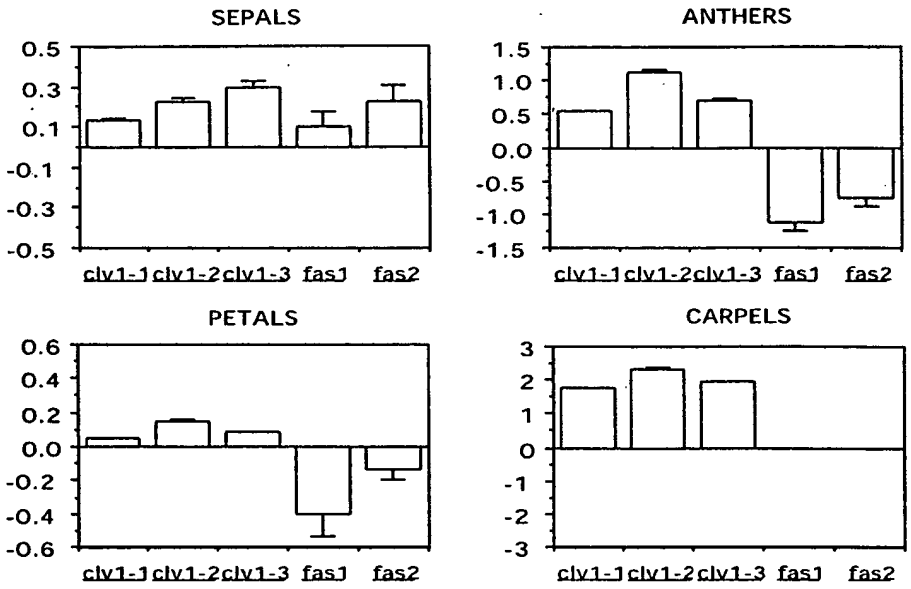

Fig. 4. The graphs show the mean deviation from wild-type floral organ number in each of the fasciated mutant lines. In both Landsberg *erecta* and Enkheim flowers there are invariantly four sepals, four petals and two carpels. Enkheim plants always have six stamens but in Landsberg *erecta* flowers one, or both of the abaxial stamens may fail to develop such that the mean number of stamens in these flowers is 5.7±0.02. The error bars represent the standard error of the means.

rower than wild-type. *Fas2* plants show a variety of leaf shapes but the leaves are also often narrower than wild-type and occasionally lanceolate, particularly the cauline leaves (Fig. 6). The roots of *fas1* plants are 60% wild-type length after 2 weeks of growth and those of *fas2* are 38% wild-type length.

The shoot apical meristems of wild-type and mutant plants

Fasciation represents a breakdown in the control of shoot apical meristem function and so may involve or result from breakdown in shoot apical meristem structure. The apical meristem of *fas2* plants can frequently be observed directly in individuals in which organ initiation has failed to such an extent that the meristem is not hidden by recently initiated leaves. These plants show that the meristem has enlarged greatly, mainly in one plane (Fig. 6). In *fas1* and *clv1* plants, direct observation of the meristem is not possible so longitudinal sections were taken though the meristems of 5-day-old *fas1*, *clv1-3*, Enkhiem and Landsberg *erecta* plants (Fig. 6). At least 4 meristems of each genotype were examined. The sections show that at this stage the meristems of both the wild-type lines used consist of a shallow dome of avacuolate cells. In Landsberg *erecta* plants the meristem measures between 50 μm and 62 μm across the base and between 20 μm and 25 μm in height. At its highest point, the meristem has 4 layers of avacuolate cells. The meristem of *clv1-3* plants is on average both broader and taller than wild-type measuring between 60 μm and 90 μm across the base, and between 25 μm and 30 μm in height. At its highest point, the *clv1-3* meristem has between 5 and 7 layers of avacuolate cells. Although the dome structure is maintained, *clv1-3* meristems have more gently sloping sides so that they are bell shaped.

In wild-type Enkheim plants the meristem measures between 50 μm and 65 μm across the base and between 25 μm and 30 μm in height. In *fas1* plants, the meristem is usually broader than wild-type being between 50 μm and 80 μm across the base but the dome shape of the wild-type is not observed. The *fas1* meristem is nearly flat, measuring between 15 μm and 23 μm in height, and having only 1 or 2 layers of avacuolate cells.

Double mutant combinations

In order to examine possible interactions between the mutations, pairwise crosses were performed between *clv1-2* and the *fas1* and *fas2* mutants. The resultant F_2 populations were screened for possible double mutant homozygotes. Plants were observed which showed the leaf morphology of the *fas* mutants and the distinctive silique phenotype of the *clv1* mutant. In the F_3, the progeny of these plants were all of similar phenotype with no segregation of distinct phenotypic classes suggesting that these F_2 plants were indeed doubly homozygous for *clv1-2* and each of the *fas* mutations. The phenotypes of the *fas1*, *clv1-2* and *fas2*, *clv1-2* double mutants were morphologically similar (as *fas1* and *fas2* plants are similar), and appear to represent the superimposition of the two phenotypes with no obvious interaction. Like *fas* mutants, the double mutants are slow growing with narrow and variable leaves, sepals and petals but

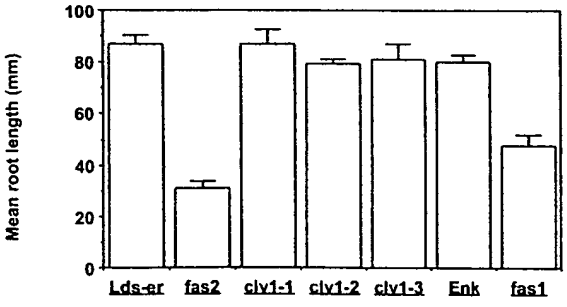

Fig. 5. The graph shows the mean root length of wild-type (Landsberg *erecta* and Enkheim) and mutant plants after two weeks growth on vertically positioned Petri dishes. The error bars represent the standard error of the means.

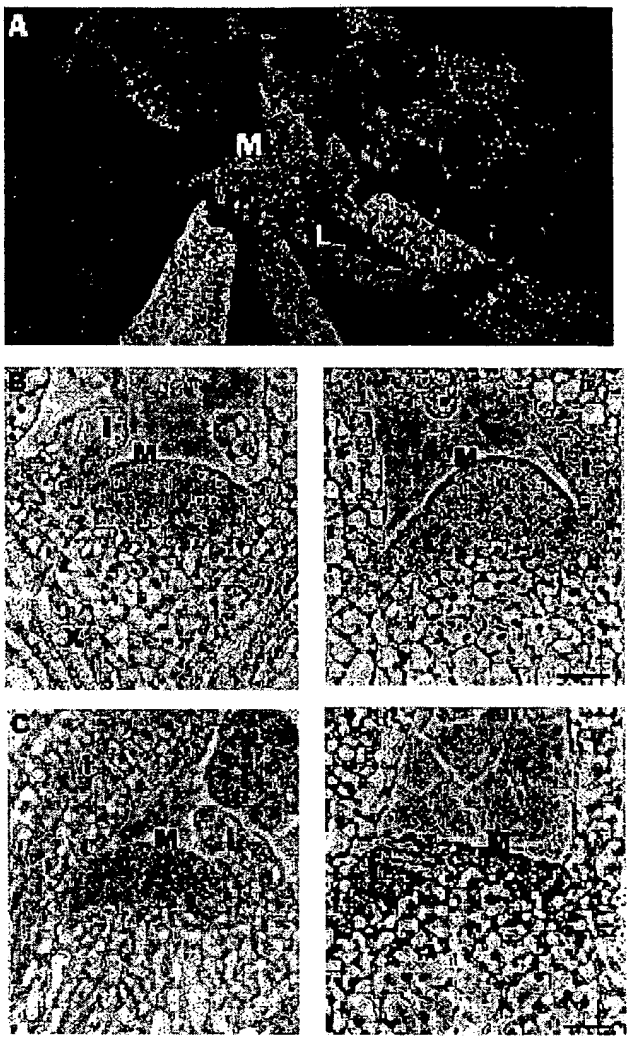

Fig. 6. (A) The photograph shows the shoot apical meristem of a *fas2* plant. Organ initiation in this plant has been affected to such an extent that the meristem is not hidden by young leaves or buds as it would be in a wild-type plant. The meristem has degenerated into a large callus-like structure (M). Note also the narrow leaf (L) on the bolting stem. (B) The photomicrographs show 6 μm median, longitudinal sections through the shoot apical meristem of a 5-day-old wild-type Enhkheim plant on the left, and a 5-day-old *fas1* plant on the right. (C) The photomicrographs show 6 μm median, longitudinal sections through the shoot apical meristems of a 5-day-old wild-type Landsberg *erecta* plant on the left, and a 5-day-old *clv1-3* plant on the right. In B and C, the plants were stained with OsO_4 during fixation. Meristematic cells are identifiable because their cytoplasm stains more densely than that of nearby, more vacuolate cells. The meristems are marked M and leaf initials are marked I. Xylem vessels are marked X. Bar, 20 μm.

like the *clv1* mutants they have club-like siliques. Such plants show stem and inflorescence fasciation and the only novelty is that flower initiation tends to become localized on one side of the apex. This gives a "brushlike" appearance with siliques and flowers clustered on one side of the stem (Fig. 7).

Similar crosses were performed between the two *fas* mutants but no obvious double mutant class could be identified in the F_2. In the F_2 plants, 99 wild-type and 73 fasciated types were found. This is in good agreement with the segregation expected of two unlinked recessive mutants of similar phenotype; 9:7 ($\chi^2 = 0.11$). However, the data are also compatible with the double mutant class having a lethal phenotype; 9:6 ($\chi^2 = 0.43$). In an attempt to resolve this, seven fasciated F_2 plants were harvested and the F_3 sown in the expectation that segregation of the other *fas* mutation might be observed. Two of the seven families segregated a seedling lethal phenotype. The affected individuals die with two to four true leaves. There is no direct evidence that the lethal phenotype is related to the interaction of *fas1* and *fas2*. So the phenotype of the double mutant class may either be the seedling-lethal or indistinguishable from the single *fas* homozygotes. Further genetic analysis is needed to resolve this.

Discussion

In order to learn about the control of meristem structure and function in plants, we have characterised three shoot apical meristem mutants of *Arabidopsis thaliana*:- *fas1*, *fas2* and *clv1*. The *fas1* and *fas2* loci were mapped. The *clv1* locus has previously been mapped by Koornneef et al. (1983) and three independent *clv1* alleles were characterised in this study. The mutants can be grouped into two classes with the *clv1* mutants making up one class, and *fas1* and *fas2* making up the other. The main features that separate these classes are that *fas1* and *fas2* mutants have darker green, abnormally shaped leaves, short roots, abnormal floral organs and a tendency for breakdown in the ability of the meristem to initiate unique and distinct organs. Conversely, *clv1* mutants have nearly wild-type leaves, wild-type roots and additional, but structurally normal, floral organs and, except for rare double organs, the plants retain the ability to initiate distinct and unique organs.

There are also features common to all the mutant phenotypes. The mutants were selected for fasciation and all show characteristic broad stems and distortions in phyllotaxy in both the vegetative and floral apex. In all cases, the fasciations are associated with enlargement and shape change in the meristem. The fasciations become progressively worse with time and can eventually lead to stem bifurcations. Following bifurcation, more normal phyllotaxy is temporarily restored.

Implications for the field theory of phyllotaxy

The association that we observe between phyllotactic distortions with meristematic enlargement is consistent with the results of other workers studying both genetic (Krickhahn and Napp-Zinn, 1975) and wound induced (Loiseau, 1959) fasciations. The observation that a more normal phyllotaxy is restored following stem bifurcation further strengthens the correlation between meristem enlargement and fasciation. Bifurcation results from the splitting of the apical meristem which presumably reduces its size. This correlation can be viewed as support for the field theory of phyllotaxy (Wardlaw, 1949). The field theory proposes that

the position of new leaves is determined by the interaction of fields of substances inhibitory to leaf initiation which are produced by recently initiated leaves. If it is assumed that the size and strength of these fields is not affected by the mutations, then the observed enlargement of the meristems would lead to alterations in the interactions of the inhibitory fields, provoking alterations in the position of new leaf initiation, and hence alterations in phyllotaxy.

It is possible that the size and/or strength of the fields are affected by the mutations. This would lead to phyllotactic distortion even in the absence of meristematic enlargement. Even so, it seems unlikely that any alteration in these fields is the primary affect of the mutations described here since this would not explain why the meristems of all the mutations are altered in size and shape, and why in all cases floral development is also affected. It therefore seems more likely that the mutations primarily affect meristem development and their phenotype should be interpreted in this light.

Implications for the independence of PZ and CZ function

The functions of the shoot apical meristem can be considered as firstly the initiation of distinct organs in a particular pattern, which is largely achieved by the peripheral zone (PZ), and secondly the maintenance of meristem size and shape which is largely achieved by the stem-cell-like activities of the central zone (CZ). In *fas1* and *fas2* plants both these functions are simultaneously disrupted such that distinct and wild-type organs are not always initiated and the size and shape of the meristem is not maintained.

In *clv1* plants, more specific alterations are observed. The mutant plants retain the ability to initiate wild-type leaves but fail to maintain apical meristem size and shape. The phenotype of *clv1* mutants clearly demonstrates the partial independence of these two meristem functions although the phenotypes of *fas1* and *fas2* indicate that this separation is not total. An attractive hypothesis to explain the *clv1* phenotype is that only a subset of cells in the meristem are affected by the mutations. The curious bell shape of some *clv1* meristems, coupled with the observation that the phenotype of the leaves of *clv1* plants is nearly wild-type, suggests that only the CZ and not the PZ is affected by the mutations. If the CZ enlarges, the PZ would be forced outward and, if the field theory of phyllotaxy is correct, this would lead to phyllotactic distortions as discussed above. Despite this enlargement, the PZ of *clv1* plants retains the ability to direct the differentiation of nearly wild-type leaves. The rare double leaves may not represent a breakdown in the normal mechanisms directing organ initiation, instead they might represent the normal functioning of these mechanisms without compensating for the increased size of the meristem. This will lead, on occasions, to two leaves initiating very close together, which could result in the observed double leaves. This contrasts with the frequent failure in distinct organ initiation observed in *fas1* and particularly in *fas2* plants. If this failure occurs at all in any one plant, it usually continues until the meristem fails altogether. This phenotype may be the result of a more general breakdown in meristem function.

One possible way to test the relative effects of the mutations described on the PZ and the CZ would be to use a PZ-specific reporter gene. Medford et al. (1991) have isolated a promoter from cauliflower that expresses specifically in the PZ of the meristem. This promoter has been fused to the β-galacturonidase reporter gene (Jefferson et al., 1987) for which a number of chromogenic substrates are available. The transfer of these constructs into plants allows histochemical localisation of gene expression. If such constructs were introduced into wild-type and mutant plants, then the relative sizes of the PZ and CZ could be studied in the mutants and compared to those of wild-type plants. In this way, it might be possible to test the theory that there are CZ-specific alterations in *clv1* meristems but less specific alterations in *fas1* and *fas2* meristems.

Implications for the relationship between the floral primordium and shoot apical meristem

Mutations at all the loci studied give rise to non-wild-type floral development. The nature of the floral phenotype in each mutant line closely parallels the phenotype of the shoot system. In *fas1* and *fas2* plants, the floral organs, like the leaves, are narrow and variable resulting in reduced fertility. In *clv1* plants, while additional organs are observed, these organs are wild-type, although occasional double floral organs are formed as were occasional double leaves. The carpels are consistently duplicated in *clv1* plants. These organs are derived from the centre of the flower primordium. The *clv1* mutation results in enlargement of the centre of the apical meristem and the carpel phenotype may involve a similar enlargement of the centre of the flower primordium. The parallel phenotype of the shoot apical meristem and the floral primordia suggests that there are common factors involved in regulating both these structures. This is consistent with the view that the floral primordium is evolutionarily derived from the shoot apical meristem. This idea is supported by genetic evidence which suggests floral organs are modified leaves. *Arabidopsis* plants mutant in genes involved in floral development may fail to produce floral organs and produce leaves in the positions where floral organs would normally develop (Bowman et al., 1989).

Attempts were made to construct all three possible double mutant combinations of *fas1*, *fas2* and *clv1-2*. The *fas2, fas1* combination may either resemble the *fas* mutants or it may be lethal. The *fas1*, *clv1-2* and *fas2*, *clv1-2* plants are similar in phenotype, suggesting that the affects of these mutation are additive.

The phenotypes of the mutants described here probably result from meristem enlargement and shape change. This in turn alters the pattern of organ initiation and to a lesser extent the structure of the organs formed. In this respect, these mutations are distinct from other groups of developmental mutants in *Arabidopsis* which affect organ identity (Meyerowitz et al., 1991), developmental timing (Rédei, 1962) and presence or absence of pattern elements (Mayer et al., 1991). It is probably not meaningful to speculate on the specific roles of the wild-type genes defined by these mutations since fasciations can be provoked by rather non-specific stimuli (Loiseau, 1959; Murai et al. 1980). However, particularly in the case of clv1 mutants where such precise changes are seen, it is possible that these genes are

involved in regulating the proliferation and differentiation of meristem cells.

We would like to thank Patrick Echlin and Brian Chapman for help with the microscopy, Joanne Pumfrey for help with double mutant construction, Mark Estelle and Stephen Day for critical reading of the manuscript and Joanne Griffiths for typing.

This work was supported by the Agriculture and Food Research Council. O.L. was supported by a Science and Engineering Research Council studentship.

References

Bowman, J. L., Smyth, D. R. and Meyerowitz, E. M. (1989). Genes directing flower development in *Arabidopsis*. *The Plant Cell* **1**, 37-52.

Brown, J. A. M., Miksche, J. P. and Smith, H. H. (1964). An analysis of 3H-thymidine distribution throughout the vegetative meristem of *Arabidopsis thaliana* L. Heynh. *Radiation Botany* **4**, 107-113.

Chang, C., Bowman, J. L., Dejohn, A. W., Lander E. S. and Meyerowitz, E. M. (1988). Restriction fragment length polymorphism linkage map of *Arabidopsis thaliana*. *Proc. Natn. Acad. Sci. U.S.A.* **85**, 6856-6860.

Finkelstein, R., Estelle, M., Martinez-Zapater, J. and Somerville, C. (1988). *Arabidopsis* as a tool for the identification of genes involved in plant development. In *Temporal and Spatial Regulation of Plant Genes.* (eds. D. P. S. Verma and R. B. Goldberg) pp. 1-25. Wien: Springer Verlag.

Haughn, G. W. and Somerville, C. R. (1988). Genetic control of morphogenesis in *Arabidopsis*. *Developmental Genetics* **9**, 73-89.

Jefferson, R. A., Kavanagh, T. A. and Bevan, M. W. (1987). Gus fusions. b-glucuronidase as a sensitive and versatile gene fusion marker in higher plants. *EMBO J.* **6**, 3901-3907.

Koornneef, M., van Eden, J., Hanhart, C. J., Stam P., Braaksma, F. J. and Feenstra, W. J. (1983). Linkage map of *Arabidopsis thaliana*. *J. Heredity* **74**, 265-272.

Krickhahn, D. and Napp-Zinn, K. (1975). Fasciation studies in *Arabidopsis thaliana* (L.) Heynh. *Arabid. Inf. Serv.* **12**, 9.

Loiseau, J.-E. (1959). Observations et experimentation sur la phyllotaxie et le fonctionnement du sommet vegetatif chez quelques Balsaminacees. *Ann. Sci. Nat. Bot. Ser. 11* **20**, 1-214.

MacArthur, J. W. (1926). Linkage studies with the tomato. *Genetics* **11**, 387-405.

Mayer, U., Tores Ruiz, R. A., Berleth, T., Misera, S. and Jurgens, G. (1991). Mutations affecting body organisation in the *Arabidopsis* embryo. *Nature* **532**, 402-407.

McKelvie, A. D. (1962). A list of mutant genes in *Arabidopsis thaliana* (L.) Heynh. *Radiation Botany* **1**, 233-241.

Medford, J. I., Scott Elmer, J. and Klee, H. J. (1991). Molecular cloning and characterisation of genes expressed in shoot apical meristems. *The Plant Cell* **3**, 359-370.

Meyerowitz, E. M., Bowman, J. L., Brockman, L. L., Drews, G. N., Jack, T., Sieburth, L. E. and Weigel, D. (1991). A genetic and molecular model for flower development in *Arabidopsis thaliana*. *Development 1991 Supplement* **1**, 157-168.

Miksche, J. P. and Brown, J. A. M. (1965). Development of vegetative and floral meristems of *Arabidopsis thaliana*. *Amer. J. Bot.* **52**, 533-537.

Murai, N., Skoog, F., Doyle, M. E. and Hanson, R. S. (1980). Relationships between cytokinin production, presence of plasmids, and fasciation caused by strains of *Corynebacterium fascians*. *Proc. Natn. Acad. Sci. U.S.A.* **77**, 619-623.

Murashige, T. and Skoog, F. (1962). A revised medium for growth and bioassays with tobacco cell cultures. *Physiol. Plant.* **15**, 473-497.

Nam, H-G., Giraudat, J., den Boer, B., Moonan, F., Loos, W. D. B., Hauge, B. M. and Goodman, H. M. (1989). Restriction fragment length polymorphism linkage map of *Arabidopsis thaliana*. *The Plant Cell* **1**, 699-705.

Rédei, G. (1962). Supervital mutants of *Arabidopsis*. *Genetics* **47**, 443-460.

Rédei, G. (1969). *Arabidopsis thaliana* (L) Heynh, a review of the genetics and biology. *Bibliographica Genetica* **21**, 1-151.

Reinholz, E. (1966). Radiation induced mutants showing changed inflorescence characteristics. *Arabid. Inf. Serv.* **3**, 19-20.

Satina, S., Blakeslee, A. F. and Avery, A. G. (1940). Demonstration of the three germ layers in the shoot apex of *Datura* by means of induced polyploidy periclinal chimeras. *Amer. J. Bot.* **27**, 895-905.

Smyth, D. R., Bowman, J. L. and Meyerowitz, E. M. (1990). Early flower development in *Arabidopsis*. *The Plant Cell* **2**, 755-767.

Usmanov, P. D. and Startsev, G. A. (1979). The appearance of stem fasciation in *Arabidopsis thaliana* F_2 by crossing the mutant 90 with LuCo. *Arabid. Inf. Serv.* **16**, 99-102.

Vaughn, J. G. (1952). Structure of the angiosperm apex. *Nature* **169**, 458-459.

Vaughn, J. G. and Jones F. R. (1953). Structure of the angiosperm inflorescence apex. *Nature* **171**, 751-752.

Vaughn, J. G. (1955). The morphology and growth of the vegetative and reproductive apices of *Arabidopsis thaliana* (L.) Heynh., *Capsella bursa-pastoris* (L.) Medic., and *Anagallis arvensis*. *J. Linn. Soc. Bot.* **55**, 279-301.

Wardlaw, C. W. (1949). Experiments on organogenesis in ferns. *Growth (Suppl.)* **13**, 93-131.

Worsdell, W. C. (1905). Fasciation: Its meaning and origin. *New Phytol.* **4**, 55-74.

(Accepted 9 July 1992)

dev1884 colour tip-in

Fig. 1. The photographs and interpretive drawings show the phyllotaxy of (A) Landsberg *erecta* wild-type and (B) two *clv1* plants. In the drawings leaves are outlined with solid lines and cotyledons are outlined with dotted lines. The leaves are numbered in order of initiation and the displaced leaves of *clv1* plants are marked with an asterisk.

Fig. 3. Photographs A-D show the typical inflorescence morphology of (A) a wild-type Landsberg *erecta* plant, (B) a *clv1-2* plant, (C) a *fas1* plant and (D) a *fas2* plant. The oldest *clv1-2* flower has been opened to show the additional floral organs. The inflorescences of *fas1* and *fas2* plants are similar in morphology being generally disorganised. The narrow sepals and petals of the *fas* mutant flowers allow anthers to protrude as shown. Photographs E and F show the bolting stem of (E) a wild-type Landsberg *erecta* plant and (F) a *fas1* plant. The wild-type stem is of even width throughout. Toward the apex, the *fas1* stem shows a typical ribbon fasciation, being broad and flat. Photographs G-J show typical rosette leaves from (G) a wild-type Landsberg *erecta* plant, (H) a *clv1-2* plant, (I) a *fas1* plant and (J) a *fas2* plant. The leaves of *clv1* plants are consistently somewhat rounder than wild-type. In the *fas* mutants the leaves are variable in shape. Typically rosette leaves of *fas1* plants are dentate as shown, while the rosette leaves of *fas2* plants are more nearly wild-type but may be asymmetrical. Particularly in *fas2* mutant plants, more extreme leaf shape abnormalities are observed later in development (see Fig. 6).

Fig. 7. The photograph shows the inflorescence of a *clv1-2, fas1* double mutant plant. The bolting stem has curled round and floral initiation has become limited to one side of the stem.

Specific and heritable genetic interference by double-stranded RNA in *Arabidopsis thaliana*

Chiou-Fen Chuang and Elliot M. Meyerowitz*

Division of Biology 156-29, California Institute of Technology, Pasadena, CA 91125

Contributed by Elliot M. Meyerowitz, January 24, 2000

We investigated the potential of double-stranded RNA interference (RNAi) with gene activity in *Arabidopsis thaliana*. To construct transformation vectors that produce RNAs capable of duplex formation, gene-specific sequences in the sense and antisense orientations were linked and placed under the control of a strong viral promoter. When introduced into the genome of *A. thaliana* by *Agrobacterium*-mediated transformation, double-stranded RNA-expressing constructs corresponding to four genes, *AGAMOUS* (*AG*), *CLAVATA3*, *APETALA1*, and *PERIANTHIA*, caused specific and heritable genetic interference. The severity of phenotypes varied between transgenic lines. *In situ* hybridization revealed a correlation between a declining *AG* mRNA accumulation and increasingly severe phenotypes in *AG* (*RNAi*) mutants, suggesting that endogenous mRNA is the target of double-stranded RNA-mediated genetic interference. The ability to generate stably heritable RNAi and the resultant specific phenotypes allows us to selectively reduce gene function in *A. thaliana*.

In *Arabidopsis thaliana*, reverse genetic techniques for isolating mutants corresponding to known sequences, such as antisense suppression (1–7), cosuppression by overexpression of the target gene (3, 8, 9), targeted gene disruption (10), or the PCR approach of screening for T-DNA insertion libraries (11, 12) have been developed, but are often insufficient and have many unanticipated difficulties. The widespread identification of differentially expressed genes, homologous genes, and interacting proteins have created a need for potent and efficient methods for obtaining their loss-of-function or reduction-of-function mutants.

Double-stranded RNA (dsRNA)-mediated interference with expression of specific genes has been observed in a number of organisms including *Caenorhabditis elegans* (13–17), plants (18, 19), *Drosophila* (20, 21), *Trypanosoma brucei* (22), and a planarian (23). Although the mechanism of RNA interference (RNAi) is not well understood, it seems to provide an effective way to discover gene function in many organisms (24–26).

To investigate the potential of dsRNA interference with gene activity in *A. thaliana*, we introduced dsRNA-expressing constructs of selected genes with previously defined functions into plants. Gene constructs delivered into plants with *Agrobacterium*-mediated transformation are stably integrated into the genome of host cells; thus, RNA expression from these constructs in transgenic plants can be persistent and heritable.

In this study, one gene from each of four major categories of genes involved in flower development was chosen, to determine the ability of RNAi to allow functional assessment of genes with diverse developmental functions in flowers. They are the floral organ identity gene *AGAMOUS* (*AG*), the floral meristem-size gene *CLAVATA3* (*CLV3*), the floral meristem identity gene *APETALA1* (*AP1*), and the floral organ number gene *PERIANTHIA* (*PAN*) (27–30). The phenotypes produced by dsRNAs corresponding to these genes are similar to those of their previously identified reduction-of-function or loss-of-function mutants (31–36). The progeny from fertile RNAi mutants, such as *CLV3* (*RNAi*) and *AP1* (*RNAi*) plants, also showed phenotypes. In addition to high specificity and heritability, a phenotypic series (weak, intermediate, and strong) was obtained from dsRNA interference. Furthermore, *in situ* hybridization indicates that endogenous target mRNA is decreased in RNAi mutants. Most constructs that are designed to produce only antisense or only sense RNA do not induce interference. Thus, specific and inheritable dsRNA interference may offer a useful alternative to classical reverse genetic screening of mutants in *A. thaliana*.

Materials and Methods

Constructs. A summary of DNA constructs is shown in Fig. 1. In p35S::A-GUS-S and p35S::A, constructs were ligated to the *Bam*HI and *Xba*I sites of pCGN1547 (37) into which an 842-bp fragment of the cauliflower mosaic virus 35S promoter and a 253-bp fragment of the 3′ end of nopaline synthase had previously been inserted in the *Asp*718/*Bam*HI and *Xba*I/*Pst*I sites, respectively (38). Constructs consisting of a 339-bp fragment of the nopaline synthase promoter, gene-specific sequences in the sense orientation and a 253-bp fragment of the 3′ end of nopaline synthase were ligated to the *Pst*I and *Hin*dIII sites of pCGN1547 and p35S::A to make pNOS::S and p35S::A-NOS::S, respectively. In p35S::A-GUS-S, the β-glucuronidase (GUS) fragment containing nucleotides 787–1,809 was used as a linker between gene-specific fragments in the antisense and sense orientations. *AG*, *CLV3*, *AP1*, and *PAN* cDNA coding sequences used in this study contain nucleotides 301–855 (27), 3–291 (28), 445–854 (29), and 27–396 (30), respectively.

***Agrobacterium*-Mediated Transformation.** *Agrobacterium* strain ASE carrying DNA constructs in pCGN1547 was used to transform *Arabidopsis* plants (T_0) by vacuum infiltration (39). Transformed *Arabidopsis* lines (T_1) were selected on Murashige/Skoog (Sigma) plates containing kanamycin (50 μg/ml). Kanamycin-resistant seedlings were then transferred to soil. Phenotypic analysis of T_1 and T_2 plants is summarized in Table 1 and Table 2, respectively.

***In Situ* Hybridization.** The *AG* cDNA clone pCIT565 containing nucleotides 9–977 (27) was used to synthesize antisense and sense probes. ^{35}S-labeled RNA probes were synthesized with Riboprobe *in vitro* Transcription Systems (Promega). The template was linearized with *Hin*dIII and transcribed by T7 RNA polymerase (antisense probe), or linearized with *Xho*I and transcribed by SP6 RNA polymerase (sense probe). Tissue was fixed in 1× PBS containing 4% paraformaldehyde/0.1% Triton X-100/0.1% Tween 20 at 4°C overnight. Fixed tissue was dehydrated with ethanol, cleared with xylene, embedded in paraffin (Paraplast Plus, Oxford Labware, St. Louis), and sectioned at 8 μm. *In situ* hybridization was performed as described by Drews

Abbreviations: dsRNA, double-stranded RNA; RNAi, RNA interference; GUS, β-glucuronidase.

*To whom reprint requests should be addressed. E-mail: meyerow@cco.caltech.edu.

The publication costs of this article were defrayed in part by page charge payment. This article must therefore be hereby marked "*advertisement*" in accordance with 18 U.S.C. §1734 solely to indicate this fact.

Article published online before print: *Proc. Natl. Acad. Sci. USA*, 10.1073/pnas.060034297. Article and publication date are at www.pnas.org/cgi/doi/10.1073/pnas.060034297

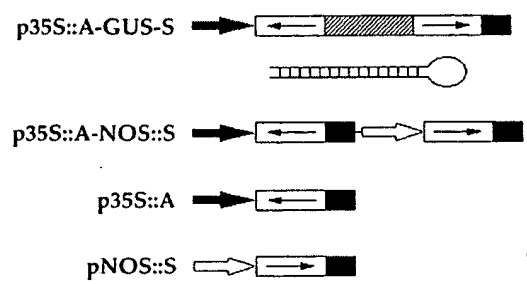

Fig. 1. Gene constructs used to analyze dsRNA effects. In p35S::A-GUS-S, gene-specific sequences (open boxes with arrows indicating the orientation) in the antisense (A) and sense (S) orientations were linked with a 1,022-bp fragment of the GUS gene (hatched box) and controlled by the 35S promoter (solid arrow). A schematic structure of the predicted dsRNA stem with a single-stranded loop generated by p35S::A-GUS-S constructs is shown. In p35S::A-NOS::S, gene-specific sequences in the antisense and sense orientations were controlled by the 35S promoter and the nopaline synthase promoter, respectively (open arrow). p35S::A contains gene-specific sequences in the antisense orientation under control of the 35S promoter. pNOS::S contains gene-specific sequences in the sense orientation driven by the nopaline synthase promoter. Solid box, the 3' end of nopaline synthase.

et al. (40), with modifications by Sakai *et al.* (41). Exposure time was 8–10 days.

Western Blot Analysis. Bud clusters (stages 1–12, including the inflorescence meristem) from one inflorescence were frozen and ground in liquid nitrogen, thawed in 30 μl of lysis buffer (50 mM Tris, pH 7.5/1 mM EDTA/100 mM NaCl/1% Nonidet P-40/0.1% SDS/0.1% Triton X-100/0.7% 2-mercaptoethanol/1 mM PMSF). The extract was mixed with 15 μl of 3× sample buffer (187 mM Tris, pH 6.8/6% SDS/30% glycerol/3% 2-mercaptoethanol/0.06% bromophenol blue), boiled for 5 min, and centrifuged (16,000 × *g* for 10 min at room temperature). Twenty microliters of the supernatant was separated on an SDS/12.5% polyacrylamide gel. The protein was transferred to nitrocellulose membrane (Schleicher & Schuell), probed with an AG-specific polyclonal antibody (42) and horseradish peroxidase-labeled secondary antibody (Amersham International), and detected with the enhanced chemiluminescence system (ECL; Amersham International).

Table 1. Effects of sense, antisense, and dsRNAs on transgenic plants

Gene	Transformed background	Transformed construct	RNAi mutants/total	%
AG	Ws*	p35S::A-GUS-S	235/236	99.6
		pNOS::A-GUS-S	2/32	6
		p35S::A-NOS::S	3/124	2
		p35S::A	0/111	0
		pNOS::S	0/95	0
CLV3	Ws	p35S::A-GUS-S	121/137	88
		p35S::A-NOS::S	2/176	1
		p35S::A	0/273	0
		pNOS::S	ND†	ND
AP1	L-*er*‡	p35S::A-GUS-S	249/260	96
		p35S::A	8/140	6
		pNOS::S	0/62	0
PAN	*crc-1*	p35s::A-GUS-S	110/126	87
		p35S::A-NOS::S	18/66	27
		p35S::A	42/76	55
		pNOS::S	2/6	33

*Ws, Wassilewskija.
†ND, not determined.
‡L-*er*, Landsberg *erecta*.

Table 2. Inheritance of genetic interference in *CLV3 (RNAi)* and *AP1 (RNAi)* mutants

T_1 plants		T_2 plants: Mutants	T_2 plants: WT*	Copy no.† in T_1 plants
CLV3 (RNAi)	Plant 1	14	8	ND‡
AP1 (RNAi)	Plant 1 (W§)	25 (W)	8	1
	Plant 2 (W)	22 (W)	8	1
	Plant 3 (I¶)	21 (I)	6	1
	Plant 4 (I/S‖)	19 (I/S)	7	1
	Plant 5 (S**)	17 (S)	5	1
	Plant 6 (S)	20 (S)	4	1

*WT, wild type.
†Number of transgene copies estimated from segregation ratios.
‡ND, not determined.
§W, weak.
¶I, intermediate.
‖I/S, intermediate/strong.
**S, strong.

Results

To make constructs that produce dsRNA, gene-specific sequences in the antisense and sense configurations were either linked with the partial GUS gene and placed under control of the constitutive 35S promoter from cauliflower mosaic virus (p35S::A-GUS-S), or controlled by the 35S promoter and the constitutive nopaline synthase promoter, respectively (p35S::A-NOS::S). A single RNA transcribed from the fusion gene in p35S::A-GUS-S can potentially form a dsRNA stem with a single-stranded loop structure (Fig. 1). Genetic interference effects of sense, antisense, and dsRNAs corresponding to *AG*, *CLV3*, *AP1*, and *PAN* are outlined in Table 1. For each of these genes, p35S::A-GUS-S constructs caused potent and specific genetic interference. However, p35S::A-NOS::S, p35S::A and pNOS::S constructs had either no, or weak, genetic interference effects. We will refer to transgenic plants carrying functional p35S::A-GUS-S constructs by listing the gene name followed by RNAi. For unknown reasons, the sense construct corresponding to *CLV3* caused toxicity in *Agrobacterium* and the sense construct of *PAN* resulted in very low transformation efficiency of *crabs claw-1* (*crc-1*) plants. Therefore, interference effects of the *CLV3* sense construct were not determined and only six *crc-1* transgenic plants containing the *PAN* sense construct were analyzed.

AG dsRNA-Mediated Genetic Interference. *AG* was chosen for initial characterization of RNAi in developing flowers. *Arabidopsis* flowers consist of four concentric whorls of organs. Most wild-type flowers have four sepals, four petals, six stamens, and two fused carpels, from the outermost first whorl to the innermost fourth whorl (Fig. 2*A*). Mutations in the *AG* gene cause homeotic alterations of the third and fourth whorls of organs in flowers (31). In severe *ag* loss-of-function mutants (Fig. 2*B*), the third whorl primordia develop into petals indistinguishable from those of the second whorl, and the fourth whorl develops into another *ag* flower, resulting in a repetitive pattern of sepals, petals, and petals (32).

The phenotypes produced by *AG* dsRNA are frequent and specific (Fig. 2 *C–I*). All but one of 236 transgenic plants showed *ag* mutant phenotypes. These *AG* (*RNAi*) mutants can be arranged into a phenotypic series based on the severity of the homeotic transformation in the third whorl and the extent of floral indeterminacy in the fourth whorl. Weak and intermediate

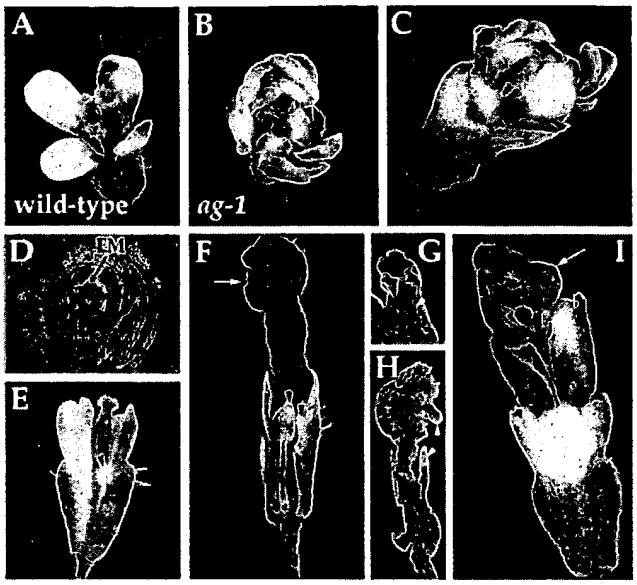

Fig. 2. Flowers of wild-type, *ag-1* and *AG (RNAi)* plants. (*A*) Wild-type flowers have four sepals, four petals, six stamens, and two carpels. (*B*) *ag-1* flowers consist of an indeterminate number of whorls of sepals and petals in the pattern (sepals, petals, petals)$_n$, with no staminoid or carpeloid tissue. (*C–I*) *AG (RNAi)* flowers with different severity of phenotypes. (*C*) Strong mutant flowers phenocopied *ag-1*. (*D*) Longitudinal section of a strong mutant flower showing a large number of sepals and petals produced by an indeterminate floral meristem (FM). (*E*) Weak mutant flower. The stamens fail to elongate and the anthers are slightly petaloid (arrowhead), with no pollen. (*F*) Intermediate mutant flower with some sepals and petals removed. Anthers are partially transformed into petaloid tissue (arrowheads). The gynoecium is bulged at the top (arrow, *F*), with inner organs such as carpels (arrowhead, *G*) and/or petals (arrowheads, *H*). (*I*) Intermediate/strong mutant flowers have the repeated pattern of sepals, petals, petals formed in outer whorls and an incomplete flower in the center (arrow). *AG (RNAi)* plants are in the Wassilewskija background; therefore, internode elongation between successive internal flowers are seen in intermediate/strong (*I*) and strong mutant flowers (*C*).

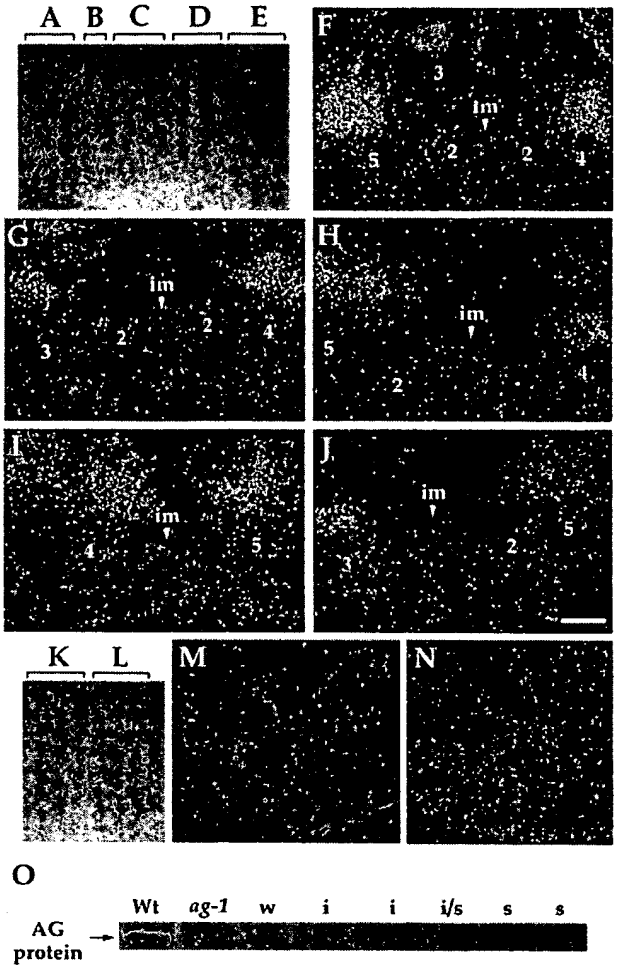

Fig. 3. Effects of *AG* dsRNA on levels of *AG* mRNA and AG protein. (*A–E*) An autoradiogram of the tissue hybridized with an *AG* anti-mRNA probe. The tissue is from wild-type (*A* and *F*), weak (*B* and *G*), intermediate (*C* and *H*), intermediate/strong (*D* and *I*), and strong (*E* and *J*) *AG (RNAi)* mutant plants. (*A–E*) Hybridization signals declined gradually with increasingly severe phenotypes. (*F–J*) The bright-field/dark-field double exposures of longitudinal section through the inflorescence meristems with stage 2–5 flowers. The silver grains representing *AG* mRNA expression were made to appear yellow with the use of a yellow filter. The number indicated corresponds to the development stage of flowers (43). im, inflorescence meristem. (Bar = 50 μm.) (*K* and *L*) An autoradiogram of the tissue hybridized with an *AG* sense probe. The tissue is from wild-type (*K* and *M*) and intermediate *AG (RNAi)* mutant plants (*L* and *N*). (*O*) Western blot analysis of AG protein. The anti-AG antibody recognizes the carboxyl-terminal part of the AG protein from aa 220–285 which is absent in the AG-1 protein (27, 42); thus, *ag-1* is a control of the specificity of the antibody. Whereas AG protein is weakly expressed in weak (w) and intermediate (i) *AG (RNAi)* mutants compared with wild type (Wt), it is not detected at levels above background in intermediate/strong (i/s) and strong (s) *AG (RNAi)* mutants.

AG (RNAi) mutant flowers showed partial homeotic transformation in the third whorl organs and slight floral indeterminacy (Fig. 2 *E–H*). However, intermediate/strong and strong *AG (RNAi)* mutant flowers showed complete transformation of the third whorl organs from stamens to petals and severe floral indeterminacy (Fig. 2 *C*, *D*, and *I*). Particularly, flowers from strong *AG (RNAi)* plants (Fig. 2*C*) are indistinguishable from those of strong *ag* mutant alleles such as *ag-1* (Fig. 2*B*). Weak, intermediate, intermediate/strong, and strong *AG (RNAi)* mutants represent 16, 32, 43, and 9%, respectively, of the transgenic plant populations. In contrast, pNOS::A-GUS-S, in which the nopaline synthase promoter was used to drive the fusion gene, and p35S::A-NOS::S constructs for *AG* caused very weak genetic interference in 2 out of 32 and 3 out of 124 transgenic plants, respectively (data not shown). Flowers from transgenic plants containing the *AG* antisense (n = 111) or sense (n = 95) construct are indistinguishable from those of wild-type plants (data not shown).

dsRNA Interferes with mRNA Accumulation. *In situ* hybridization was performed to determine the target of dsRNA interference. The earliest expression of *AG* in wild-type flowers is in stage three, in those cells that will give rise to the third- and fourth-whorl organ primordia. Later, *AG* expression is restricted to the stamen and the carpel primordia (Fig. 3*F*) (27). The autoradiogram of the tissue hybridized with an *AG* anti-mRNA probe showed that hybridization signals declined with increasingly severe phenotypes in *AG (RNAi)* mutants (Fig. 3 *A–E*), consistent with the observation that *AG* mRNA accumulation is decreased in *AG (RNAi)* mutants (Fig. 3 *G–J*). These results suggest that endogenous mRNA is a target of dsRNA-mediated genetic interference. When used as a standard control for *in situ* hybridization, an *AG* sense probe hybridized with the tissue from *AG (RNAi)* mutants but not with that from wild type (Fig. 3 *K–N*), suggesting that *AG* antisense RNA is produced in *AG (RNAi)* mutants. Reverse transcription–PCR analysis with *GUS*- and *AG*-specific primers also showed that expression levels of both strands of *AG* RNA from the fusion gene in p35S::A-GUS-S increase with increasingly severe phenotypes (data not shown).

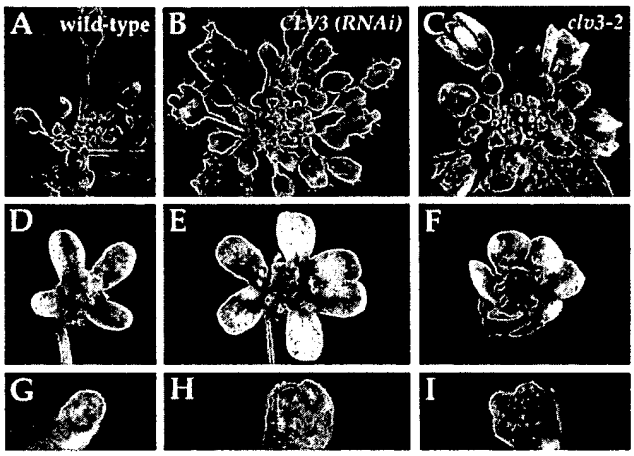

Fig. 4. Phenotypes of wild-type, *CLV3 (RNAi)*, and *clv3–2* plants. Wild-type and *CLV3 (RNAi)* mutants are in the ecotype Wassilewskija, whereas *clv3–2* is in the ecotype Landsberg *erecta* which has reduced internode elongation. The inflorescence meristems are enlarged in *CLV3 (RNAi)* (*B*) and *clv3–2* (*C*) compared with wild type (*A*). (*D*) Wild-type flower. (*E*) *CLV3 (RNAi)* and (*F*) *clv3–2* flowers have additional organs. (*G–I*) Cross section of gynoecia showing that the wild-type gynoecium (*G*) consists of two carpels, and gynoecia in *CLV3 (RNAi)* (*H*) and *clv3–2* (*I*) have four carpels.

Furthermore, Western blot analysis of total protein from wild-type and *AG (RNAi)* mutants with an AG-specific polyclonal antibody (42) demonstrated that the severity of phenotypes is correlated with a reduction of the AG protein level in *AG (RNAi)* mutants. AG protein is weakly expressed in weak and intermediate *AG (RNAi)* mutants. In contrast, it is not detected at levels above background in intermediate/strong and strong *AG (RNAi)* mutants (Fig. 3*O*).

Genetic Interference by *CLV3* and *AP1* dsRNAs. We further assessed the effectiveness and specificity of dsRNA with the *CLV3* and *AP1* genes. Plants with mutations in the *CLV3* gene have enlarged meristems and extra floral organs, especially carpels (Fig. 4 *C*, *F*, and *I*) (33). The majority of *CLV3 (RNAi)* mutants (89%, n = 121) have flowers with extra carpels (Fig. 4*H*); however, only 2% of those plants (n = 108) also have extra sepals, petals, and stamens (Fig. 4*E*). In addition, some *CLV3 (RNAi)* mutant plants (26%, n = 121) have enlarged shoot apical meristems with distortions in phyllotaxy (Fig. 4*B*) and bifurcation, flattening, and broadening of the stem (data not shown). In contrast, only 1% (n = 176) of plants transformed with p35S::A-NOS::S for *CLV3* have the extra carpel phenotype. *clv3* mutant phenotypes were not observed in transgenic plants containing the *CLV3* antisense construct (n = 273).

Mutations in the *AP1* gene result in homeotic alterations of the outer two whorls and a partial or complete conversion of a floral meristem into an inflorescence meristem (34, 35). In weak *ap1* mutant alleles, the first and second whorls consist of mosaic sepaloid organs and staminoid petals, respectively (Fig. 5*B*). In intermediate *ap1* mutant alleles, flowers have leaf-like first whorl organs and leaf-like or staminoid second whorl organs (Fig. 5*C*). In strong *ap1* mutant alleles, bract-like organs are produced in the first whorl and petals are usually absent in the second whorl (Fig. 5*D*). In addition, secondary flowers usually arise from the axils of the first whorl organs in flowers of intermediate and strong *ap1* mutant alleles (Fig. 5 *C* and *D*). About 96% of transgenic plants (n = 260) containing the *AP1* dsRNA-expressing construct, p35S::A-GUS-S, produced flowers similar to those of *ap1* mutant alleles (Fig. 5 *E–H*). Weak (Fig. 5*E*), intermediate (Fig. 5*F*), intermediate/strong (Fig. 5*G*), and strong (Fig. 5*H*) phenotypes were observed in 94, 1, 3, and 2%, respectively, of *AP1 (RNAi)* mutants (n = 249). In contrast, transgenic plants containing the *AP1* construct in the antisense orientation (6%, n = 140) had very weak mutant phenotypes (data not shown). The *AP1* sense construct did not cause mutant phenotypes in transgenic plants (n = 62; data not shown).

One *CLV3 (RNAi)* T_1 plant and 6 *AP1 (RNAi)* T_1 plants of variable severity were selfed to examine the inheritance of genetic interference (Table 2). The progeny from each selected plant showed similar severity of phenotypes to those of the selfed parents, and the severity of phenotypes is constant between mutant siblings of each lineage. In addition, the progeny of *AP1 (RNAi)* plants had 3:1 (mutant/wild type) segregation ratios, suggesting that each of the 6 *AP1 (RNAi)* T_1 plants contained one copy of the transgene. This result indicates that dsRNA-expressing constructs, which are integrated into the plant genome, are stably inherited in a Mendelian fashion, and that the RNAi effect persists to, or recurs in, new generations of plants.

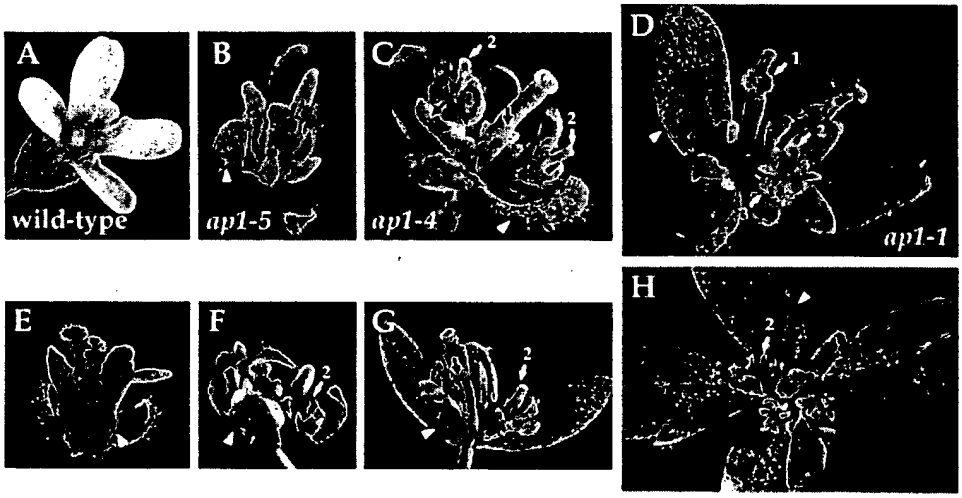

Fig. 5. Phenotypes of wild-type, *ap1* and *AP1 (RNAi)* flowers. (*A*) Wild-type flower. (*B*) *ap1–5* flower. (*C*) *ap1–4* flower. (*D*) *ap1–1* flower. (*E–H*) Flowers from weak (*E*), intermediate (*F*), intermediate/strong (*G*), and strong (*H*) *AP1 (RNAi)* plants. Arrowheads indicate leaf- or bract-like first whorl organs. The numbered arrows indicate the primary (1), secondary (2), and tertiary (3) flowers. The black arrows in *C* and *G* indicate leaf-like or staminoid second-whorl organs.

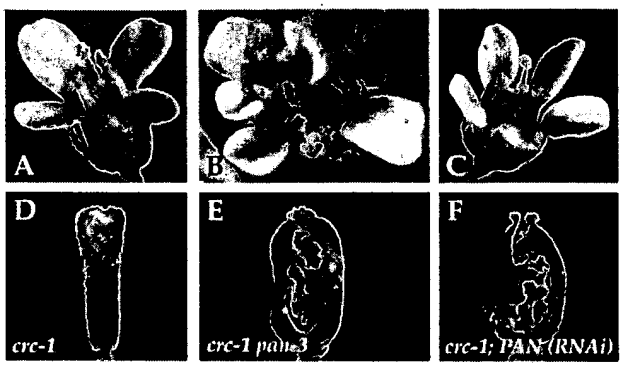

Fig. 6. Effects of PAN dsRNA on *crc-1* transgenic plants. (*A* and *D*) *crc-1*. (*B* and *E*) *crc-1 pan-3* and (*C* and *F*) *crc-1; PAN (RNAi)* flowers have extra organs and unfused gynoecia.

RNA-Mediated Interference with *PAN*. Flowers of plants mutant for *pan* are characterized by an increase in the organ number in the first two whorls, and a decrease in the organ number in the third whorl. Mutant flowers usually have five sepals, five petals, five stamens, and two carpels (36). When introduced into wild-type plants, the dsRNA-expressing construct of *PAN* caused either no, or weak, extra organ phenotypes. Reverse transcription–PCR analysis showed that *PAN* mRNA was reduced by 30–90% in *PAN (RNAi)* plants compared with wild-type plants (data not shown), suggesting that a small portion of PAN activity is sufficient for its function in wild-type plants. This hypothesis is consistent with results from previous immunohistochemical analysis showing that the mutant *pan-1* and *pan-2* alleles, with high expressivity of the extra organ phenotype, are likely null alleles (30).

Whereas flowers homozygous for strong mutant alleles show high penetrance of the extra organ phenotype, only the first few flowers from homozygotes of weak mutant alleles show the phenotype. However, both strong and weak *pan* alleles cause high penetrance of unfused carpel phenotypes in a *crc-1* genetic background (Fig. 6 *A*, *B*, *D*, and *E*) (30, 44), suggesting that *crc* mutants provide a more sensitive background than wild type in which to observe phenotypic effects of *PAN* reduction-of-function mutations. Therefore, RNA-expressing constructs corresponding to *PAN* were introduced into a *crc-1* homozygous background to further assess the potential of RNA-mediated interference with *PAN*. Similar to *pan* alleles, *PAN* dsRNA-expressing constructs, p35S::A-GUS-S (87%, n = 126) and p35S::A-NOS::S (27%, n = 66), caused extra organ number and unfused carpels in *crc-1* (Fig. 6 *C* and *F*). Antisense (55%, n = 76) and sense (33%, n = 6) sequences corresponding to *PAN* have similar RNAi effects as well (data not shown), suggesting that low levels of dsRNAs might be produced in such a case and weak interference with *PAN* activity is sufficient to confer an unfused carpel phenotype in *crc-1*.

Discussion

This study shows that dsRNA-mediated genetic interference can operate in *A. thaliana* to efficiently induce sequence-specific inhibition of gene function. Although the technique of RNA microinjection has been widely used in *C. elegans* (13–15, 44), *Drosophila* (20, 21), and planarians (23), methods for RNA injection into zygotes of *A. thaliana* are not available. However, *Agrobacterium*-mediated transformation provides a convenient and efficient method to introduce dsRNA-expressing constructs into the plant genome. Therefore, RNAi in transgenic plants is persistent and inherited instead of being transient and unstable as in RNA-injected animals (13–15, 20, 21, 23, 45) and transiently transfected cells (22). In addition, inducible and tissue-specific promoters might be used to obtain regulated RNAi.

In this study, two kinds of dsRNA-expressing constructs, p35S::A-GUS-S and p35S::A-NOS::S, were used to investigate RNAi effects. p35S::A-NOS::S is less potent at inducing genetic interference than p35S::A-GUS-S, perhaps because of unequal expression levels of sense and antisense RNAs by two promoters of different strength. The nopaline synthase promoter is much weaker than the 35S promoter, suggested by the observation that pNOS::A-GUS-S has weaker genetic interference than p35S::A-GUS-S. These results suggest that equal and high levels of both strands of each RNA in each cell are essential for inducing potent RNAi. If this is true, use of two strong promoters of similar strength should improve RNAi effects of dsRNA-expressing constructs in which sense and antisense RNAs are produced separately; however, use of two identical promoters in a construct should be avoided to prevent cosuppression (46).

dsRNAs corresponding to four genes selected in this study caused potent and specific genetic interference, suggesting that dsRNA-mediated gene silencing can occur in the tissues where these genes normally function. In addition, a phenotypic series can be obtained from RNAi mutants. The fact that the severity of phenotypes varied between T_1 individuals is possibly because of variable transgene copy number and/or positional effects of particular DNA insertion events. However, our results suggest that severity of phenotypes in *API (RNAi)* T_1 plants is not related to the transgene copy number.

CLV3 dsRNA seems predominantly to block gene function in a subset of the cells where it is normally expressed. *CLV3* is expressed in the inflorescence and the floral meristems (28). Mutations in the *CLV3* gene cause enlarged meristems and extra floral organs (33). About 89% of *CLV3 (RNAi)* plants have flowers with extra carpels but only 26% of *CLV3 (RNAi)* plants have enlarged inflorescence meristems. This result suggests a strong suppression of the *CLV3* gene function in the center of the floral meristem but less suppression of its function in the inflorescence meristem. It is probably because of differential activity of the 35S promoter which drives expression of dsRNA in these tissues. It is also possible that some tissues could partially resist RNAi (25), or that some phenotypes (such as enlarged inflorescence meristems) are less sensitive to the level of gene activity.

When used as controls for RNAi experiments, the sense and antisense constructs of *PAN* also had the ability to induce genetic interference in a *crc-1* homozygous background; so did the *API* antisense construct in wild-type plants. It has been suggested that low levels of dsRNA might be produced from transgenes that are designed to produce only antisense or only sense RNA, via the readthrough transcription from transgenes arranged as an inverted repeat, or transcription from a transgene whose 3′ end is adjacent to an endogenous promoter (19, 24, 25, 47). Alternatively, it seems possible that cellular RNA-dependent RNA polymerase could be involved in the conversion of single-stranded RNA to dsRNA in a cell-specific manner, suggested by the cloning and *in vitro* catalytic analysis of an RNA-dependent RNA polymerase from tomato (25, 48).

In situ hybridization revealed a correlation between decreasing levels of *AG* mRNA accumulation and increasing severity of phenotypes in *AG (RNAi)* plants, suggesting that the mechanism blocking mRNA accumulation could be responsible for dsRNA interference. This result is consistent with previous findings that endogenous mRNA is a target of dsRNA-mediated genetic interference (13, 14, 22, 23). In addition, a recent report of isolation of an RNaseD homolog from *C. elegans* mutants which are resistant to RNAi suggests that RNAi works by dsRNA-directed, enzymatic RNA degradation (49).

Whatever the mechanism by which RNAi acts to reduce specific mRNA levels, the experiments described here show that it is a useful method for determining the loss-of-function phe-

notypes of genes involved in development and meristem activity in *A. thaliana*.

We thank John Bowman and Yuval Eshed for critical reading of the manuscript; Xavier Ambroggio, Catherine Baker, Chieh Chang, Toshiro Ito, Jeff Long, Kazuaki Ohashi, Carolyn Ohno, G. Venugopala Reddy, Doris Wagner, Frank Wellmer, and Eva Ziegelhoffer for their comments on the manuscript; Amani Zewail for technical assistance; and Toshiro Ito for providing the anti-AG antibody. This work was supported by National Institutes of Health Grant GM45697 to E.M.M.

1. Baier, M. & Dietz, K. J. (1999) *Plant Physiol.* **119,** 1407–1414.
2. Coles, J. P., Phillips, A. L., Croker, S. J., Garcia-Lepe, R., Lewis, M. J. & Hedden, P. (1999) *Plant J.* **17,** 547–556.
3. Haldrup, A., Naver, H. & Scheller, H. V. (1999) *Plant Cell* **17,** 689–698.
4. Huang, N. C., Liu, K. H., Lo, H. J. & Tsay, Y. F. (1999) *Plant Cell* **11,** 1381–1392.
5. Nanjo, T., Kobayashi, M., Yoshiba, Y., Sanada, Y., Wada, K., Tsukaya, H., Kakubari, Y., Yamaguchi-Shinozaki, K. & Shinozaki, K. (1999) *Plant J.* **18,** 185–193.
6. Ni, M., Tepperman, J. M. & Quail, P. H. (1998) *Cell* **95,** 657–667.
7. Yoshizumi, T., Nagata, N., Shimada, H. & Matsui, M. (1999) *Plant Cell* **11,** 1883–1896.
8. Bell, E., Creelman, R. A. & Mullet, J. E. (1995) *Proc. Natl. Acad. Sci. USA* **92,** 8675–8679.
9. Naver, H., Haldrup, A. & Scheller, H. V. (1999) *J. Biol. Chem.* **274,** 10784–10789.
10. Kempin, S. A., Liljegren, S. J., Block, L. M., Rounsley, S. D., Yanofsky, M. F. & Lam, E. (1997) *Nature (London)* **389,** 802–803.
11. Mckinney, E. C., Ali, N., Traut, A., Feldmann, K. A., Belostotsky, D. A., McDowell, J. M. & Meagher, R. B. (1995) *Plant J.* **8,** 613–622.
12. Winkler, R. G., Frank, M. R., Galbraith, D. W., Feyereisen, R. & Feldmann, K. A. (1998) *Plant Physiol.* **118,** 743–750.
13. Fire, A., Xu, S., Montgomery, M. K., Kostas, S. A., Driver, S. E. & Mello, C. C. (1998) *Nature (London)* **391,** 806–811.
14. Montgomery, M. K., Xu, S. & Fire, A. (1998) *Proc. Natl. Acad. Sci. USA* **95,** 15502–15507.
15. Shi, Y. & Mello, C. (1998) *Genes Dev.* **12,** 943–955.
16. Tabara, H., Grishok, A. & Mello, C. C. (1998) *Science* **282,** 430–431.
17. Timmons, L. & Fire, A. (1998) *Nature (London)* **395,** 854 (lett.).
18. Voinnet, O., Vain, P., Angell, S. & Baulcombe, D. C. (1998) *Cell* **95,** 177–187.
19. Waterhouse, P. M., Graham, M. W. & Wang, M.-B. (1998) *Proc. Natl. Acad. Sci. USA* **95,** 13959–13964.
20. Kennerdell, J. R. & Carthew, R. W. (1998) *Cell* **95,** 1017–1026.
21. Misquitta, L. & Paterson, B. M. (1999) *Proc. Natl. Acad. Sci. USA* **96,** 1451–1456.
22. Ngo, H., Tschudi, C., Guli, K. & Ullu, E. (1998) *Proc. Natl. Acad. Sci. USA* **95,** 14687–14692.
23. Alvarado, A. S. & Newmark, P. A. (1999) *Proc. Natl. Acad. Sci. USA* **96,** 5049–5054.
24. Montgomery, M. K. & Fire, A. (1998) *Trends Genet.* **14,** 255–258.
25. Fire, A. (1999) *Trends Genet.* **15,** 358–363.
26. Sharp, P. A. (1999) *Genes Dev.* **13,** 139–141.
27. Yanofsky, M. F., Ma, H., Bowman, J. L., Drews, G. N., Feldmann, K. A. & Meyerowitz, E. M. (1990) *Nature (London)* **346,** 35–39.
28. Fletcher, J. C., Brand, U., Running, M. P., Simon, R. & Meyerowitz, E. M. (1999) *Science* **283,** 1911–1914.
29. Mendel, M. A., Gustafson-Brown, C., Savidge, B. & Yanofsky, M. F. (1992) *Nature (London)* **360,** 273–277.
30. Chuang, C.-F., Running, M. P., Williams, R. W. & Meyerowitz, E. M. (1999) *Genes Dev.* **13,** 334–344.
31. Bowman, J. L., Smyth, D. R. & Meyerowitz, E. M. (1989) *Plant Cell* **1,** 37–52.
32. Bowman, J. L. (1994) in *Arabidopsis: An Atlas of Morphology and Development*, ed. Bowman, J. L. (Springer, New York), pp. 216–221.
33. Clark, S. E., Running, M. P. & Meyerowitz, E. M. (1995) *Development (Cambridge, U.K.)* **121,** 2057–2067.
34. Bowman, J. L., Alvarez, J., Weigel, D., Meyerowitz, E. M. & Smyth, D. R. (1993) *Development (Cambridge, U.K.)* **119,** 721–743.
35. Irish, V. F. & Sussex, I. M. (1990) *Plant Cell* **2,** 741–753.
36. Running, M. P. & Meyerowitz, E. M. (1996) *Development (Cambridge, U.K.)* **122,** 1261–1269.
37. McBride, K. E. & Summerfelt, K. R. (1990) *Plant Mol. Biol.* **14,** 269–276.
38. Krizek, B. A. & Meyerowitz, E. M. (1996) *Proc. Natl. Acad. Sci. USA* **93,** 4063–4070.
39. Bechtold, N., Ellis, J. & Pelletier, G. (1993) *C. R. Acad. Sci.* **316,** 1194–1199.
40. Drews, G. N., Bowman, J. L. & Meyerowitz, E. M. (1991) *Cell* **65,** 991–1002.
41. Sakai, H., Medrano, L. J. & Meyerowitz, E. M. (1995) *Nature (London)* **378,** 199–203.
42. Ito, T., Takahashi, N., Shimura, Y. & Okada, K. (1997) *Plant Cell Physiol.* **38,** 248–258.
43. Smyth, D. R., Bowman, J. L. & Meyerowitz, E. M. (1990) *Plant Cell* **2,** 755–767.
44. Alvarez, J. & Smyth, D. R. (1999) *Development (Cambridge, U.K.)* **126,** 2377–2386.
45. Tabara, H., Sarkissian, M., Kelly, W. G., Fleenor, J., Grishok, A., Timmons, L., Fire, A. & Mello, C. C. (1999) *Cell* **99,** 123–132.
46. Baulcombe, D. C. & English, J. J. (1996) *Curr. Opin. Biotechnol.* **7,** 173–180.
47. Kooter, J. M., Matzke, M. A. & Meyer, P. (1999) *Trends Plant Sci.* **4,** 340–347.
48. Schiebel, W., Pélissier, T., Riedel, L., Thalmeir, S., Schiebel, R., Kempe, D., Lottspeich, F., Sänger, H. L. & Wassenegger, M. (1998) *Plant Cell* **10,** 2087–2101.
49. Ketting, R. F., Haverkamp, T. H., van Luenen, H. G. & Plasterk, R. H. (1999) *Cell* **99,** 133–141.

The Plant Journal (2001) 25(4), 417–425

Size constraints for targeting post-transcriptional gene silencing and for RNA-directed methylation in *Nicotiana benthamiana* using a potato virus X vector

Carole L. Thomas[1], Louise Jones[2], David C. Baulcombe[2] and Andrew J. Maule[1,*]
[1] *Department of Virus Research and*
[2] *The Sainsbury Laboratory, John Innes Centre, Norwich Research Park, Colney, Norwich NR4 7UH, UK*

Received 11 August 2000; revised 20 November 2000; accepted 1 December 2000.
*For correspondence (fax +44 1603 450045; e-mail andy.maule@bbsrc.ac.uk).

Summary

Using a recombinant potato virus X (PVX) vector, we investigated the relationship between the length of RNA sequence identity with a transgene and the ability to promote post-transcriptional gene silencing (PTGS) and transgene methylation. The lower size limit required for targeting reporter transgene mRNA *de novo* using PTGS was 23 nucleotides (nt) of complete identity, a size corresponding to that of small RNAs associated with PTGS in plants and RNA interference (RNAi) in animals. The size and sequence specificity were also explored for PTGS-associated transgene methylation and for the targeting of the vector RNA. The PTGS-competent short sequences resulted in similar patterns of methylation. In all cases, including specific sequences of 33 nt with or without symmetrical cytosine residues, the methylation was distributed throughout the transcribed region of the transgene. In contrast, short sequences lacking symmetrical cytosines were less efficient at promoting PTGS of the transgene mRNA. Short *gfp* sequences in the PVX vector provided as effective a target for the degradation of viral RNA as was found for PVX carrying the complete *gfp* cDNA. Short sequences were able to initiate PTGS of an endogenous gene, phytoene desaturase, although this occurred in the absence of DNA methylation. This experimental approach provides important insights into the relationship between short RNA sequences and PTGS.

Keywords: post-transcriptional gene silencing, methylation, transgenes, homology, minimal size, small RNAs.

Introduction

Post-transcriptional gene silencing (PTGS) is based on a homology-dependent degradation of RNA in the cytoplasm. The target RNA may be derived from transgenes, endogenous genes or viruses. Although originally identified in plants as the underlying mechanism obtained from the transgenic expression of virus-derived sequences, PTGS is now recognized as a fundamental process related to a wide range of epigenetic phenomena (reviewed by Depicker and Van Montagu, 1997; Fagard and Vaucheret, 2000; Plasterk and Ketting, 2000; Stam *et al.*, 1997; Van den Boogaart *et al.*, 1998). It is also apparent that PTGS is not restricted to plants, being mechanistically related to quelling in *Neurospora* (Cogoni and Macino, 1999; Cogoni *et al.*, 1996) and RNAi in *Caenorhabditis elegans* (Fire *et al.*, 1998); *Escherichia coli* (Tchurikov *et al.*, 2000); *Drosophila melanogaster* (Kennerdell and Carthew, 1998; Misquitta and Paterson, 1999); fish (Wargelius *et al.*, 1999; Yx *et al.*, 2000); and mammals (Wianny and Zernicka-Goetz, 2000). Particularly compelling is the involvement of homologous genes in *Neurospora, C. elegans* and *Arabidopsis thaliana* (Cogoni and Macino, 1999; Dalmay *et al.*, 2000a; Mourrain *et al.*, 2000; Smardon *et al.*, 2000) and the association of small RNAs with PTGS and RNAi in plants (Hamilton and Baulcombe, 1999) and *Drosophila* (Hammond *et al.*, 2000; Zamore *et al.*, 2000), respectively. In plants, small RNAs were found associated with silenced transgenes and virus infection; small RNAs of the same size (21 and 23 nt) were shown to activate the homology-dependent degradation of target RNAs in cell free extracts of *Drosophila* embryos, and to generate further similar RNAs as products (Zamore

et al., 2000). For plants, it was also proposed (Hamilton and Baulcombe, 1999) that these small RNAs might constitute cellular signals for the induction of PTGS, both locally and at more distal regions of the plant. However, it has not been shown that such short lengths of RNA are capable of promoting PTGS-mediated targeting of homologous RNA *de novo*.

The potential for RNA to interact with genomic sequences has been shown (Wassenegger *et al.*, 1994), even when the RNA is generated outside the nucleus. Hence infection of transgenic plants with cytoplasmically replicating RNA viruses resulted in *de novo* methylation of the transgene if the viral RNA contained regions of homology with the genomic DNA (Jones *et al.*, 1998, Jones *et al.*, 1999). If the homology corresponded to the transgene promoter, transcriptional gene silencing ensued. Homology corresponding to the transgene mRNA sequence was associated with PTGS. In this case, methylation was restricted to the transcribed region, but spread beyond the initial region of homology (Jones *et al.*, 1999). Although a tight correlation between methylation and PTGS has been shown (English *et al.*, 1996; Ingelbrecht *et al.*, 1994; Jones *et al.*, 1998; Sijen *et al.*, 1996; Van Houdt *et al.*, 1997), the relevance of methylation for PTGS remains uncertain. It has been suggested, however, that methylation could be involved in the amplification and maintenance of transgene-mediated PTGS (Dalmay *et al.*, 2000b; Jones *et al.*, 1999).

In this paper, we have used the ability of potato virus X (PVX) carrying sequences derived from the *Aequoria victoria* green fluorescent protein gene (*gfp*) to silence *gfp* expression in non-silenced *gfp*-transgenic *Nicotiana benthamiana* plants to assess the size and sequence requirements for promoting PTGS of *gfp* mRNA and transgene methylation. The data support the view that short homologous RNA sequences of 23 nt can target PTGS to *gfp* mRNA *de novo*, but that towards the lower size limits efficiency may be influenced by the sequence itself.

Results

Nucleic acid homology of 23 nt is sufficient to direct PTGS to, and de novo *methylation of, a GFP transgene*

To determine the shortest homologous RNA sequence able to target PTGS to *gfp* mRNA, fragments of *gfp* DNA were cloned into a PVX cDNA vector and the virus inoculated to *gfp*-transgenic *N. benthamiana*. The *gfp* fragments, generated by DNaseI digestion, were size selected (<100 bp) before cloning, and the resultant clones were sequenced. The orientation and origin of the fragments are shown in Figure 1(a). Surprisingly, there was a strong 3′ bias in the source distribution of the cloned fragments, although there was an equal distribution of clones in the sense (S) and antisense (AS) orientations (Figure 1a). These cloned fragments were compared with PVX-GFP containing the complete *gfp* cDNA for their ability to direct silencing. The plants were scored visually for silencing of *gfp* expression 25 (Figure 1b), 34 and 41 days post-infection (dpi). Under UV illumination silencing was seen as the loss of green GFP fluorescence to

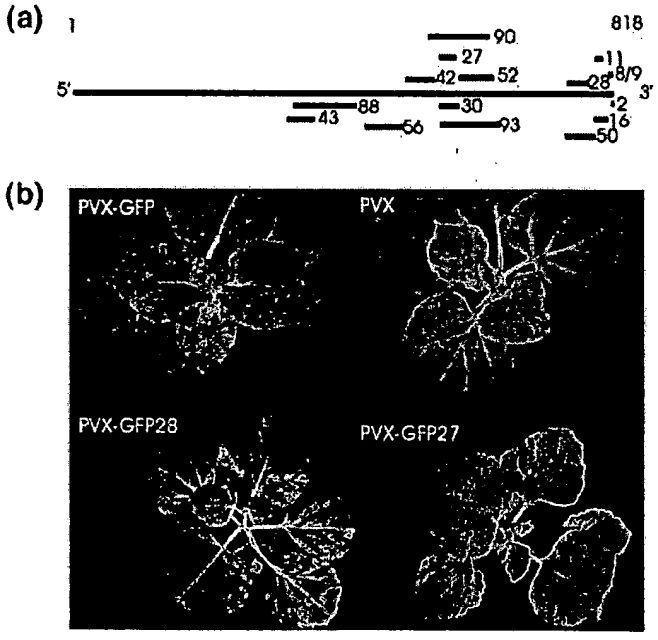

Figure 1. Effect of random *gfp* fragments on directing silencing to *gfp* transgene mRNA.
(a) Origin of random *gfp* DNAse I fragments of <100 nt inserted in the PVX vector for testing as promoters of *gfp* PTGS. Numbers indicate the size of the fragments. Sequences above the line were cloned in the S orientation, those below in the AS orientation.
(b) Phenotypes of plants observed under UV illumination at 25 dpi with PVX-GFP, PVX (no insert), PVX-GFP28 (28 nt) or PVX-GFP27 (27 nt).

Table 1. Silencing of *gfp* with PVX containing 20–30 nt homology to three distinct regions of *gfp* DNA

gfp region	Size (nt)	Nucleotide position	Sense (S/AS)	Silencing (+/–)
Region 1	20	316–335	S	–
	20	316–335	AS	–
	23	316–338	S	–
	23	316–338	AS	+
	27	316–342	S	+
	27	316–342	AS	+
	30	316–345	S	+
	30	316–345	AS	+
Region 2	20	550–569	AS	–
	21	550–570	S	–
	23	550–572	S	–
	27[a]	550–576	S	+
	30[a]	550–579	AS	+
Region 3	20	746–765	AS	–
	22	746–767	S	–
	23	746–768	S	+
	23	746–768	AS	+
	27	746–772	AS	+
	28[a]	746–773	S	+
	30	746–775	S	+
	30	746–775	AS	+

[a]Sequences also tested from the preliminary random fragmentation of *gfp*.

reveal red chlorophyll fluorescence (Figure 1b). The range of fragments required to promote silencing showed a sharp cut-off in size, with fragments of 27 nt and larger being effective, but fragments of 16 nt and less being ineffective. Fragments in either sense or antisense orientation were effective.

Although all fragments of 27 nt and larger were able to direct silencing, there was a marked difference in their relative effectiveness. In contrast to the response to PVX-GFP, which resulted in rapid and complete silencing (full red fluorescence) by 20 dpi, many of the smaller fragments took longer and showed a patchy silencing phenotype in the early stages of the infection. The largest variation was seen at 25 days (Figure 1b) when comparing PVX-GFP27 (27 nt), PVX-GFP28 (28 nt) and PVX-GFP (818 nt). Close to the minimal size for successful silencing, just a 1 nt difference in the length of homologous RNA had a dramatic effect on silencing efficiency. Eventually all the competent RNA fragments produced leaves showing an extensively red fluorescent phenotype.

To obtain a more precise estimate of the size limit for silencing, a targeted approach was taken whereby nested synthetic oligonucleotides of 20, 23 27 and 30 nt to three different regions of *gfp* (nt 316–345, nt 550–579 and nt 746–775) were inserted into the PVX vector. In most cases insertions in both orientations were obtained. With the contribution from the flanking nucleotides from the *SmaI* cloning site, a range of *gfp* homologies of 20–30 nt resulted (Table 1). The recombinant PVX variants were inoculated onto *N. benthamiana* and again scored for the initiation of silencing. After 45 dpi, silencing was seen when the homology was 23 nt or longer (Table 1). There were two exceptions (PVX *gfp* homology 316–338 and 550–572 in the S orientation), which failed to initiate silencing despite having 23 nt *gfp* homology. However, close to the lower limit for silencing, homologous sequences in the AS orientation appeared to be more efficient (data not shown). No viruses with homologous sequences of less than 23 nt initiated *gfp* silencing. Consistent with the random approach, initiation of silencing was slower and patchy with the smaller fragments (data not shown).

Surprisingly, one 27-mer *gfp*-specific oligonucleotide (nt 746–772) did not initiate silencing (data not shown), even though it covered a 23 nt region (nt 746–768) which was competent for silencing (Table 1). However, sequencing of these 27 nt identified an error in the sequence which divided the 27 nt into 12 and 14 nt of identity with *gfp*.

Previously, in the same experimental system (Jones *et al.*, 1999), we had shown that GFP-specific RNA in the PVX vector was able to direct methylation of the transcribed region of the *gfp* transgene, irrespective of whether the 5′ or 3′ regions of the sequence were used as inducers. To see whether the short *gfp* fragments retained their capacity as inducers of methylation, genomic DNA from completely silenced tissues of plants infected with PVX-GFP28 (28S nt), PVX-GFP43 (43AS nt) or PVX-GFP were subjected to analysis using *Sau96I* and Southern blotting with the complete *gfp* cDNA, as before (Jones *et al.*, 1999). *Sau96I*, which has a recognition sequence GGNCC, is sensitive to methylation of canonical or symmetrical cytosine residues (CpG or CpNpG), or non-symmetrical C residues when the nt 3′ to GGNCC is not a G residue. The organization of the 35S:*gfp* transgene, the location of restriction sites, and the sizes of digestion products of a non-methylated GFP transgene are shown in Figure 2(a). In non-silenced, infected tissue (Figure 2b, lane 1) only the two major *gfp*-specific fragments of 0.56 and 0.28 kb were detected. In contrast, in silenced, infected tissue additional fragments of 0.36, 0.84 and 1.3 kb were detected; the pattern of fragments was the same for all the samples (Figure 2b, lanes 2–4). This indicated a partial methylation at the three *Sau96I* sites internal to the *gfp* sequence, but no methylation at the flanking sites in the non-transcribed 35S and tnos portions of the transgenes. Incomplete RNA-directed methylation was also a feature of previous, related studies (Jones *et al.*, 1998, Jones *et al.*, 1999). The complete digestion of the DNA with *Sau96I* was confirmed by re-probing the Southern blot for *hsp70* DNA, as shown by the detection of just a single 1.4 kbp band in all lanes (Figure 2c).

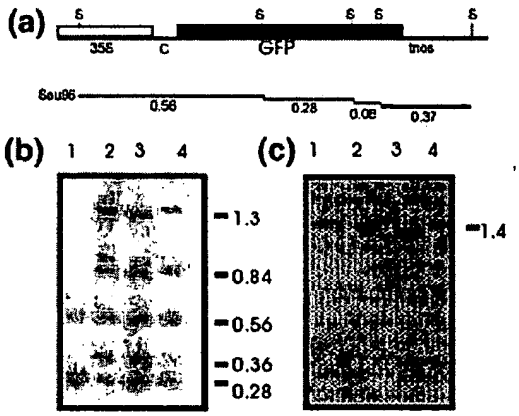

Figure 2. Methylation associated with PTGS of *gfp* initiated using short, homologous *gfp* sequences.
(a) Structure of the *gfp* transgene is shown as including the 35S promoter (35S; open box), the chitinase endoplasmic reticulum targeting signal sequence (C), *gfp* coding sequence (solid box), and the nopaline synthase terminator (tnos). *Sau96*I restriction sites and sizes of the expected digestion products in kilobases are shown below.
(b,c) Southern blot analyses of genomic DNA samples from tissue infected with PVX, non-silenced leaves (lane 1), PVX-GFP silenced (lane 2), PVX-GFP43 (43 nt *gfp*) silenced (lane 3), and PVX-GFP28 (28 nt *gfp*) silenced (lane 4) leaves of *gfp*-transgenic *N. benthamiana* plants. The same blot was probed sequentially with *gfp* (b) and *hsp70* (c) cDNAs. Sizes (in kilobases) of relevant DNA fragments are indicated.

Table 2. Silencing of *gfp* with PVX containing oligonucleotides (33 nt) with or without symmetrical cytosine residues

PVX-Oligo	Nucleotide position	Polarity (S/AS)	CNG or CG	Silencing (+/–)
A	786–818	S	No	+
B	786–818	AS	No	+
C	497–529	AS	No	+
D	508–540	S	Yes	+
E	508–540	AS	Yes	+
F	746–778	S	Yes	+
G	746–778	AS	Yes	+
GFP28	746–773	S	Yes	+
GFP	1–818	S	Yes	+
PVX	NA	NA	NA	–

Canonical CpG and CpNpGp are not essential for de novo *methylation for a GFP transgene*

The identification of short sequences capable of initiating PTGS allowed us to test the effect of specific RNA sequences for the capacity to induced methylation, particularly to address the importance of canonical CpG or CpNpG residues. Unfortunately, the shortest competent fragment for silencing (23 nt) did not allow *gfp*-specific sequences completely devoid of C residues to be tested. It has been suggested that methylation of symmetrically located Cs may provide nucleation centres for the spread of methylation to adjacent non-symmetrical C residues (Finnegan *et al.*, 1998). To test the significance of CpG or CpNpG for inducing methylation, two regions of *gfp* devoid of symmetrical C residues were identified, and corresponding S and AS synthetic oligonucleotides inserted into the PVX vector. The regions identified (Table 2) made it possible to use sequences of 33 nt, which had the advantage of increasing the efficiency of PTGS induction. Adjacent sequences containing symmetrical C residues were tested in parallel (Table 2). Unfortunately, the sense oligonucleotide corresponding to *gfp* nt 497–529 was unstable in the PVX vector, and could not be analysed further.

PVX-oligo-A to -G, PVX-GFP28, PVX-GFP and wild-type PVX were all agro-inoculated to *gfp-N. benthamiana* and scored for silencing after 25 days (Table 2). All the viruses carrying *gfp* sequences effectively initiated silencing. Although some constructs were more effective than others at 25 dpi, by 41 dpi the silencing from each construct was complete. This experiment was repeated five times using two plants per construct. The least efficient initiators of silencing were always the oligonucleotides devoid of symmetrical C residues, irrespective of orientation. For reference, these were always weaker than PVX-GFP28 (Figure 1b). No correlation between the strength of silencing and the number of symmetrical C residues in the initiator sequence could be made.

It was possible that the inefficient initiation of *gfp* PTGS by PVX-oligo-A to -C could be attributable to reduced transgene methylation as a result of triggering with a GFP fragment devoid of canonical cytosines. Hence genomic DNA isolated from fully PVX-oligo-silenced tissue at 22 dpi was digested with *Sau96*I and analysed by Southern blot hybridization with a GFP probe to assess the extent of methylation. In this case *Sau96*I digestion gave fragments of 0.56, 0.37 and 0.28 kb for non-silenced samples (Figure 3, lane 1), and additional fragments of 1.3 and 0.84 kb in silenced samples (Figure 3, lanes 2–9). Equivalent data were obtained using a second methylation-sensitive restriction enzyme, *Alu*I (data not shown). Hybridization of the same blots with a probe for *hsp70* confirmed that the pattern of fragments was not due to incomplete digestion of the DNA samples (data not shown).

PTGS targeted to gfp *using small oligonucleotides is able to target recombinant virus for degradation*

When PTGS is directed in a *gfp*-transgenic line by PVX-GFP, the strong silencing targets *gfp* mRNA and PVX-GFP RNA for degradation, and PVX-GFP is prevented from further accumulation (Ruiz *et al.*, 1998). This effect is a combination of the strength of the PTGS response and the potential of PVX containing all the *gfp* cDNA to be seen as a target for degradation. Experiments involving transgenic plants displaying constitutive PTGS-based virus resistance

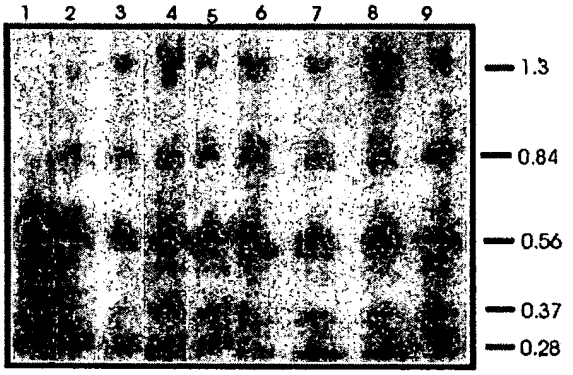

Figure 3. Methylation associated with PTGS of *gfp* induced with recombinant PVX carrying specific *gfp* oligonucleotides.
Southern blot analysis of genomic DNA samples from non-silenced tissues infected with PVX (no insert) (lane 1), and silenced tissues infected with PVX-GFP28 (28 nt; lane 2) or PVX-GFPoligo-A to -G (lane 3–9). The blot was probed with *gfp* cDNA. Sizes (in kilobases) of relevant DNA fragments are indicated.

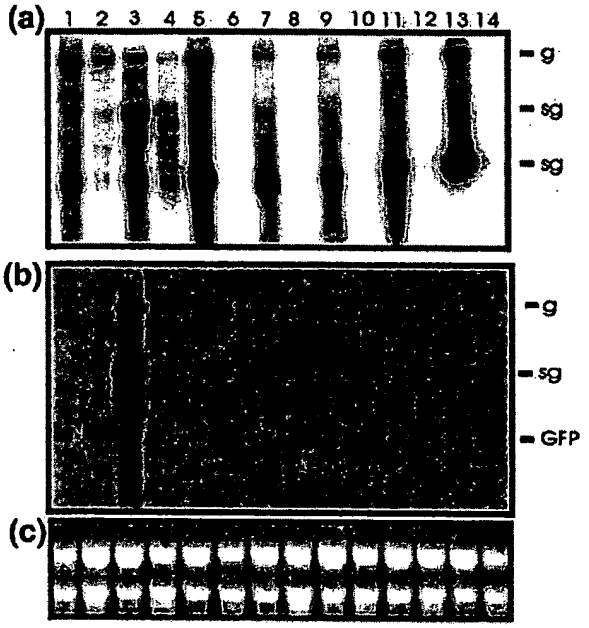

Figure 4. PTGS-mediated targeting of PVX RNA and *gfp* mRNA species.
Northern blot analysis of samples from non-silenced (lanes 1, 2, 3, 5, 7, 9, 11, 13) or silenced (lanes 4, 6, 8, 10, 12, 14) tissues infected with non-recombinant PVX (lanes 1 and 2), PVX-GFP (lanes 3 and 4), PVX-GFP28 (lanes 5 and 6), PVX-oligo-A (S and lacking symmetrical C residues; lanes 7 and 8), PVX-oligo-B (AS and lacking symmetrical C residues; lanes 9 and 10), PVX-oligo-D (S and with symmetrical C residues; lanes 11 and 12) or PVX-oligo-E (AS and with symmetrical C residues; lanes 13 and 14). Non-silenced tissues were harvested at 14 dpi, except for the sample in lane 2, which was harvested with silenced tissues at 27 dpi. Total RNA (10 μg) was probed for either (a) PVX-specific or (b) GFP-specific sequences. Equal gel loadings were confirmed by ethidium bromide staining of ribosomal RNAs (c). The positions of the genomic (g) and subgenomic (sg) PVX RNAs and the *gfp* transgene mRNA (GFP) are marked.

have identified 60 nt as being the smallest region of homology able to tag a recombinant virus for degradation (Sijen *et al.*, 1996). To determine if regions of homology of less than 60 nt were able to identify the recombinant PVX RNAs as targets in a *de novo*-directed PTGS system, and whether the canonical C content might influence the efficiency of targeting, GFP and PVX RNA levels were assessed in tissues silenced by PVX-GFP, PVX-GFP28 and PVX-oligo-A, -B, -D and -E (Table 2). Total RNA from infected, non-silenced tissue 14 dpi, and from silenced tissue 27 dpi, was subjected to Northern analysis using probes for PVX (Figure 4a) or *gfp* (Figure 4b) sequences. The PVX probe detected genomic and subgenomic RNAs for both PVX-GFP and PVX. The *gfp* probe detected *gfp*-transgene mRNA and PVX-GFP; PVX-GFP28 or PVX-oligo RNAs were not detected. The levels of PVX RNA, that accumulated in leaves of *gfp*-transgenic plants at 14 dpi, and in upper leaves at 27 dpi, are shown (Figure 4a, lanes 1 and 2). As previously demonstrated for PVX-GFP (Ruiz *et al.*, 1998), the levels of viral RNAs in the silenced tissue at 27 dpi (Figure 4a, lanes 4, 6, 8, 10, 12, 14) were dramatically reduced compared to the non-silenced tissue at 14 dpi (Figure 4a, lanes 3, 5, 7, 9, 11, 13). The mobility shift of the subgenomic PVX RNA in Figure 4(a), lane 4, and the absence of hybridization with the *gfp* probe (Figure 4b, lane 4), indicates that residual PVX RNA in silenced tissue results from recombination. The absence of recombined PVX in tissues silenced using PVX-oligo suggests that the smaller inserted sequences reduce the propensity for recombination (Figure 4, lanes 5–14). This was confirmed by RT–PCR analysis of extracts of infected plants using primers that enabled the detection of recombinant and wild-type PVX (data not shown). When the 14 and 27 dpi RNA samples were analysed using the *gfp* probe, the expected dramatic reduction in *gfp* mRNA levels was observed in silenced tissues (27 dpi; Figure 4b, lanes 4, 6, 8, 10, 12 and 14). Actually, *gfp* mRNA was reduced even at 14 dpi in tissues infected with PVX-GFP (Figure 4b, lane 3), indicating that the mRNA was more prone to degradation than the virus at this time. The equal loss of PVX-oligo-A, -B, -D and -E RNAs at 27 dpi showed that the content of symmetrical cytosine residues had no influence on the mechanism of RNA targeting and degradation. The loss of these RNAs and PVX-GFP28 also showed that homology as short as 28 nt was sufficient to provide an effective target.

PTGS of an endogenous gene using short regions of homology

To determine whether PTGS of an endogenous gene could be initiated by short regions of homology in PVX, oligonucleotides were designed to different regions of the endogenous phytoene desaturase gene (*pds*). This is a

Table 3. Silencing of phytoene desaturase with PVX containing PDS-specific oligonucleotides

PVX-PDSoligo	Size (nt)	Nucleotide position	Polarity (S/AS)	Silencing (+/–)
1	34	1326–1359	S	–
2	34	1326–1359	AS	–
3	52	1326–1381	S	–
4	52	1326–1381	AS	+
5	33	1498–1530	S	+
6	33	1498–1530	AS	+
7	51	1498–1548	S	+
8	51	1498–1548	AS	+
9	34	1639–1672	S	–
10	34	1639–1672	AS	–
PDS	368	1322–1690	S	+
PVX	NA	NA	NA	–

single-copy, low expressed gene in *N. benthamiana* which has been shown to be susceptible to virus-induced PTGS with a 368 bp fragment of the *N. benthamiana pds* gene (Kumagai *et al.*, 1995; Ruiz *et al.*, 1998). Silencing of *pds* causes suppression of carotenoid biosynthesis so that the affected plants become susceptible to photo-bleaching (Demmig-Adams and Adams, 1992).

Recombinant PVX were constructed carrying *pds* S and AS oligonucleotides specific to different regions within the 3′ half of *N. benthamiana pds* (Table 3). The oligonucleotides, including the contribution from flanking nucleotides in the PVX cloning site, were either 33, 34, 51 or 52 nt, sizes that reproducibly gave strong silencing of the *gfp* transgene. The *pds* sequences were cloned in both orientations into the PVX vector and agro-inoculated onto *N. benthamiana*. As a positive control, 368 bp of *pds* from *N. benthamiana* (corresponding to 1322–1690 nt of the tomato cDNA (Kumagai *et al.*, 1995; Pecker *et al.*, 1992) was used. At 25 dpi plants were scored for the presence of photo-bleaching, indicative of silencing of PDS (Table 3). Unlike the situation with PVX-stimulated silencing of the *gfp*-transgene with sequences longer than 23 nt, not all the PVX-PDSoligo constructs were able to initiate silencing. Broadly, they fell into two classes: those that did, and those that did not cause photo-bleaching (Table 3). Sequences from the *pds* region including nts 1498–1548 were effective irrespective of orientation, whereas the flanking regions were generally ineffective, the exception being AS oligonucleotide 4 (nts 1326–1381). Hence plants infected with PVX-PDSoligos –4 to –8 (Figure 5a, panels 4–8) all showed photo-bleaching, albeit to different degrees. Plants infected with PVX-PDSoligos1–3, 9 and 10 (Figure 5a, panels 1–3, 9, 10) failed to show photo-bleaching, even after 45 d.p.i.

The wide variation in phenotype (more-or-less photo-bleaching) amongst those sequences effective for *pds* silencing revealed some trends. Photo-bleaching was strongest when triggered by sequences in the AS rather than the S orientation (Figure 5a, compare panels 5 and 6; 7 and 8, where 6 and 8 result from the action of AS *pds* sequences 6 and 8). This orientation bias was not observed with larger fragments of *pds* (Ruiz *et al.*, 1998). To confirm that the phenotype related to *pds* mRNA levels, RNA samples from photo-bleached leaves were subjected to semiquantitative duplex RT–PCR (Figure 5b). In comparison with the relative accumulation of *pds* and *ubiquitin* mRNAs in non-silenced tissues infected with PVX (without PDS sequences), both PVX-PDSoligo-7 (S) and PVX-PDSoligo-8 (AS) infections led to a reduction (relative to *ubiquitin*) of *pds* mRNA. This was marginal for PVX-PDSoligo-7, but clear for PVX-PDSoligo-8. It also appeared that larger oligonucleotides (51–52 nt) were more efficient than smaller oligonucleotides (33–34 nt) at initiating silencing (Figure 5a, compare panels 2 and 4; 5 and 7; 6 and 8). However, in the case of PVX-PDSoligo-5 to –8 (Figure 5a, panels 5–8), which cover the same area of *pds*, the AS oligo-6 (33 nt; Figure 5a, panel 6) was more efficient than the S oligo-7 (51 nt; Figure 5a, panel 7). This indicates that orientation may have a stronger influence than size on the silencing of *pds*.

We have previously demonstrated that *de novo* methylation is not associated with silencing of the endogenous gene *rbcs* (Jones *et al.*, 1999). To determine if the same was true of silencing triggered by PVX-PDS or a PVX-PDSoligo, DNA was isolated from *pds* silenced leaf tissue and analysed using methylation sensitive enzymes, *Hin*dIII, and *Hae*III. When probed with *pds* cDNA, there was an identical hybridization profile obtained for both non-silenced and silenced leaf tissue, indicating that *de novo* methylation is not associated with silencing of *pds* (data not shown).

Discussion

By using random fragments of *gfp* and *gfp* oligonucleotides in a virus vector, we were able to assess indirectly the influence of size and sequence on the capacity to direct PTGS *de novo* to *gfp* mRNA in *gfp*-transgenic plants. The shortest length of *gfp* homology with the ability to target silencing to *gfp* mRNA was 23 nt. This correlates well with the size of small RNAs associated previously with PTGS in plants (Hamilton and Baulcombe, 1999; although originally sized at ≈25 nt, improved techniques have provided a more accurate size assessment as 21 and 23 nt, unpublished data), and with the size requirement for RNAi in other systems. Fortuitously, the failure to observe silencing with the 27 nt with incomplete identity with *gfp* (due to the presence of a sequence error) showed that it was necessary for the short initiating sequence to have complete homology with the target. One likely consequence is

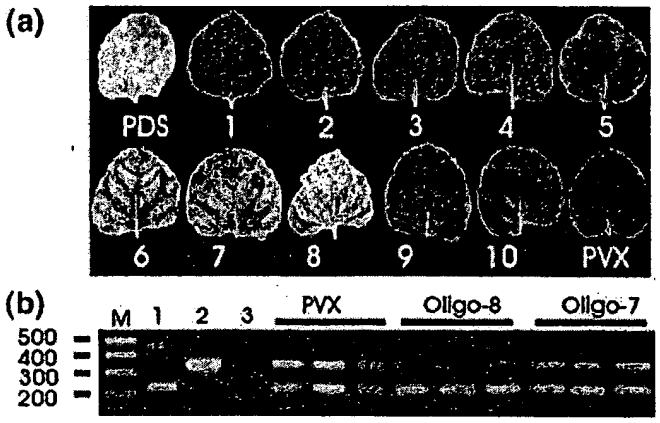

Figure 5. Correlation of the *pds*-silenced phenotype with *pds* mRNA levels.
(a) Phenotype PVX-PDSoligo-1 to -10 infection on the upper leaves of *N. benthamiana* at 26 dpi in relation to that seen after infection with PVX-PDS or PVX (without insert).
(b) Ethidium bromide-stained gel of products obtained after RT–PCR analysis of mRNAs from tissues infected with PVX, PVX-PDSoligo-7 or PVX-PDSoligo-8. Three samples from each of three individual plants were analysed using primers for *ubiquitin* mRNA (lower band) and *pds;* a representative from each plant is shown. Control reactions with RNA isolated from PVX-infected tissue (non-silenced) were carried out separately using primers for *ubiquitin* (lane 1) and *pds* (lane 2). The corresponding bands were never seen in the absence of reverse transcriptase (lane 3). The sizes (bp) of the markers (M) are indicated on the left of the gel.

that the occurrence of PTGS will be determined by the presence or absence of stretches of 23 nt of identity rather than by the mean (percentage) homology between inducer and target.

The efficiency of initiation of silencing increased dramatically when the size of the *gfp* fragment was increased by only a few nt. This may reflect the increase in probability that the exact 23 nt of *gfp* would be generated by a processive cleavage of ds PVX-GFPFrag RNA, as proposed for the cleavage mechanism in *Drosophila* cell-free extracts. The lower size limit for PTGS initiation at 23 nt not only provides evidence that they have the potential to act as signals for inducing PTGS, but also provides an experimental link between the physical identification of small RNAs in plants and their function in *Drosophila* cell-free extracts.

The quantitative nature of the silencing response with short homologous sequences has also been noted for RNAi in *Trypanosoma brucei* (Ngô *et al.*, 1998) and in *Drosophila* cell-free extracts (Tuschl *et al.*, 1999). In the former, 59 nt of homology induced mRNA degradation, but the effect was much stronger with 100–450 nt. In the cell-free extracts, weak RNA degrading activity was directed by dsRNA of 149 nt of homology, but 505 nt was markedly stronger. Surprisingly, a 49 nt RNA was inactive (Tuschl *et al.*, 1999), although the 21–23 nt fraction purified following cell-free RNAi was active in targeting RNA in a new reaction (unpublished data in Zamore *et al.*, 2000).

Logically, if short homologous regions are capable of inducing PTGS, we might expect them to be effective in targeting homologous RNA in the cytoplasm. Previously, Sijen *et al.* (1996) showed that as little as 60 nt homology between a recombinant PVX vector and a transgene could target the virus for degradation to give resistance. Our data show that the same effect can be achieved with just 28 nt homology. In contrast, when silenced transgenes composed of fragments of the tomato spotted wilt virus (TSWV) N gene fused to *gfp* were analysed for their ability to target TSWV, resistance was seen only when >110 nt of N were present in the transgene (Pang *et al.*, 1997). In our experiments, the source of the 28 nt homology would be the sum of the RNA degradation products from the recombinant virus and the transgene mRNA, conceivably a higher dose than found in the other experimental system.

We attempted to use short, homologous RNA sequences to silence an endogenous gene (PDS). While this was effective in some cases, particularly for sequences in the centre of the region analysed, the effect was not reproducible even when 51–52 nt fragments were used. As for the shorter *gfp* homologous sequences, effectiveness was also variably influenced by sequence orientation. The reason for this is unknown when the likely source of the PTGS inducer is viral dsRNA. However, analysis of the silenced plants reinforces the view that there is a fundamental difference between endogenous genes and transgenes in the interaction of cytoplasmically derived RNA and genomic DNA, reflected in their methylation status in silenced tissues. There was no *de novo* methylation of *pds.*

As silencing directed by recombinant RNA viruses probably has the capacity to trigger the degradation of existing homologous mRNAs in the cytoplasm, we could not determine with certainty whether the short sequences we tested could interact directly with genomic DNA, potentially to direct *de novo* methylation. However, the influence of symmetrical C residues on the efficiency of PTGS might indicate a direct interaction from the input recombinant virus. Also, it is clear from the RNA-directed methylation of transgenic viroid sequences (Pélissier and Wassenegger, 2000) that short homologous DNA

sequences (30 bp) can be invoked as targets for methylation. Why we found that PVX-GFP28 (28 nt *gfp*) led to DNA methylation, but PVX-PDSoligo-6 (33 nt *pds*) did not, even though both infections initiated silencing, remains to be determined. However, it would appear that the plant can distinguish between a transgene and an endogenous gene as substrates for RNA-directed methylation. Surprisingly, PTGS induced by ds viral RNA carrying a very short homologous region led to methylation throughout the transcribed region of the transgene. Since the transgene mRNA appeared to be more susceptible than the viral RNA to targeted degradation (Figure 4b), it is conceivable that it could act as the primary target in the cytoplasm of the short region of sequence homology from the virus. The processive degradation of the target mRNA (Zamore *et al.*, 2000) could release further *gfp* fragments that additively direct methylation throughout the transcribed region of the transgene. This can also lead to subsequent targeting of RNAs with homology to adjacent regions (Jones *et al.*, 1999; Ruiz *et al.*, 1998). Whether methylation is just an indicator of this capacity for spreading the PTGS specificity, or whether it is an active component, remains a key question.

Experimental procedures

Plant material

Transgenic *Nicotiana benthamiana* plants (line 16c) carrying a single 35S::*gfp*::tnos transgene have been described previously (Ruiz *et al.*, 1998).

Recombinant PVX viruses

Fragments of GFP5 (Haseloff *et al.*, 1997) DNA were generated by limited DNaseI digestion in the presence of Mn^{2+} (Melgar and Goldthwait, 1968). The digested DNA was size-fractionated in a 1.5% agarose gel and fragments of <100 bp cloned into the *Sma*I site of a PVX vector (pGR107; Jones *et al.*, 1999), adjacent to a duplicated subgenomic coat protein promoter. Cloning synthetic oligonucleotides into the *Sma*I site similarly generated other recombinant PVXs. In determining the precise size of the gfp-homologous sequence in the PVX vector, the contribution of the sequences comprising the *Sma*I cloning site were also taken into account. The vector pGR107 expresses an infectious PVX RNA from a CaMV 35S promoter after introduction into plant cells using *Agrobacterium tumefaciens* pGV3101 stab inoculation ('agro-inoculation'). PVX-GFP contained a full-length gfp cDNA cloned into the *Sma*I site (Ruiz *et al.*, 1998). PVX-PDS similarly contained a 368 bp fragment of *N. benthamiana* pds cDNA (Ruiz *et al.*, 1998). Varying numbers of plants (three to ten) were agro-inoculated with the PVX constructs discussed in the text. Without exception, all plants infected with the same construct gave a consistent phenotype (either they did or did not initiate silencing).

GFP imaging

Observation and photographic recording of GFP fluorescence was as previously described (Voinnet *et al.*, 1998).

Southern blot analysis

Genomic DNA was extracted from leaves using the 'DNAeasy' kit (Qiagen, Chatsworth, CA, USA) according to the manufacturer's instructions. DNA digestion with methylation-sensitive restriction enzymes and gel-blot analysis was as described (Jones *et al.*, 1998). ^{32}P-labelled hybridization probes corresponded to the entire gfp sequence, a 368 bp *N. benthamiana* pds cDNA fragment or 450 bp of the *N. benthamiana* heat-shock protein 70 (hsp70) cDNA.

RNA extraction and analysis

Total RNA was extracted using RNA isolator (Genosys Biotechnologies Inc., The Woodlands, TX, USA) following the manufacturer's instructions. RNA electrophoresis and gel-blot analysis were performed as described previously (Jones *et al.*, 1998) and hybridized with *gfp and* PVX probes. For semiquantitative RT–PCR analysis, three leaves showing the *pds* silenced phenotype were sampled from each of three individual plants infected with either PVX-PDSOligo-7 or -8, or from similarly aged leaves infected with PVX. Poly(A)+ RNA was isolated from 10 µg total RNA using Dynabeads (Dynal AS, Oslo, Norway) as per the manufacturers instructions. cDNA was synthesized using Expand reverse transcriptase (Roche Diagnostics GmbH, Mannheim, Germany), and used in a duplex PCR reaction containing oligonucleotides specific for amplifying *ubiquitin* and *pds* mRNAs. Semi-quantitative PCR of cDNA derived from the equivalent of 1 µg of total RNA was performed using the following conditions: 95°C/5 min for 1 cycle, 95°C/30 sec, 55°C/1 min, 72°C/1 min for 22, 26 or 30 cycles and 72°C/10 min for 1 cycle, for each sample. The linear phase of DNA amplification (26 cycles) was determined by electrophoresing the PCR products on a 1.5% agarose gel. The *pds* oligonucleotides were designed to detect *pds* mRNA and not the *pds* sequences within PVX-PDSOligo-7 or -8.

Acknowledgements

We are grateful to Andrew Hamilton, Olivier Voinnet and colleagues for valuable comments on the work and the manuscript prior to submission. The John Innes Centre and The Sainsbury Laboratory are supported by the Biotechnology and Biological Research Council and the Gatsby Charitable Foundation, respectively. The work was carried out under the UK Ministry of Agriculture Fisheries and Food Licence PHL 24A/2921.

References

Cogoni, C. and Macino, G. (1999) Gene silencing in *Neurospora crassa* requires a protein homologous to RNA-dependent RNA polymerase. *Nature*, **399**, 166–169.

Cogoni, C., Ireland, J.T., Schumacher, M., Schmidhauser, T.J., Selker, E.U. and Macino, G. (1996) Transgene silencing of the *al-1* gene in vegetative cells of *Neurospora* is mediated by a cytoplasmic effector and does not depend on DNA: DNA interactions or DNA methylation. *EMBO J.* **15**, 3153–3163.

Dalmay, T., Hamilton, A., Rudd, S., Angell, S. and Baulcombe, D.C. (2000a) An RNA-dependent RNA polymerase gene in *Arabidopsis* is required for posttranscriptional gene silencing mediated by a transgene but not by a virus. *Cell*, **101**, 543–553.

Dalmay, T., Hamilton, A., Muller, E. and Baulcombe, D.C. (2000b)

Potato virus X amplicons in *Arabidopsis* mediate genetic and epigenetic gene silencing. *Plant Cell*, **12**, 369–379.

Demmig-Adams, B. and Adams, W.W. (1992) Photoprotection and other responses of plants to high light stress. *Annu. Rev. Plant Physiol. Plant Mol. Biol.* **43**, 599–626.

Depicker, A. and Van Montagu, M. (1997) Post-transcriptional gene silencing in plants. *Curr. Opin. Cell Biol.* **9**, 372–382.

English, J.J., Mueller, E. and Baulcombe, D.C. (1996) Suppression of virus accumulation in transgenic plants exhibiting silencing of nuclear genes. *Plant Cell*, **8**, 179–188.

Fagard, M. and Vaucheret, H. (2000) (Trans) gene silencing in plants: how many mechanisms? *Annu. Rev. Plant Physiol. Plant Mol. Biol.* **51**, 167–194.

Finnegan, E.J., Genger, R.K., Peacock, W.J. and Dennis, E.S. (1998) DNA methylation in plants. *Annu. Rev. Plant Physiol. Plant Mol. Biol.* **49**, 223–247.

Fire, A., Xu, S., Montgomery, M.K., Kostas, S.A., Driver, S.E. and Mello, C.C. (1998) Potent and specific genetic interference by double-stranded RNA in *Caenorhabitis elegans. Nature*, **391**, 806–811.

Hamilton, A.J. and Baulcombe, D.C. (1999) A species of small antisense RNA in posttranscriptional gene silencing in plants. *Science*, **286**, 950–952.

Hammond, S.M., Bernstein, E., Beach, D. and Hannon, G.J. (2000) An RNA-directed nuclease mediates post-transcriptional gene silencing in *Drosophila* cells. *Nature*, **404**, 293–296.

Haseloff, J., Siemering, K.R., Prasher, D.C. and Hodge, S. (1997) Removal of a cryptic intron and subcellualr localization of green fluorescent protein are required to mark transgenic *Arabidopsis* plants brightly. *Proc. Natl Acad. Sci. USA*, **94**, 2122–2127.

Ingelbrecht, I., Van Houdt, H., Van Montagu, M. and Depicker, A. (1994) Posttranscriptional silencing of reporter transgenes in tobacco correlates with DNA methylation. *Proc. Natl Acad. Sci. USA*, **91**, 10502–10506.

Jones, A.L., Thomas, C.L. and Maule, A.J. (1998) *De novo* methylation and co-suppression induced by a cytoplasmically replicating plant RNA virus. *EMBO J.* **17**, 6385–6393.

Jones, L., Hamilton, A.J., Voinnet, O., Thomas, C.L., Maule, A.J. and Baulcombe, D.C. (1999) RNA–DNA interactions and DNA methylation in post-transcriptional gene silencing. *Plant Cell*, **11**, 2291–2301.

Kennerdell, J.R. and Carthew, R.W. (1998) Use of dsRNA-mediated genetic interference to demonstrate that *frizzled* and *frizzled 2* act in the wingless pathway. *Cell*, **95**, 1017–1026.

Kumagai, M.H., Donson, J., Della-Cioppa, G., Harvey, D., Hanley, K. and Grill, L.K. (1995) Cytoplasmic inhibition of carotenoid biosynthesis with virus-derived RNA. *Proc. Natl Acad. Sci. USA*, **92**, 1679–1683.

Melgar, E. and Goldthwait, D.A. (1968) Deoxyribonucleic acid nucleases. II. The effects of metals on the mechanism of action of deoxyribonuclease I. *J. Biol. Chem.* **243**, 4409–4416.

Misquitta, L. and Paterson, B.M. (1999) Targeted disruption of gene function in *Drosophila* by RNA interference (RNA-i): a role for *nautilus* in embryonic somatic muscle formation. *Proc. Natl Acad. Sci. USA*, **96**, 1451–1456.

Mourrain, P., Béclin, C., Elmayan, T. *et al.* (2000) *Arabidopsis SGS2* and *SGS3* genes are required for posttranscriptional gene silencing and natural virus resistance. *Cell*, **101**, 533–542.

Ngô, H., Tschudi, C., Gull, K. and Ullu, E. (1998) Double-stranded RNA induces mRNA degradation in *Trypanosoma brucei. Proc. Natl Acad. Sci. USA*, **95**, 14687–14692.

Pang, S.-Z., Jan, F.-J. and Gonsalves, D. (1997) Nontarget DNA sequences reduce the transgene length necessary for RNA-mediated tospovirus resistance in transgenic plants. *Proc. Natl Acad. Sci. USA*, **94**, 8261–8266.

Pecker, I., Chamovitz, D., Linden, H., Sandmann, G. and Hirschberg, J. (1992) A single polyeptide catalysing the conversion of phytoene to ξ-carotene is transcriptionally regulated during tomato fruit ripening. *Proc. Natl Acad. Sci. USA*, **89**, 4962–4966.

Pélissier, T. and Wassenegger, M. (2000) A DNA target of 30 bp is sufficient for RNA-directed DNA methylation. *RNA*, **6**, 55–65.

Plasterk, R.H. and Ketting, R.F. (2000) The silence of the genes. *Curr. Opin. Genet. Devel.* **10**, 562–567.

Ruiz, M.T., Voinnet, O. and Baulcombe, D.C. (1998) Initiation and maintenance of virus-induced gene silencing. *Plant Cell*, **10**, 937–946.

Sijen, T., Wellink, J., Hiriart, J.-B. and Van Kammen, A. (1996) RNA-mediated virus resistance: role of repeated transgenes and delineation of targeted regions. *Plant Cell*, **8**, 2277–2294.

Smardon, A., Spoerke, J.M., Stacey, S.C., Klein, M.E., Mackin, N. and Maine, E.M. (2000) EGO-1 is related to RNA-directed RNA polymerase and functions in germ-line development and RNA interference in *C. elegans. Curr. Biol.* **10**, 169–178.

Stam, M., Mol, J.N.M. and Kooter, J.M. (1997) The silence of genes in transgenic plants. *Ann. Rev. Bot.* **79**, 3–12.

Tchurikov, N.A., Chistyakova, L.G., Zavilgelsky, G.B., Manuhov, I.V., Chernov, B.K. and Golova, Y.B. (2000) Gene-specific silencing by expression of parallel complementary RNA in *Escherichia coli. J. Biol. Chem.* **275**, 26523–26529.

Tuschl, T., Zamore, P.D., Lehmann, R., Bartel, D.P. and Sharp, P.A. (1999) Targeted mRNA degradation by double-stranded RNA *in vitro. Genes Dev.* **13**, 3191–3197.

Van den Boogaart, T., Lomonossoff, G.P. and Davies, J.W. (1998) Can we explain RNA-mediated virus resistance by homology-dependent gene silencing? *Mol. Plant–Microbe Interact.* **11**, 717–723.

Van Houdt, H., Ingelbrecht, I., Van Montagu, M. and Depicker, A. (1997) Post-transcriptional silencing of a neomycin phospho-transferase II transgene correlates with the accumulation of unproductive RNAs and with increased cytosine methylation of 3′ flanking regions. *Plant J.* **12**, 379–392.

Voinnet, O., Vain, P., Angell, S. and Baulcombe, D.C. (1998) Systemic spread of sequence-specific transgene RNA degradation is initiated by localized introduction of ectopic promoterless DNA. *Cell*, **95**, 177–187.

Wargelius, A., Ellingsen, S. and Fjose, A. (1999) Double-stranded RNA induces specific developmental defects in zebrafish embryos. *Biophys. Res. Commun.* **263**, 156–161.

Wassenegger, M., Heimes, S., Riedel, L. and Sänger, H.L. (1994) RNA-directed *de novo* methylation of genomic sequences in plants. *Cell*, **76**, 567–576.

Wianny, F. and Zernicka-Goetz, M. (2000) Specific interference with gene function by double-stranded RNA in early mouse development. *Nat. Cell Biol.* **2**, 70–75.

Yx, L., Farrell, M.J., Liu, R., Mohanty, N. and Kirby, M.L. (2000) Double-stranded RNA injection produces null phenotypes in zebrafish. *Dev. Biol.* **217**, 394–405.

Zamore, P.D., Tuschl, T., Sharp, P.A. and Bartel, D.P. (2000) RNAi: double-stranded RNA directs the ATP-dependent cleavage of mRNA at 21–23 nucleotide intervals. *Cell*, **101**, 25–33.

Developmental Cell, Vol. 5, 891–901, December, 2003, Copyright ©2003 by Cell Press

EXHIBIT E

Imprinting of the *MEA* Polycomb Gene Is Controlled by Antagonism between MET1 Methyltransferase and DME Glycosylase

Wenyan Xiao,[1] Mary Gehring,[1]
Yeonhee Choi,[1] Linda Margossian,[1]
Hong Pu,[2] John J. Harada,[3]
Robert B. Goldberg,[4] Roger I. Pennell,[2]
and Robert L. Fischer[1,*]
[1]Department of Plant and Microbial Biology
University of California, Berkeley
Berkeley, California 94720
[2]Ceres, Incorporated
3007 Malibu Canyon Road
Malibu, California 90265
[3]Section of Plant Biology
Division of Biological Sciences
University of California, Davis
Davis, California 95616
[4]Department of Molecular, Cell, and Developmental Biology
University of California, Los Angeles
Los Angeles, California 90095

Summary

The *MEA* Polycomb gene is imprinted in the *Arabidopsis* endosperm. DME DNA glycosylase activates maternal *MEA* allele expression in the central cell of the female gametophyte, the progenitor of the endosperm. Maternal mutant *dme* or *mea* alleles result in seed abortion. We identified mutations that suppress *dme* seed abortion and found that they reside in the *MET1* methyltransferase gene, which maintains cytosine methylation. Seeds with maternal *dme* and *met1* alleles survive, indicating that suppression occurs in the female gametophyte. Suppression requires a maternal wild-type *MEA* allele, suggesting that *MET1* functions upstream of, or at, *MEA*. DME activates whereas MET1 suppresses maternal *MEA::GFP* allele expression in the central cell. MET1 is required for DNA methylation of three regions in the *MEA* promoter in seeds. Our data suggest that imprinting is controlled in the female gametophyte by antagonism between the two DNA-modifying enzymes, MET1 methyltransferase and DME DNA glycosylase.

Introduction

Imprinting results in genes being expressed or silenced according to their parental origin (Ferguson-Smith and Surani, 2001; Reik and Walter, 2001). Imprinting occurs in mammals and plants and plays an important role in the reproductive strategies of both groups (Moore, 2001). In mammals, many of the imprinted genes control prenatal growth (Tycko and Morison, 2002); they are expressed in the extraembryonic membranes that serve as a conduit for the flow of nutrients from the mother to the embryo (Reik and Walter, 2001). In plants, the endosperm performs a similar function and is also a critical site for gene imprinting (Martienssen, 1998; Moore, 2001). Although some imprinted genes are essential for plant reproduction (Gehring et al., 2003), little is known about how imprinting is initiated and maintained in plants.

In mammals, one of the mechanisms of gene imprinting involves differential 5-cytosine methylation of alleles during gametogenesis that is then transmitted to the embryo (Ferguson-Smith and Surani, 2001; Li, 2002; Reik and Walter, 2001). In plants, DNA methylation is also responsible, at least in part, for many epigenetic phenomena (Martienssen and Colot, 2001). These include transcriptional silencing of transposons, transgenes, and pathogen DNA, as well as the silencing of genes that control flowering time, floral organ identity, fertility, and leaf morphology (Finnegan et al., 1996; Jacobsen et al., 2000; Kakutani et al., 1996; Miura et al., 2001; Soppe et al., 2000). DNA methyltransferases have been identified that establish and maintain patterns of symmetric (CpG and CpNpG) and asymmetric (CpNpN) cytosine methylation in the plant genome (Cao and Jacobsen, 2002a, 2002b; Finnegan and Dennis, 1993; Lindroth et al., 2001). This methylation is intimately related to histone modifications, chromatin remodeling, and the accessibility of DNA to transcription factors (Jackson et al., 2002; Johnson et al., 2002; Martienssen and Colot, 2001; Soppe et al., 2002). Genetic crosses between plants with wild-type and hypomethylated genomes suggest that DNA methylation is necessary for endosperm development and seed viability (Adams et al., 2000). However, the role that DNA methylation plays in the imprinting of specific genes has not yet been established.

The endosperm and embryo of flowering plants are derived from two fertilization events that occur in the female gametophyte. In *Arabidopsis*, a haploid megaspore undergoes three mitotic divisions to form an eight-nucleus, seven-cell female gametophyte containing the egg, central, synergid, and antipodal cells; the fusion of two haploid nuclei makes the nucleus of the central cell diploid. Fertilization of the egg cell by a sperm cell gives rise to a diploid embryo that ultimately generates the organs, tissues, and meristems of the plant. Fertilization of the central cell by a second sperm cell generates the triploid endosperm that supports embryo or seedling growth and development by producing storage proteins, lipids, and starch, and by mediating the transfer of maternal-derived nutrients to be absorbed by the embryo (Brown et al., 1999).

The *MEDEA* (*MEA*) gene is imprinted in the *Arabidopsis* endosperm. Only the maternal *MEA* allele is expressed (Kinoshita et al., 1999; Luo et al., 2000; Vielle-Calzada et al., 1999). *MEA* encodes a SET domain Polycomb group protein (Grossniklaus et al., 1998; Kiyosue et al., 1999; Luo et al., 1999). Polycomb group proteins repress gene transcription by remodeling chromatin at specific regions within the genome (Francis and Kingston, 2001). *MEA* prevents the onset of central cell proliferation prior to fertilization, represses endosperm growth after fertilization, and represses gene expression in the female

*Correspondence: rfischer@uclink.berkeley.edu

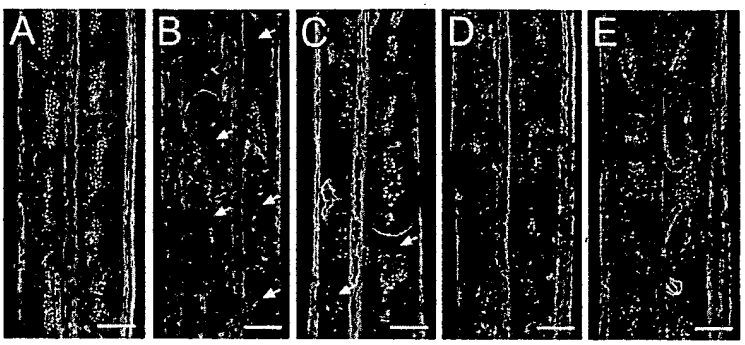

Figure 1. Effect of *dme* and *dme* Suppressor Mutations on Seed Viability

Siliques were dissected and photographed 14 days after self-pollination. The scale bars represent 0.5 mm. Arrows indicate aborted seeds. Siliques shown in (D) and (E) were F_1 progeny from a self-pollinated plant heterozygous for *DME/dme-1* and heterozygous for the *dme* suppressor (line 1424 described in Experimental Procedures).

(A) Wild-type silique.

(B) Heterozygous *DME/dme-1* silique.

(C) Silique is heterozygous for *DME/dme-1* and heterozygous for the *dme* suppressor mutation.

(D) Silique is heterozygous for *DME/dme-1* and homozygous for the *dme* suppressor mutation.

(E) Silique is homozygous for the *dme* suppressor mutation.

gametophyte and seed (Chaudhury et al., 1997; Kiyosue et al., 1999; Kohler et al., 2003). Because *MEA* is an essential imprinted gene, loss-of-function alleles have parent-of-origin effects on seed viability. A seed that inherits a mutant maternal *mea* allele aborts regardless of the genotype of the silent paternal allele (Chaudhury et al., 1997; Grossniklaus et al., 1998; Kiyosue et al., 1999).

The *DEMETER* (*DME*) gene is necessary for maternal *MEA* allele expression in the *Arabidopsis* central cell and endosperm (Choi et al., 2002). As a result, seed viability depends only on the maternal *DME* allele, and seed abortion results from maternal inheritance of a mutant *dme* allele regardless of the genotype of the paternal *DME* allele. *DME* is primarily expressed in the central cell of the female gametophyte where it is required to activate expression of the maternal *MEA* allele. *MEA* expression persists after the central cell is fertilized to form the endosperm, even though *DME* does not. Ectopic *DME* expression in cauline leaves and in endosperm activates *MEA* and paternal *MEA* allele expression, respectively, suggesting that differential expression of DME in maternal (expressed) and paternal (not expressed) reproductive organs is responsible, at least in part, for imprinting *MEA* in the endosperm.

DME encodes a large protein with DNA glycosylase and nuclear localization domains (Choi et al., 2002). Most DNA glycosylases function in a base excision DNA repair pathway that excises damaged, modified, or mispaired bases, nicks the DNA, and replaces the abasic sites with normal bases (Bruner et al., 2000; Jiricny, 2002). Ectopic expression of *DME* in cauline leaves causes single-stranded breaks in the *MEA* promoter, consistent with its DNA glycosylase function and with the view that DME acts directly on *MEA* (Choi et al., 2002). Mutagenesis of a conserved aspartic acid to asparagine in the putative DME glycosylase catalytic site abolishes the ability of the mutated *DME* transgene to complement a *dme* mutation (Y.C. and R.L.F., unpublished results). This further supports the idea that DME is a DNA glycosylase. The mechanism used by DME to regulate the transcription of the maternal *MEA* allele transcription is unknown.

We isolated four mutations that suppress *dme*-mediated seed abortion to understand how *MEA* gene imprinting is regulated. Map-based cloning revealed that all four mutations represented distinct lesions in the *MET1* gene (*met1-5* to *met1-8*). *MET1*, an *Arabidopsis* ortholog of the mammalian Dnmt1 methyltransferase gene, maintains cytosine methylation at CpG sites (Finnegan and Dennis, 1993; Kishimoto et al., 2001; Lindroth et al., 2001) and indirectly influences methylation at CpNpG and CpNpN sites (Cao and Jacobsen, 2002a). Inheritance of a maternal *met1* mutant allele by a female gametophyte was sufficient for complete suppression of *dme*-mediated seed abortion, whereas inheritance of a paternal *met1* mutant allele had little or no effect. Suppression of *dme* by *met1* mutations requires a maternal wild-type *MEA* allele, suggesting that *met1* mutations act upstream of *MEA* to rescue *dme* seed viability. Maternal *MEA::GFP* allele transcription in the central cell and endosperm, prevented by a maternal *dme* mutant allele, is fully restored when maternal *dme* and *met1* mutant alleles are inherited together. Bisulfite sequencing experiments revealed three regions of cytosine methylation in the *MEA* promoter that are hypomethylated in *met1* mutant seeds. These results suggest that DNA methylation plays an important role in the control of *MEA* imprinting and seed viability, and that these processes are controlled by antagonism between MET1 and DME enzymes in the female gametophyte.

Results

Identification of Mutations that Suppress *dme*-Mediated Seed Abortion

We mutagenized *DME/dme* heterozygous seed and identified four mutant lines that suppressed *dme*-mediated seed abortion (see Experimental Procedures). Whereas seeds from wild-type plants rarely abort (Figure 1A), self-pollinated heterozygous *DME/dme-1* siliques (Figure 1B) have a 1:1 segregation ratio of viable and nonviable seeds (272:250, $\chi^2 = 0.9$, $P > 0.4$) because inheritance of a maternal mutant *dme* allele is sufficient to cause seed abortion (Choi et al., 2002). By contrast, plants heterozygous for *DME/dme-1* and heterozygous

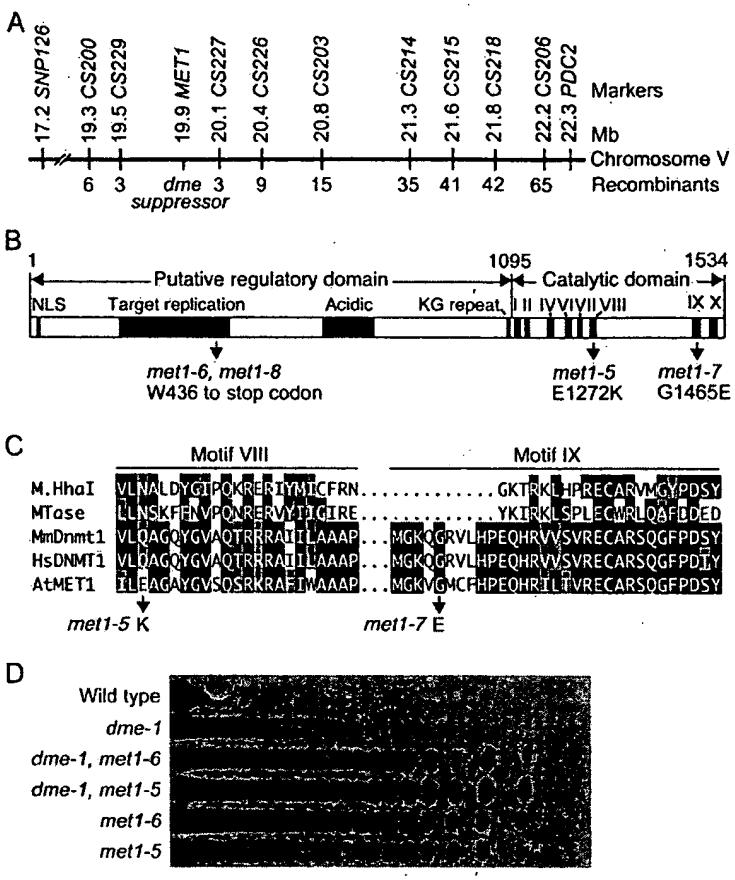

Figure 2. *dme* Suppressor Mutations Reside in the *MET1* Gene

(A) Map-based cloning of a *dme* suppressor mutant allele. The position of the *MET1* gene relative to SSLP molecular markers, and the number of recombinants between the *dme* suppressor (*met1-5*) and molecular markers, are shown.

(B) Position of *met1* alleles relative to conserved domains in the MET1 protein. The MET1 amino-terminal regulatory domain includes a nuclear localization signal (NLS), a sequence for targeting MET1 enzyme to DNA replication foci, a plant-specific acidic region of glutamic and aspartic acid residues, and lysine/glycine repeats by which the regulatory domain is fused to the catalytic domain. The catalytic domain has eight of ten conserved motifs found in prokaryotic DNA methyltransferases (Posfai et al., 1989). The codon (UGG) for tryptophan at position 436 was mutated to a stop codon in the *met1-6* (UAG) and *met1-8* (UGA) mutant alleles. *met1-5* and *met1-7* missense mutations altered the amino acid sequence in conserved motifs VIII and IX, respectively.

(C) Comparison of motif VIII and motif IX domains among DNA methyltransferases. The positions of the *met1-5* and *met1-7* mutations in the conserved motifs are shown. M. HhaI, *Haemophilus haemolyticus* methylase (GenBank accession number P05102); MTase, *Bacillus subtilis* phages ϕ3T DNA methyltransferase (accession number CTBPPT); MmDnmt1, *Mus musculus* DNA methyltransferase 1 (accession number P13864); HsDNMT1, *Homo sapiens* DNA methyltransferase 1 (accession number NP_001370); AtMET1, *Arabidopsis thaliana* DNA methyltransferase 1 (accession numbers AT5G49160 and AF139372).

(D) The *met1-5* and *met1-6* mutations result in genome hypomethylation. DNA was isolated from seedlings and digested with HpaII, blotted, and hybridized to a probe complementary to the 180 base pair centromere repeats (Kankel et al., 2003). Seedlings were homozygous for the indicated mutant alleles.

for its suppressor have a 3:1 segregation ratio of viable and nonviable seeds (Figure 1C; 184:63, $\chi^2 = 0.03$, $P > 0.85$). Seed abortion was completely suppressed in plants heterozygous for *DME/dme-1* and homozygous for its suppressor mutation (Figure 1D; 2 aborted seeds among 231checked), as well as in control plants homozygous for the wild-type *DME* allele and the *dme* suppressor (Figure 1E; 1 aborted seed among 135 checked). Mapping experiments showed that the *dme* suppressor mutations are near the bottom of chromosome 5 (Figure 2A) and are therefore genetically unlinked to *DME*, which is located near the top of chromosome 5. These results show that second-site suppressor mutations compensated for loss-of-function mutations in the maternal *dme* allele and restored seed viability.

dme Suppressor Mutations Are Loss-of-Function *met1* Alleles

High-resolution gene mapping experiments showed that a *dme* suppressor mutation resides in a 0.6 Mb region spanning the *MET1* gene (Figure 2A). MET1 is an *Arabidopsis* ortholog of mammalian Dnmt1 methyltransferase, which maintains methylation at CpG sites (Finnegan and Kovac, 2000). Certain phenotypes associated with homozygous *dme* suppressor plants (e.g., late flowering and abnormal patterning of floral organs) were similar to those observed in transgenic plants bearing an antisense *MET1* gene (Finnegan et al., 1996; Ronemus et al., 1996), suggesting that *dme* suppressor mutations might reside in the *MET1* gene. We determined the sequence of the *MET1* gene in all four mutant lines and found that each line harbored a lesion in the *MET1* gene (Figure 2B). These new *met1* alleles are distinct from those previously reported (Kankel et al., 2003; Saze et al., 2003), and are designated *met1-5* to *met1-8*.

In eukaryotes, MET1 and MET1-related proteins have an amino-terminal putative regulatory domain and a carboxy-terminal catalytic domain (Finnegan and Kovac, 2000; Posfai et al., 1989). The *met1-6* and *met1-8* alleles represent base pair changes that generate a stop codon at amino acid 436 in the MET1 polypeptide (Figure 2B). These alleles are likely to be null alleles, as the truncated polypeptide encoded by the *met1-6* and *met1-8* alleles lacks a large portion of the putative regulatory domain as well as the entire catalytic domain. The *met1-5* and *met1-7* alleles have base pair changes that alter single amino acids residing in catalytic domain motifs that are conserved in prokaryotic and eukaryotic cytosine 5-methyltransferases (Figures 2B and 2C). It is likely that these amino acids are critical for MET1 enzyme activity,

as *met1-5* and *met1-7* suppress *dme*-mediated seed abortion to the same extent as null alleles *met1-6* and *met1-8* (data not shown).

Plants homozygous for mutations in the *MET1* gene display DNA hypomethylation (Kankel et al., 2003; Saze et al., 2003). As shown in Figure 2D, the 180 base pair repeated centromere DNA from wild-type and homozygous *dme-1* mutant plants is highly methylated and cannot be cleaved by the methylation-sensitive restriction endonuclease HpaII. By contrast, these centromeric repeats are hypomethylated in the genome of homozygous *met1-5* or *met1-6* plants, as well as in plants homozygous for both *dme-1* and *met1* alleles (Figure 2D). Thus, full suppression of *dme*-mediated seed abortion is associated with missense and nonsense mutations that cause DNA hypomethylation.

Distinct Developmental Abnormalities in Plants with Mutant *dme* and *met1* Alleles

Both *DME* and *MET1* are required for stable, reproducible patterns of floral and vegetative development (Choi et al., 2002; Finnegan and Kovac, 2000). Homozygous *dme-1* or *met1* plants, as well as antisense *MET1* transgenic plants, display sporadic developmental abnormalities (Choi et al., 2002; Finnegan et al., 1996; Kakutani et al., 1996; Kankel et al., 2003; Ronemus et al., 1996). Plants homozygous for both *dme-1* and *met1-6* mutant alleles have distinctive sporadic phenotypes. For example, homozygous *dme-1 met1-6* mutant siliques were sometimes distended (Figure 3A), and ovules appeared to be converted to leaf-like organs (Figure 3B) or carpel-like organs tipped with stigmatic papillae and connected by a funiculus to the placenta (Figure 3C). Sometimes a single flower (Figure 3D) or influorescence shoot (Figure 3E) emerged from a homozygous *dme-1 met1-6* silique. In the extreme cases, the pattern of producing flowers in siliques was reiterated multiple times (Figure 3F). These sporadic phenotypes increased in frequency with each generation, were detected in about 15% of the F_3 homozygous *dme-1 met1-6* plants, and were not observed in control homozygous F_3 *dme-1* or F_3 *met1-6* plants. Analysis of subsequent generations was not possible because F_3 homozygous *dme-1 met1-6* plants are sterile. These distinct mutant phenotypes suggest a genetic interaction between DME and MET1 is necessary to generate stable, reproducible patterns of floral and vegetative development.

Maternal *met1* Allele Suppresses *dme*-Mediated Seed Abortion

Inheritance of a maternal *DME* allele is vital for seed viability, while a paternal *DME* allele is dispensable (Choi et al., 2002). As a result, *DME/dme-1* heterozygous plants pollinated with wild-type pollen produce siliques with a 1:1 segregation ratio of viable and aborted seeds (Choi et al., 2002) and essentially all of the viable F_1 progeny inherit a maternal wild-type *DME* allele (Table 1). By contrast, *DME/dme-1 MET1/met1-6* plants pollinated with wild-type pollen generate siliques with a 3:1 ratio of viable to aborted seeds (140:44, $\chi^2 = 0.1$, $P > 0.8$). All viable F_1 progeny that inherited a maternal mutant *dme-1* allele also inherited a maternal mutant *met1-6* allele (Table 1), indicating that *dme-1 met1-6* female gametophytes pollinated with wild-type pollen produce viable seed. We observed a 1:1:1 segregation ratio of viable progeny with *dme-1 met1-6*, *DME met1-6*, and *DME MET1* maternal alleles (Table 1; $\chi^2 = 4.8$, $P > 0.1$), showing that pollinated *dme-1 met1-6* and *DME met1-6* female gametophytes produced equal numbers of viable seeds. Thus, *met1-6* is a fully penetrant suppressor of *dme* in the female gametophyte.

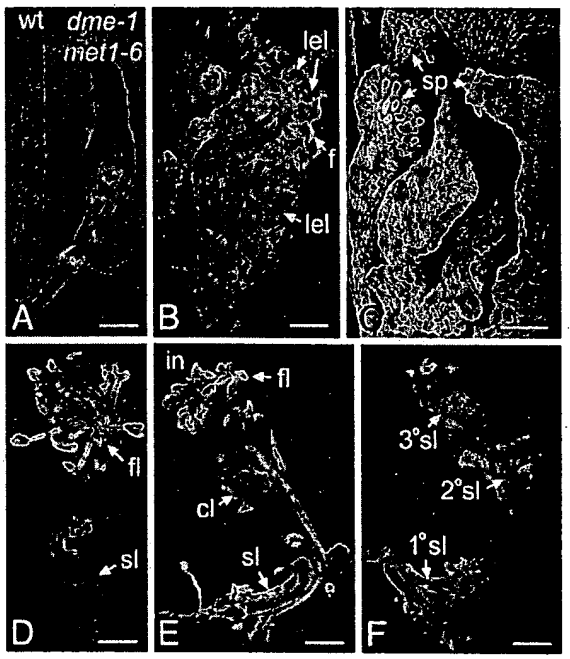

Figure 3. Developmental Abnormalities in Homozygous *dme-1 met1-6* Plants

Heterozygous *DME/dme-1 MET1/met1-6* plants were self-pollinated, F_1 homozygous *dme-1 met1-6* plants were self-pollinated, and phenotypes of F_2 homozygous *dme-1 met1-6* plants were analyzed.

(A) Siliques from wild-type and homozygous *dme-1 met1-6* plants. wt, wild-type. The scale bar represents 2 mm.

(B) Dissected homozygous *dme-1 met1-6* silique showing ovule converted to leaf-like (lel) structures connected by a funiculus (f) to the placenta. The scale bar represents 0.5 mm.

(C) Scanning electron micrograph of homozygous *dme-1 met1-6* ovules converted to leaf-like structures with stigmatic papilla (sp). The scale bar represents 50 μm.

(D) Flower (fl) emerging from a mature homozygous *dme-1 met1-6* silique (sl). The scale bar represents 2 mm.

(E) Influorescence shoot (in) with cauline leaves (cl) and flowers (fl) emerging from a mature *dme-1 met1-6* silique (sl). The scale bar represents 2 mm.

(F) Generation of primary (1°sl), secondary (2°sl), and tertiary (3°sl) siliques in a *dme-1 met1-6* homozygous plant. The scale bar represents 2 mm.

A recessive mutation in the *DECREASE IN DNA METHYLATION1* (*DDM1*) gene, *ddm1-2*, encoding a chromatin-remodeling SWI2/SNF2-like protein (Jeddeloh et al., 1999), also causes genome hypomethylation. When *DME/dme-1 DDM1/ddm1-2* plants were self-pollinated, we observed siliques with a 1:1 ratio of viable to aborted seeds (742:716, $\chi^2 = 0.46$, $P = 0.5$), suggesting that the *ddm1-2* mutation did not suppress *dme*-mediated seed abortion. These results show that the genetic

Table 1. Effect of a Maternal *met1* Allele on Transmission of Maternal *dme* and *mea* Mutant Alleles

Genetic Cross		Maternal Alleles of Viable F_1 Seedlings				
Maternal Parent	Paternal Parent	N[a]	%	Genotype		
DME/dme-1	Wild-type	94	1	*dme-1*		
			99	*DME*		
DME/dme-1, MET1/met1-6	Wild-type	86	25	*dme-1*	*met1-6*	
			0	*dme-1*	*MET1*	
			30	*DME*	*met1-6*	
			45	*DME*	*MET1*	
MEA/mea-3	Wild-type	89	6	*mea-3*		
			94	*MEA*		
MEA/mea-3, MET1/met1-6	Wild-type	64	2		*met1-6*	*mea-3*
			0		*MET1*	*mea-3*
			45		*met1-6*	*MEA*
			53		*MET1*	*MEA*
DME/dme-1, MEA/mea-3, MET1/met1-6	Wild-type	68	0	*dme-1*	*met1-6*	*mea-3*
			0	*dme-1*	*MET1*	*mea-3*
			0	*DME*	*met1-6*	*mea-3*
			0	*DME*	*MET1*	*mea-3*
			24	*dme-1*	*met1-6*	*MEA*
			0	*dme-1*	*MET1*	*MEA*
			41	*DME*	*met1-6*	*MEA*
			35	*DME*	*MET1*	*MEA*

[a]Number of F_1 seedlings checked.

interaction between the *met1* and *dme* mutations is a specific one.

Suppression of *dme* by *met1-6* Requires a Maternal Wild-Type *MEA* Allele

DME functions upstream of *MEA* to control seed viability (Choi et al., 2002). Like *DME*, inheritance of a maternal *MEA* allele is needed for seed viability while a paternal *MEA* allele is dispensable (Grossniklaus et al., 1998; Kiyosue et al., 1999; Luo et al., 1999). As a result, *MEA/mea-3* heterozygous plants pollinated with wild-type pollen produce siliques with a 1:1 segregation ratio of viable and aborted seed (88:84, $\chi^2 = 0.1$, $P > 0.8$), and most viable F_1 progeny inherit a maternal wild-type *MEA* allele (Table 1).

Do *met1* mutations function upstream of, at the level of, or downstream of *MEA* to suppress *dme*-mediated seed abortion? We addressed this question genetically by determining whether *met1* mutations suppress *mea*-mediated seed abortion. If downstream, a *met1* mutation would be expected to suppress *mea*-mediated seed abortion, whereas no suppression would be expected if *met1* functions at the level of *MEA* or upstream of *MEA*. To distinguish between these alternatives, *MEA/mea-3 MET1/met1-6* heterozygous plants were pollinated with wild-type pollen and the percentage of seed abortion and genotypes of F_1 progeny were analyzed. Siliques had a 1:1 segregation ratio of viable and aborted seeds (107:84, $\chi^2 = 2.7$, $P > 0.1$) and essentially all of the viable F_1 progeny inherited a maternal wild-type *MEA* allele (Table 1). Thus, a maternal *met1-6* allele does not suppress *mea*-mediated seed abortion, suggesting *MET1* functions either at the level of *MEA* or upstream of *MEA*.

If *MET1* functions upstream of, or at, *MEA*, then a wild-type *MEA* allele should be necessary for *met1* suppression of *dme*-mediated seed abortion. To test this hypothesis, *DME/dme-1 MET1/met1-6 MEA/mea-3* heterozygous plants were pollinated with wild-type pollen and the genotypes of viable F_1 progeny were determined. All viable F_1 progeny that inherited a maternal mutant *dme-1* allele also inherited a mutant *met1-6* allele and a wild-type *MEA* allele (Table 1). Thus, a wild-type maternal *MEA* allele is required for suppression of *dme* by *met1-6* in the female gametophyte. These results indicate that *met1* functions upstream of, or at, *MEA* in the female gametophyte to rescue the seed abortion caused by a maternal mutant *dme* allele.

DME and *MET1* Antagonism Regulates *MEA* Gene Expression

DME is necessary for *MEA* RNA accumulation (Choi et al., 2002) and *MEA* RNA, present in wild-type flowers, is not detected in homozygous *dme-1* flowers (Figure 4). Suppression of *dme* by *met1* mutations might be due, at least in part, to restoration of *MEA* gene expression. To test this idea, we isolated RNA from homozygous mutant *dme-1 met1-6* flowers and measured the

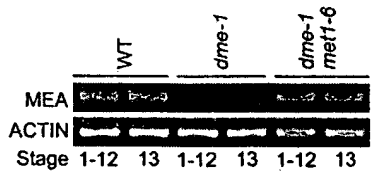

Figure 4. *MET1* and *DME* Genes Antagonistically Regulate *MEA* RNA Accumulation

RNA was isolated from developing floral buds (stage 1–12) and open flowers (stage 13). The approximate level of *MEA* RNA was determined by semiquantitative RT-PCR as described (Choi et al., 2002). Floral stages are as described (Bowman, 1994). Plants were homozygous for the indicated mutant alleles. WT, wild-type.

level of *MEA* RNA using reverse transcriptase polymerase chain reaction (RT-PCR) procedures. We found that the level of *MEA* RNA in *dme-1 met1-6* flowers was similar to that in wild-type (Figure 4). This result shows that MET1 is necessary for suppression of *MEA* expression in a *dme* mutant genetic background.

To understand the spatial and temporal control of *MEA* gene expression by *MET1* and *DME* during ovule and seed development, we analyzed the effect of *met1* and *dme-1* mutations on transcription of a *MEA::GFP* transgene consisting of 4.2 kb of *MEA* 5′-flanking sequences ligated to the *GFP* reporter gene (Choi et al., 2002). Essentially all (>99%) prefertilization ovules from control transgenic plants homozygous for the *MEA::GFP* transgene displayed strong fluorescence in the central cell nucleus and cytoplasm prior to fertilization. In a plant homozygous for the *MEA::GFP* transgene and heterozygous for *DME /dme-1*, we detected a 1:1 segregation ratio of fluorescent and nonfluorescent ovules (164:149, $\chi^2 = 0.7$, $P > 0.4$), suggesting that female gametophytes inheriting the *dme-1* mutant allele did not express the *MEA::GFP* transgene (Figure 5A). By contrast, in a plant homozygous for the *MEA::GFP* transgene, *DME/dme-1*, and *MET1/met1-6*, a 3:1 segregation ratio of fluorescent and nonfluorescent ovules (253:99, $\chi^2 = 1.8$, $P > 0.25$) was observed, suggesting that female gametophytes inheriting *dme* and *met1* mutant alleles expressed the *MEA::GFP* transgene (Figure 5B). To verify this hypothesis, we examined ovules from plants homozygous for the *MEA::GFP* transgene, *dme-1*, and *met1-6*. We found that essentially all ovules contained fluorescent central cells (Figure 5C; 241 fluorescent among 245 checked). These experiments reveal that *MET1* represses *MEA* promoter activity in a *dme* mutant central cell.

Activation of the *MEA::GFP* transgene by DME in the central cell is sufficient for postfertilization transcription of the *MEA::GFP* transgene in the endosperm, when DME is no longer expressed (Choi et al., 2002). As a result, we observed a 1:1 segregation of fluorescent and nonfluorescent seeds 24 hr (Figure 5D; 92:105, $\chi^2 = 0.9$, $P > 0.4$) and 90 hr (Figure 5G; 165:151, $\chi^2 = 0.6$, $P > 0.5$) after plants homozygous for the *MEA::GFP* transgene and heterozygous for *DME/dme-1* were pollinated with wild-type pollen. To determine whether activation of a *MEA::GFP* transgene in a *dme met* mutant female gametophyte likewise persists after fertilization, we pollinated flowers homozygous for the *MEA::GFP* transgene, and heterozygous for *DME/dme-1, MET1/met1-6* with wild-type pollen and observed GFP fluorescence in the endosperm of F_1 seeds. We observed a 3:1 segregation of fluorescent and nonfluorescent seeds 24 hr (Figure 5E; 253:99, $\chi^2 = 1.8$, $P > 0.25$) and 90 hr (Figure 5H; 304:123, $\chi^2 = 3.3$, $P > 0.08$) after pollination, showing that *MEA::GFP* transcription persists in the endosperm after fertilization of *dme met1* female gametophytes. Thus, prefertilization activation of *MEA* promoter activity in a *dme met1* central cell is not suppressed postfertilization by a wild-type paternal *MET1* allele. Consistent with this conclusion, essentially all F_1 seeds fluoresced 24 hr (Figure 5F; 157 fluorescent among 161 checked) and 90 hr (Figure 5I; 207 fluorescent among 209 checked) after pollination of flowers homozygous for the *MEA::GFP* transgene, *dme-1*, and *met1-6*. These results show that two DNA-modifying enzymes, DME glycosylase and MET1 methyltransferase, antagonistically regulate *MEA* expression in the central cell and endosperm.

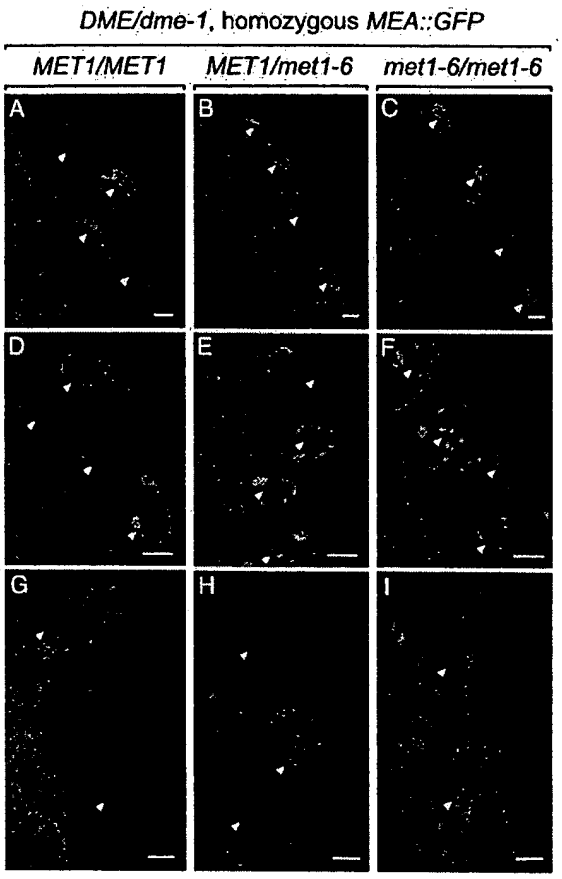

Figure 5. *MET1* and *DME* Genes Antagonistically Regulate *MEA* Promoter Activity

The GFP and chlorophyll fluorescence was converted to green and red, respectively.

(A–C) Fluorescence micrographs of stage 12 ovules. Arrows point to central cells. The genotype of the plant is shown above the fluorescence micrographs. The scale bars represent 0.04 mm.

(D–F) Fluorescence micrographs of seeds photographed 24 hr after a cross with wild-type pollen. The genotype of the pistil donor is shown above the fluorescence micrographs. The scale bars represent 0.16 mm.

(G–I) Fluorescence micrographs of seeds photographed 90 hr after a cross with wild-type pollen. The genotype of the pistil donor is shown above the fluorescence micrograph. The scale bars represent 0.32 mm.

MET1 Is Necessary for Cytosine Methylation in the *MEA* Promoter

What is the mechanism by which MET1 suppresses *MEA* gene transcription in a *dme* mutant central cell? We previously did not detect 5-methylcytosine residues in 2 kb of *MEA* 5′-flanking sequences from L*er* (Landsberg *erecta* ecotype) seeds or leaves, suggesting that DNA methylation does not play a direct role in the regulation of maternal *MEA* allele gene expression (Choi et al., 2002). However, the involvement of MET1 in the control of maternal *MEA* allele expression (Figure 4) prompted

us to examine the entire 4.2 kb *MEA* promoter that regulates expression of the *MEA::GFP* transgene (Figure 5), and to compare the patterns of methylation in wild-type and *met1* genetic backgrounds.

Because DNA methylation is often associated with genes that are not expressed, we initially analyzed DNA isolated from stamens (Columbia *glabrous* [Col *gl*] ecotype), an organ where *MEA* expression is not detected (data not shown). Using bisulfite sequencing methods (see Experimental Procedures), we identified three regions with significant cytosine methylation at −0.5 kb (−585 to −521), −3 kb (−3099 to −3071), and −4 kb (−4235 to −3800) relative to the translation start site of *MEA*. In wild-type seeds (Col *gl* ecotype), DNA sequence analysis of approximately 20 top strand and 20 bottom strand clones revealed clusters of eight, four, and five methylated CpG sites in the −4 kb, −3 kb, and −0.5 kb regions, respectively (Figures 6A and 6C). In addition, the −4 kb region contained six CpNpG and 28 CpNpN methylated sites on the top strand, and four CpNpG and 46 CpNpN methylated sites on the bottom strand (Figure 6B; Supplemental Figure S1 at http://www.developmentalcell.com/cgi/content/full/5/6/891/DC1). Similar results were obtained when wild-type seeds were isolated from L*er* ecotype plants, except that the level of CpG methylation at −0.5 kb was reduced to approximately 10%, which may explain why it was not detected previously (Choi et al., 2002). These results show that the 4.2 kb *MEA* promoter contains three regions with cytosine methylation.

To determine whether MET1 is responsible for maintaining cytosine methylation in the *MEA* promoter, we measured the level of cytosine methylation in *met1-6* mutant seeds (Col *gl* ecotype). We found that CpG methylation in the −4 kb, −3 kb, and −0.5 kb regions was dramatically reduced to 8%, 1%, and 0.7% in homozygous *met1-6* seeds compared with 81%, 21%, and 61% in wild-type Col *gl*, respectively (Figure 6A). Methylation at CpNpG and asymmetric CpNpN sites was also substantially reduced in *met1-6* mutant seeds (Figure 6B). A similar reduction in cytosine methylation was observed in plants homozygous for the *met1-5* allele (data not shown). Thus, *MET1* is necessary to maintain cytosine methylation at the three distinct sites in the *MEA* promoter.

Discussion

We isolated mutations that suppress *dme*-mediated seed abortion to understand how *MEA* imprinting is regulated. All mutations resided in the *MET1* methyltransferase gene that maintains cytosine methylation. Suppression requires a maternal wild-type *MEA* allele, suggesting that *MET1* functions upstream of, or at, *MEA*. DME activates whereas MET1 suppresses *MEA* gene expression. Three regions in the *MEA* promoter are hypomethylated in *met1* mutant seeds. Our analyses suggest a mechanism for the regulation of imprinted genes that are maternally expressed and paternally silenced in the endosperm. In the central cell of the female gametophyte, the MET1 methyltransferase represses *MEA* gene transcription, but expression of *DME* DNA glycosylase specifically in the central cell overcomes *MET1*-mediated silencing and activates the maternal *MEA* allele expression that persists during endosperm development.

Control of *MEA* Imprinting and Seed Viability in the Female Gametophyte by Antagonists DME and MET1

Like DME DNA glycosylase, MET1 methyltransferase functions in the female gametophyte. This conclusion is based upon data showing that inheritance of maternal mutant *met1* allele by the female gametophyte is sufficient to rescue maternal *MEA* expression in the central cell and endosperm of *dme* mutant plants (Figure 5) and to restore seed viability (Figure 1; Table 1). In the genetic crosses shown in Figure 5 and Table 1, the paternal parents were wild-type, and the maternal heterozygous *met1* parents were derived from mutagenized plants that were never homozygous for *met1* mutant alleles. Because rescue does not require that either parent be homozygous for a mutant *met1*allele, these data strongly suggest that MET1 methyltransferase, like DME DNA glycosylase (Choi et al., 2002), functions in the female gametophyte to control *MEA* imprinting and seed viability. This hypothesis is consistent with *MET1* being necessary for epigenetic inheritance during plant gametogenesis (Saze et al., 2003) and suggests that genes in the central cell, as well as in the egg, are epigenetically modified by *MET1*.

In the maternal parent, MET1 methyltransferase functions at, or upstream of, *MEA* and controls imprinting and seed viability. This is based upon our demonstration that rescue of *dme*-mediated seed abortion by the maternal *met1* allele requires a wild-type maternal *MEA* allele (Table 1). MET1 methyltransferase may suppress maternal *MEA* allele expression by directly methylating the *MEA* promoter. This idea is supported by the fact that MET1 methyltransferase is responsible for maintaining cytosine methylation in three regions of the *MEA* promoter (Figure 6). Alternatively, it is also possible that MET1 methylates, and thereby suppresses, an unknown gene that in turn activates maternal *MEA* expression. In either case, we propose that passive postmeiotic demethylation associated with mitoses during *met1* mutant female gametophyte development allows the maternal *MEA* allele to be expressed in the absence of DME DNA glycosylase activity (Figure 5).

After fertilization, MET1 may be relatively unimportant for control of the expression of the maternal *MEA* allele. This is because the postfertilization expression of *MEA* is stably maintained (Figure 5), even though the MET1 methyltransferase is expressed (M.G. and R.L.F., unpublished results) and its antagonist, DME DNA glycosylase, is not expressed at that time. Thus, wild-type *MET1* alleles cannot reestablish silencing of the maternal *MEA* allele in the endosperm (Figure 5), suggesting that epigenetic modification of the maternal *MEA* allele by DME DNA glycosylase cannot be reversed by MET1 methyltransferase in the endosperm.

Models for the Antagonistic Interaction between MET1 and DME

The discovery of an antagonistic relationship between MET1 and DME has provided important information about DME function. In the absence of DME DNA glycosylase activity in a *dme* mutant female gametophyte,

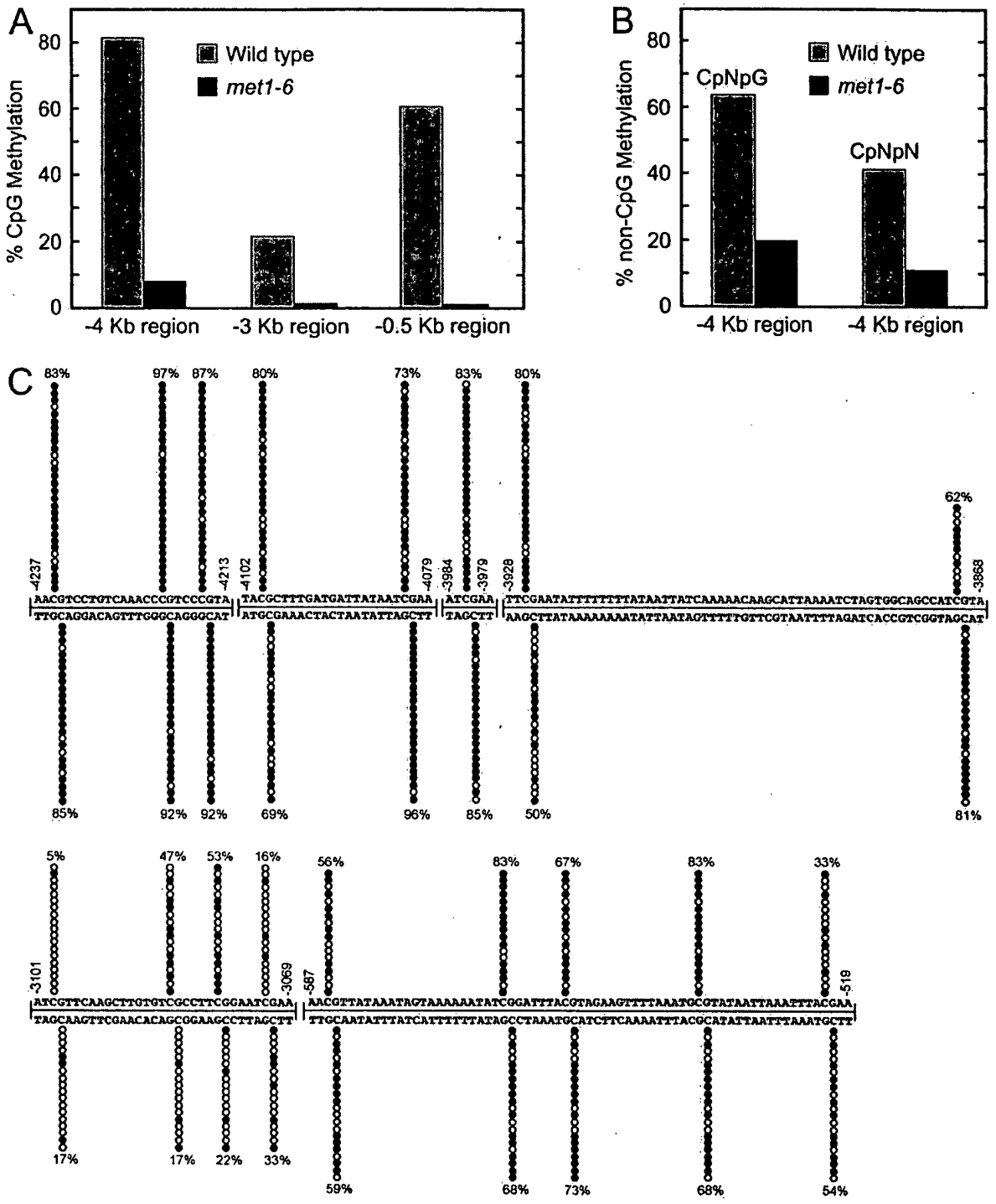

Figure 6. Pattern of DNA Methylation in the *MEA* Promoter

Percentage of CpG (A) and non-CpG (B) methylation in three regions of the *MEA* promoter isolated from wild-type and *met1-6* mutant seeds. (C) shows converted and nonconverted CpG sites in the sequenced clones in the three regions. Methylated and unmethylated cytosines are indicated by black and white circles, respectively. Number of sequences is relative to the translation start site of *MEA*.

MET1 methyltransferase maintains suppression of the maternal *MEA* allele (Figure 5) by maintaining patterns of DNA methylation. Thus, in wild-type plants, an essential function of DME is to overcome MET1 methyltransferase activity in the central cell of the female gametophyte.

How does DME overcome MET1-mediated DNA methylation and activate maternal *MEA* allele transcription in the central cell? One model is that DME DNA glycosylase excises 5-methylcytosine. Completion of the base excision DNA repair process would result in insertion of

a cytosine into the abasic site created by excision of 5-methylcytosine by DME. In support of this model, other related mammalian DNA glycosylases have been shown to excise 5-methylcytosine from the genome (Jost et al., 2001). Moreover, *ROS1*, the gene most closely related to *DME* in the *Arabidopsis* genome, represses DNA methylation-mediated transgene silencing in vivo and functions to excise 5-methylcytosine in vitro (Gong et al., 2002). Alternatively, DME may use a more indirect mechanism to overcome MET1-mediated silencing of the maternal *MEA* allele. For example, DNA nicking associated with the base excision DNA repair process may facilitate nucleosome sliding and alter chromatin structure, allowing access of transcription factors to activate *MEA* gene transcription or preventing maintenance of *MEA* promoter methylation by MET1. This possibility is consistent with the broad pattern of nicks in the *MEA* promoter induced in vivo by DME (Choi et al., 2002).

DME acts as an antagonist to MET1 in the central cell to control endosperm imprinting and seed viability. Because chromosomes inherited by the endosperm are not transmitted to progeny, DME- and MET1-based epigenetic modification of maternal alleles in the central cell need not be reset at the next generation. Thus, the imprinting mechanism in plants regulated by two DNA-modifying enzymes, MET1 methyltransferase and DME glycosylase, is fundamentally different from that in mammals, where epigenetic modification including CpG methylation of imprinted genes is reset at every generation.

Experimental Procedures

Isolation of Mutations that Suppress *dme*

Mutant *dme* alleles are not transmitted maternally (Choi et al., 2002), and in the Col *gl* ecotype are transmitted paternally at a reduced level. Thus, 15% of the progeny from self-pollinated *DME/dme* plants inherit the mutant *dme* allele, instead of the expected 75%. To isolate *dme* suppressors we selected lines with increased transmission of the *dme* mutant allele. Measuring transmission rate was facilitated by the fact that *dme-1* and *dme-2* mutant alleles (Choi et al., 2002) are due to insertion of a pSKI015 T-DNA (Weigel et al., 2000) with a BAR gene, which confers resistance to glufosinate ammonium herbicide (Basta; Crescent Chemical Co.). M_1 seeds from *DME/dme-1* or *DME/dme-2* self-pollinated plants were treated with ethylmethanesulfonate (EMS; Ohad et al., 1996). Approximately 8,000 M_1 plants were grown and M_2 seeds from four consecutive siliques were separately harvested, germinated, and the number of 7-day-old seedlings counted. Seedlings were sprayed with Basta and 4 days later the number of Basta-resistant seedlings was counted. When the percentage of Basta-resistant M_2 seedlings significantly exceeded 15%, the percentage of M_3 seed abortion in self-pollinated M_2 siliques was determined. Four putative *dme* suppressor lines (212, 1424, 6683, and 7598) were identified with a 3:1 segregation ratio of viable and aborted seeds. Lines were crossed to wild-type (Col *gl*) six times to remove additional mutations.

Cloning of *dme* Suppressors

Line 212 was crossed to Ler, F_1 plants were self-pollinated, and the percentage of seed abortion was determined in 50 F_2 plants. DNA from F_2 plants was isolated and the position of mutation 212 was mapped relative to molecular markers *SNP126* (17.2 Mb) and *PDC2* (22.3 Mb). This procedure was used to map lines 1424, 6683, and 7598. A population of approximately 600 F2 plants was used to map 212 between markers *CS229* (19.5 Mb) and *CS227* (20.1 Mb), a region that spans the *MET1* gene (19.9 Mb). By DNA sequencing, we identified a lesion in the *MET1* gene from homozygous 212 (*met1-5*), 1424 (*met1-6*), 6683 (*met1-7*), and 7598 (*met1-8*) plants. Primers for molecular markers are *CS200* 5′-TGACAAACCATTTTATT TCATCG-3′ and 5′-TGAGAGAAATCGCAGCCC-3′; *CS229* 5′-TTCT AGAGAAAAGTGGCTCACG-3′ and 5′-TTGTAATCTGAATTAGCATA TCATG-3′; *CS227* 5′-AAAAAGACTTTTTCGACAAATCA-3′ and 5′-GTG GCAGCCGCTGTAAAT-3′; *CS226* 5′-AGGGTAGCTTCGGTTCGG-3′ and 5′-ATGCATGGGAATTGTGGG-3′, *CS203* 5′-CTGTCAAGTGTC AACAATCACC-3′ and 5′-AGAATCTCAAACCCGTTATTCG-3′; *CS214* 5′-CCTGCAAGTAAGGCCCAA-3′ and 5′-TCGCCATTGCAACTTTCA-3′; *CS215* 5′-TTGTTGCTCTTCAAATTTCTCG-3′ and 5′-GAGAGTGA AATCTCTCTTGAAACG-3′; *CS218* 5′-TTTGGCATCATCGCTCAA-3′ and 5′-ACCCTTTCGAAATTCCGC-3′; *CS206* 5′-TGCCATCGCAAA AACTT-3′ and 5′-TCTCAATACCCTCCCAATCG-3′.

Plant Materials

To prevent accumulation of epigenetic abnormalities, homozygous *dme-1* and *met1-6* plants were generated from self-pollinated heterozygous *DME/dme-1 MET1/met1-6* plants. To determine plant genotype, DNA was isolated, PCR amplified, and when necessary digested with restriction endonucleases. The *dme-1* allele was detected by amplifying the BAR gene (*BAR-F* 5′-ATCTACCATGAGCC CAGAAC-3′ and *BAR-R* 5′-GTCATCAGATCTCGGTGACG-3′). The *DME* allele was detected by PCR amplification across the T-DNA insertion site (*SKB-6* 5′-CACTGAGATTAATTCTTCAGACTCGTG-3′ and *SKES2.5* 5′-TTCAGACTCAGAGTCACCTTGC-3′). The *MET1* and *met1-6* alleles were distinguished by amplification with dCAPs (Neff et al., 1998) primers (*1424dBglII* 5′-TGTGACTGAGAACCGCTGT CAGGATCGTTTAAAGAGATC-3′ and *1424F* 5′-CGTACTATAAGAC CTCCGAAG-3′) followed by digestion with BglII. *MEA* and *mea-3* alleles were distinguished as described (Yadegari et al., 2000).

Microscopy

Scanning electron microscopy (Bowman, 1994) and GFP fluorescence microscopy (Yadegari et al., 2000) were performed as described.

Bisulfite Genomic DNA Sequencing

Stamens were collected from wild-type Col *gl* open flowers. Late heart and torpedo stage seeds were isolated from Col *gl* wild-type plants. Heterozygous *met1-6* Col *gl* plants were self-pollinated, homozygous *met1-6* F_1 progeny were identified, self-pollinated, and late heart and torpedo stage homozygous *met1-6* seeds were isolated. DNA (0.3–0.7 μg) was digested with the restriction enzymes XhoI, NdeI, and PstI or HindIII in a 20 μl reaction, boiled 2 min, placed on ice for 1 min, and treated with 2.2 μl of fresh 3 M NaOH at 37°C for 15 min. The rest of the treatment was as described (Jacobsen et al., 2000) except that the DNA was treated with 208 μl sodium bisulfite solution, and the bisulfite conversion was at 55°C for 15 min and 95°C for 30 s for 30 cycles. Two microliters of 50 μl of bisulfite-treated DNA was used in each PCR reaction. PCR reactions were 50 μl with 400–600 nM primers and 0.5 μl Ex Taq DNA polymerase and 1× dNTPs (Takara). PCR conditions were 95°C 5 min, 5 cycles of 95°C 15 s, 60°C 3 min, 72°C 3 min followed by 10 cycles of 95°C 15 s, 60°C 1 min, 72°C 2 min then 30 cycles of 95°C 15 s, 50°C 1 min 30 s, 72°C 2 min, and finally 72°C for 5 min. For some reactions a 50°C annealing temperature was used for all cycles.

The bottom strand of the *MEA* promoter from −4248 to −1 (relative to the translation start site) was sequenced in Col *gl* stamens, a tissue where *DME* and *MEA* are not expressed. The promoter was amplified as 14 overlapping segments. Primer pairs are: mea3979F 5′-CTARATTTTAATTTRCRRTRTACCRC-3′ and mea4510R 5′-GGT TAYTAYATGTTGGTAATAATAAG-3′; mea4445F 5′-CATTAAAATCT ARTRRCARCCATCRTAAATAART-3′ and mea4879R 5′-TGGGAA GAGAYTGTTGYTTGAATGAGA-3′; mea4800F 5′-CCAAACACACTT TCTTAAARCTTTATATACATCTTTCT-3′ and mea5234R 5′-GAGAA YGATYYAGYAATGTATAGATGGG-3′; mea5212F 5′-CATTCCCATC TATACATTTRCTRRATCRTTC-3′ and mea5582R 5′-TYYAAAYGTA TYTGAAGGTTAYGTTTAA-3′; mea5487F 5′-CTTTTRRTCTAATRTR RTRRTRRARRCTAA-3′ and mea6106R 5′-TTYGTTATAAATYYTTG TGTTAAAAYGTAAAT-3′; mea6020F 5′-CATTTARTTAACRTTATAA ARARTAAAAA-3′ and mea6244R 5′-GTGTTTGAYYATTAYATGGA TAAAGTT-3′; mea6167F 5′-TAATATTATRTACAACACACATTTAAT CTT-3′ and mea6424R 5′-TAAAAAYATGTYYAAAYTTATGGTAAT GAAAAG-3′; mea6271F 5′-TCCATCTRCCRRCTRTRTTCATCRRTA AACC-3′ and mea6589R 5′-GAAAATGGGATGATAYTGTTTYTTGA

ATGTG-3'; mea6610F 5'-TCTTACATCCTCTRTTCCTTCACA-3' and mea6812R 5'-GAAAGAGGAAAGATAGAGGGAGGA-3'; mea6790F 5'-CCTCCCTCTATCTTTCCTCT-3' and mea6994R 5'-AGATGTAGA GATGGGAATGGAGAA-3'; mea6938F 5'-CCACARTCTCTCARRA AAACCARAATRCTCTRT-3' and mea7386R 5'-TGTAATAYATAYAY YAGTTYAYAAAATTGAGA-3'; mea7320F 5'-CRRCRRATARACTTA ACCTCCCCATTCRT-3' and mea7627R 5'-TGTGAYATATATAYGG GTTAAATTYYTAGYAAGA-3'; mea7529F 5'-TATTTRACATATTATAC TCATCTCTTRAAT-3' and mea7935R 5'-GTYATTATATATATTAGT ATTYATTYYTAG-3' and mea7871F 5'-TTCTTCCATATATRCATAAT ATATAARC-3' and mea8396R 5'-GGATTTYATAAYYTAGTYAATTYA TATATG-3'.

PCR products were cloned into the TOPO TA cloning vector pCR2.1 (Invitrogen). Between four and seven individual clones were sequenced for each segment. Additional clones were sequenced from the three segments (mea3970F to mea4510R, mea5212F to mea5582R, and mea7529F to mea7935R) that showed nonconversion of a specific cytosine in two or more clones. The methylation status of the three segments on the top and bottom strand was determined in seeds. Top strand primers are: mea3970TF 5'-TGT GAAAGAYTAGATTTTAATTTGYGGTG-3' and mea4455TR 5'-CCA CTARATTTTAATRCTTRTTTTTRATAATT-3'; mea4383TF 5'-GGAA GATTGTTAAATGTYAAATATTTAATT-3' and mea4583TR 5'-AACA CARCCRRCTRATRRACCATCCTC-3'; mea5028TFc 5'-GGTTGATG TTGGAATTTTATATATAATTTTG-3' and mea5337TRc 5'-CCACAAC TCTAAACCACATTAACATCAC-3'; and mea7520TFc 5'-GATGAT TATGTGTAAGATATTTGATATATT-3' and mea7933TRc 5'-CATTA TATATTAATATTCATTCCTAACT-3'. For wild-type seeds, between 18 and 30 clones were sequenced for each strand. For *met1* seeds, between 12 and 23 clones were sequenced for each strand.

Acknowledgments

We thank Brandon Le, Yuping Bi, Laurie McGregor, Alex Navid, Tina Le, Tzung-Fu Hsieh, and Kendra Custard for help in identifying mutations that suppress *dme*. We are grateful to Tetsu Kinoshita for helpful discussions. We thank Eric Richards for providing a probe to the 180 base pair centromeric repeat. This research was supported by grants from the USDA (2002-01400) and Ceres, Inc. (B970602) to R.L.F. and an NSF Graduate Research fellowship to M.G.

Received: October 6, 2003
Revised: October 28, 2003
Accepted: November 5, 2003
Published online: November 24, 2003

References

Adams, S., Vinkenoog, R., Spielman, M., Dickinson, H.G., and Scott, R.J. (2000). Parent-of-origin effects on seed development in *Arabidopsis thaliana* require DNA methylation. Development *127*, 2493–2502.

Bowman, J.L. (1994). Flowers: introduction. In *Arabidopsis*: An Atlas of Morphology and Development, J.L. Bowman, ed. (New York: Springer-Verlag), pp. 135–145.

Brown, R.C., Lemmon, B.E., Nguyen, H., and Olsen, O.-A. (1999). Development of endosperm in *Arabidopsis thaliana*. Sex. Plant Reprod. *12*, 32–42.

Bruner, S.D., Norman, D.P., and Verdine, G.L. (2000). Structural basis for recognition and repair of the endogenous mutagen 8-oxoguanine in DNA. Nature *403*, 859–866.

Cao, X., and Jacobsen, S.E. (2002a). Locus-specific control of asymmetric and CpNpG methylation by the DRM and CMT3 methyltransferase genes. Proc. Natl. Acad. Sci. USA *99*, 16491–16498.

Cao, X., and Jacobsen, S.E. (2002b). Role of the *Arabidopsis* DRM methyltransferases in de novo DNA methylation and gene silencing. Curr. Biol. *12*, 1138–1144.

Chaudhury, A.M., Luo, M., Miller, C., Craig, S., Dennis, E.S., and Peacock, W.J. (1997). Fertilization-independent seed development in *Arabidopsis thaliana*. Proc. Natl. Acad. Sci. USA *94*, 4223–4228.

Choi, Y., Gehring, M., Johnson, L., Hannon, M., Harada, J.J., Goldberg, R.B., Jacobsen, S.E., and Fischer, R.L. (2002). DEMETER, a DNA glycosylase domain protein, is required for endosperm gene imprinting and seed viability in *Arabidopsis*. Cell *110*, 33–42.

Ferguson-Smith, A.C., and Surani, M.A. (2001). Imprinting and the epigenetic asymmetry between parental genomes. Science *293*, 1086–1089.

Finnegan, E.J., and Dennis, E.S. (1993). Isolation and identification by sequence homology of a putative cytosine methyltransferase from *Arabidopsis thaliana*. Nucleic Acids Res. *21*, 2383–2388.

Finnegan, E.J., and Kovac, K.A. (2000). Plant DNA methyltransferases. Plant Mol. Biol. *43*, 189–201.

Finnegan, E.J., Peacock, W.J., and Dennis, E.S. (1996). Reduced DNA methylation in *Arabidopsis* results in abnormal plant development. Proc. Natl. Acad. Sci. USA *93*, 8449–8454.

Francis, N.J., and Kingston, R.E. (2001). Mechanisms of transcriptional memory. Nat. Rev. Mol. Cell Biol. *2*, 409–421.

Gehring, M., Choi, Y., and Fischer, R.L. (2003). Imprinting and seed development. Plant Cell, in press.

Gong, Z., Morales-Ruiz, T., Ariza, R.R., Roldan-Arjona, T., David, L., and Zhu, J.-J. (2002). ROS1, a repressor of transcriptional gene silencing in *Arabidopsis*, encodes a DNA glycosylase/lyase. Cell *111*, 803–814.

Grossniklaus, U., Vielle-Calzada, J.-P., Hoeppner, M.A., and Gagliano, W.B. (1998). Maternal control of embryogenesis by *MEDEA*, a polycomb-group gene in *Arabidopsis*. Science *280*, 446–450.

Jackson, J.P., Lindroth, A.M., Cao, X., and Jacobsen, S.E. (2002). Control of CpNpG DNA methylation by the KRYPTONITE histone H3 methyltransferase. Nature *416*, 556–560.

Jacobsen, S.E., Sakai, H., Finnegan, E.J., Cao, X., and Meyerowitz, E.M. (2000). Ectopic hypermethylation of flower-specific genes in *Arabidopsis*. Curr. Biol. *10*, 179–186.

Jeddeloh, J.A., Stokes, T.L., and Richards, E.J. (1999). Maintenance of genomic methylation requires a SWI2/SNF2-like protein. Nat. Genet. *22*, 94–97.

Jiricny, J. (2002). An APE that proofreads. Nature *415*, 593–594.

Johnson, L.M., Cao, X., and Jacobsen, S.E. (2002). Interplay between two epigenetic marks: DNA methylation and histone H3 lysine 9 methylation. Curr. Biol. *12*, 1360–1367.

Jost, J.-P., Oakeley, E.J., Zhu, B., Benjamin, D., Thiry, S., Siegmann, M., and Jost, Y.-C. (2001). 5-Methylcytosine DNA glycosylase participates in the genome-wide loss of DNA methylation occurring during mouse myoblast differentiation. Nucleic Acids Res. *29*, 4452–4461.

Kakutani, T., Jeddeloh, J.A., Flowers, S.K., Munakata, K., and Richards, E.J. (1996). Developmental abnormalities and epimutations associated with DNA hypomethylation mutations. Proc. Natl. Acad. Sci. USA *93*, 12406–12411.

Kankel, M.W., Ramsey, D.E., Stokes, T.L., Flowers, S.K., Haag, J.R., Jeddeloh, J.A., Riddle, N.C., Verbsky, M.L., and Richards, E.J. (2003). *Arabidopsis* MET1 cytosine methyltransferase mutants. Genetics *163*, 1109–1122.

Kinoshita, T., Yadegari, R., Harada, J.J., Goldberg, R.B., and Fischer, R.L. (1999). Imprinting of the *MEDEA* polycomb gene in the *Arabidopsis* endosperm. Plant Cell *11*, 1945–1952.

Kishimoto, N., Sakai, H., Jackson, J., Jacobsen, S.E., Meyerowitz, E.M., Dennis, E.S., and Finnegan, E.J. (2001). Site specificity of the *Arabidopsis* MET1 DNA methyltransferase demonstrated through hypermethylation of the SUPERMAN locus. Plant Mol. Biol. *46*, 171–183.

Kiyosue, T., Ohad, N., Yadegari, R., Hannon, M., Dinneny, J., Wells, D., Katz, A., Margossian, L., Harada, J., Goldberg, R.B., and Fischer, R.L. (1999). Control of fertilization-independent endosperm development by the *MEDEA* polycomb gene in *Arabidopsis*. Proc. Natl. Acad. Sci. USA *96*, 4186–4191.

Kohler, C., Hennig, L., Spillane, C., Pien, S., Gruissem, W., and Grossniklaus, U. (2003). The Polycomb-group protein MEDEA regulates seed development by controlling expression of the MADS-box gene PHERES1. Genes Dev. *17*, 1540–1553.

Li, E. (2002). Chromatin modification and epigenetic reprogramming in mammalian development. Nat. Rev. Genet. *3*, 662–673.

Lindroth, A.M., Cao, X., Jackson, J.P., Zilberman, D., McCallum, C.M., Henikoff, S., and Jacobsen, S.E. (2001). Requirement of CHROMOMETHYLASE3 for maintenance of CpXpG methylation. Science *292*, 2077–2080.

Luo, M., Bilodeau, P., Koltunow, A., Dennis, E.S., Peacock, W.J., and Chaudhury, A.M. (1999). Genes controlling fertilization-independent seed development in *Arabidopsis thaliana*. Proc. Natl. Acad. Sci. USA *96*, 296–301.

Luo, M., Bilodeau, P., Dennis, E.S., Peacock, W.J., and Chaudhury, A. (2000). Expression and parent-of-origin effects for *FIS2*, *MEA*, and *FIE* in the endosperm and embryo of developing *Arabidopsis* seeds. Proc. Natl. Acad. Sci. USA *97*, 10637–10642.

Martienssen, R. (1998). Chromosomal imprinting in plants. Curr. Opin. Genet. Dev. *8*, 240–244.

Martienssen, R.A., and Colot, V. (2001). DNA methylation and epigenetic inheritance in plants and filamentous fungi. Science *293*, 1070–1074.

Miura, A., Yonebayashi, S., Watanabe, K., Toyama, T., Shimada, H., and Kakutani, T. (2001). Mobilization of transposons by a mutation abolishing full DNA methylation in *Arabidopsis*. Nature *411*, 212–214.

Moore, G. (2001). Genetic conflict, genomic imprinting and establishment of the epigenotype in relation to growth. Reproduction *122*, 185–193.

Neff, M.M., Neff, J.D., Chory, J., and Pepper, A.E. (1998). dCAPS, a simple technique for the genetic analysis of single nucleotide polymorphisms: experimental applications in *Arabidopsis thaliana* genetics. Plant J. *14*, 387–392.

Ohad, N., Margossian, L., Hsu, Y.-C., Williams, C., Repetti, P., and Fischer, R.L. (1996). A mutation that allows endosperm development without fertilization. Proc. Natl. Acad. Sci. USA *93*, 5319–5324.

Posfai, L., Bhagwat, A.S., Posfai, G., and Roberts, R.J. (1989). Predictive motifs from cytosine methyltransferases. Nucleic Acids Res. *17*, 2421–2435.

Reik, W., and Walter, J. (2001). Genomic imprinting: parental influence on the genome. Nat. Rev. Genet. *2*, 21–32.

Ronemus, M.J., Galbiati, M., Ticknor, C., Chen, J., and Dellaporta, S.L. (1996). Demethylation-induced developmental pleiotropy in *Arabidopsis*. Science *273*, 654–657.

Saze, H., Scheid, O.M., and Paszkowski, J. (2003). Maintenance of CpG methylation is essential for epigenetic inheritance during plant gametogenesis. Nat. Genet. *34*, 65–69.

Soppe, W.J.J., Jacobsen, S.E., Alonso-Blanco, C., Jackson, J.P., Kakutani, T., Koornneef, M., and Peeters, A.J.M. (2000). The late flowering phenotype of *fwa* mutants is caused by gain-of-function epigenetic alleles of a homeodomain gene. Mol. Cell *6*, 791–802.

Soppe, W.J.J., Jasencakova, Z., Andreas, H., Tetsuji, K., Armin, M., Huang, M.S., Jacobsen, S.E., Ingo, S., and Fransz, P.F. (2002). DNA methylation controls histone H3 lysine 9 methylation and heterochromatin assembly in *Arabidopsis*. EMBO J. *21*, 6549–6559.

Tycko, B., and Morison, I.M. (2002). Physiological functions of imprinted genes. J. Cell. Physiol. *192*, 245–258.

Vielle-Calzada, J.-P., Thomas, J., Spillane, C., Coluccio, A., Hoeppner, M.A., and Grossniklaus, U. (1999). Maintenance of genomic imprinting at the *Arabidopsis medea* locus requires zygotic DDM1 activity. Genes Dev. *13*, 2971–2982.

Weigel, D., Ahn, J.H., Blazquez, M.A., Borevitz, J.O., Christensen, S.K., Frankhauser, C., Ferrandiz, C., Kardailsky, I., Malancharuvil, E.J., Neff, M.M., et al. (2000). Activation tagging in *Arabidopsis*. Plant Physiol. *122*, 1003–1013.

Yadegari, R., Kinoshita, T., Lotan, O., Cohen, G., Katz, A., Choi, Y., Katz, A., Nakashima, K., Harada, J.J., Goldberg, R.B., et al. (2000). Mutations in the FIE and MEA genes that encode interacting polycomb proteins cause parent-of-origin effects on seed development by distinct mechanisms. Plant Cell *12*, 2367–2381.

Note Added in Proof

Recently it was shown that DME and MET1 regulate another gene, *FWA*, which is imprinted in the endosperm (Kinoshita et al., 2003). DME activates expression of the maternal *FWA* allele, whereas MET1 represses expression of the paternal *FWA* allele. Thus, control of maternal-specific expression by MET1 and DME may be a general mechanism for endosperm imprinting in *Arabidopsis*.

Kinoshita, T., Miura, A., Choi, Y., Kinoshita, Y., Cao, X., Jacobsen, S.E., Fischer, R.L., and Kakutani, T. (2003). A one-way control of *FWA* imprinting in *Arabidopsis* endosperm by DNA methylation. Science, in press.